ISSN 1881-7815 Online ISSN 1881-7823

BST BioScience Trends

Volume 9, Number 6
December, 2015

IRCA BSSA

IACMHR

www.biosciencetrends.com

BST
BioScience Trends

ISSN: 1881-7815
Online ISSN: 1881-7823
CODEN: BTIRCZ
Issues/Year: 6
Language: English
Publisher: IACMHR Co., Ltd.

BioScience Trends is one of a series of peer-reviewed journals of the International Research and Cooperation Association for Bio & Socio-Sciences Advancement (IRCA-BSSA) Group and is published bimonthly by the International Advancement Center for Medicine & Health Research Co., Ltd. (IACMHR Co., Ltd.) and supported by the IRCA-BSSA and Shandong University China-Japan Cooperation Center for Drug Discovery & Screening (SDU-DDSC).

BioScience Trends devotes to publishing the latest and most exciting advances in scientific research. Articles cover fields of life science such as biochemistry, molecular biology, clinical research, public health, medical care system, and social science in order to encourage cooperation and exchange among scientists and clinical researchers.

BioScience Trends publishes Original Articles, Brief Reports, Reviews, Policy Forum articles, Case Reports, News, and Letters on all aspects of the field of life science. All contributions should seek to promote international collaboration.

Editorial Board

Editorial Office

Pearl City Koishikawa 603,
2-4-5 Kasuga, Bunkyo-ku,
Tokyo 112-0003, Japan
Tel: +81-3-5840-8764
Fax: +81-3-5840-8765
E-mail: office@biosciencetrends.com

BioScience Trends

Editorial and Head Office

Pearl City Koishikawa 603, 2-4-5 Kasuga, Bunkyo-ku,
Tokyo 112-0003, Japan

Tel: +81-3-5840-8764, Fax: +81-3-5840-8765
E-mail: office@biosciencetrends.com
URL: www.biosciencetrends.com

Editorial Board Members

CONTENTS

Volume 9, Number 6, 2015

Review

Original Articles

Brief Report

Subject Index

Guide for Authors

Copyright

Review

DOI: 10.5582/bst.2015.01154

Dehydroepiandrosterone improves the ovarian reserve of women with diminished ovarian reserve and is a potential regulator of the immune response in the ovaries

Jiali Zhang[1,2], Xuemin Qiu[1,2], Yuyan Gui[1,2], Yingping Xu[1,2], Dajin Li[1,2], Ling Wang[1,2,*]

[1] *Laboratory for Reproductive Immunology, Hospital & Institute of Obstetrics and Gynecology, IBS, Fudan University Shanghai Medical College, Shanghai, China;*
[2] *Shanghai Key Laboratory of Female Reproductive Endocrine-related Disorders, Shanghai, China.*

Summary **Diminished ovarian reserve (DOR) has a high morbidity rate worldwide and has become a primary cause of infertility. DOR is a daunting obstacle in *in vitro* fertilization (IVF) and leads to poor ovarian response, high cancellation rates, poor IVF outcomes, and low pregnancy rates. Abnormal autoimmune function may also contribute to DOR. Dehydroepiandrosterone (DHEA) is a C19 androgenic steroid. DHEA is secreted mainly by the adrenal gland, and its secretion declines with age. DHEA has a pro-inflammatory immune function that opposes cortisol. The cortisol to DHEA ratio increases with age, which may lead to decreased immune function. DHEA supplementation helps improve this situation. A number of clinical case control studies and several prospective randomized clinical trials have observed a positive effect of DHEA supplementation in women with DOR. However, the underlying mechanism by which DHEA improves ovarian reserve remains unclear. DHEA functions as an immune regulator in many different tissues in mammals and may also play an important role in regulating the immune response in the ovaries. The conversion of DHEA to downstream sex steroids may allow it to regulate the immune response there. DHEA can also enhance the Th1 immune response and regulate the balance of the Th1/Th2 response. DHEA treatment can increase selective T lymphocyte infiltration in mice, resulting in a decline in the CD4+ T lymphocyte population and an upregulation of the CD8+ T lymphocyte population in ovarian tissue, thus regulating the balance of CD4+/CD8+ T cells. This review mainly focuses on how DHEA supplementation affects regulation of the immune response in the ovaries.**

Keywords: Dehydroepiandrosterone (DHEA), diminished ovarian reserve (DOR), immune response, cytokine, lymphocytes, endocrino-immune network

1. Introduction

Ovarian reserve decreases within a certain range as women age. Women with a lower ovarian reserve outside of this range are identified as having diminished ovarian reserve (DOR). Reduced ovarian reserve consists of a decline in the number of primordial follicles, a decrease in the size of the dynamic reserve of small antral follicles, and a deterioration in oocyte quality. These changes are evident as women age. Some genetic mutations and disorders of the endocrine system can accelerate or modulate the rate at which the ovarian reserve is exhausted and cause premature ovarian insufficiency (POI) (*1*). Among the various causes of DOR, abnormal immune function may be a great contributor to this phenomenon (*2*). Patients with DOR often become infertile and have a poor response to *in vitro* fertilization (IVF) (*3,4*). Researchers have developed different protocols to solve this problem, but none of them has proven to be ideal for such patients (*5-7*). Dehydroepiandrosterone (DHEA) is a C19 androgenic steroid that has been found to be effective in many areas. Decades of observational

**Address correspondence to:*
Dr. Ling Wang, Obstetrics & Gynecology Hospital of Fudan University, 413 Zhaozhou Road, Shanghai 200011, China.
E-mail: dr.wangling@fudan.edu.cn

studies both in clinical settings and in animals have found that the levels of DHEA(S) are inversely associated with cardiovascular risk, morbidity, and mortality (*8*). In ovariectomized rabbits, DHEA was found to protect against atherosclerosis because it alleviated inflammation in endothelial cells (*9*). DHEA is able to cross the brain-blood barrier. DHEA also has neuroactive characteristics and it has positive effects on human mood, emotions, and behaviors (*10,11*). In 2000, Casson *et al*. were the first to use DHEA supplementation in women with DOR to improve the response to ovarian stimulation (*12*). Many researchers have devoted their attention to the effects of DHEA supplementation in women with DOR. Narkwichean *et al*. conducted a meta-analysis that showed that DHEA administration resulted in a significant increase in the number of oocytes retrieved in women with DOR according to some clinical trials. However, more clinical trials must be performed to verify the results (*13*). In ovariectomized sheep, DHEA supplementation was effective at *in vivo* ovarian folliculogenesis (*14*). Similar results have been observed with Wistar rats in an *in vivo* model (*15*). However, the underlying mechanism by which DHEA improves ovarian reserve remains unclear. DHEA can regulate immune cell function (*16*), and it may regulate the function of many different types of tissue in mammals. Utilizing a human subcutaneous preadipocyte cell line, Chub-S7, McNeils *et al*. found that DHEA inhibition of the amplification of glucocorticoid action was mediated by 11β-hydroxysteroid dehydrogenase type 1 (11β-HSD1) (*17*). Lazaridis *et al*. performed an *in vitro* study that showed that DHEA also served as a neurosteroid, directly interacting with nerve growth factor (NGF) to prevent neuronal apoptosis (*18*). In ovariectomized rats, DHEA showed the potential to correct oxidative stress-induced endothelial dysfunction (*19*). Thus, DHEA may play an important role in regulating the immune response in the ovaries. DHEA treatment may also modulate the lymphocyte response in both human and animal trials (*20,21*). The current review mainly focuses on how DHEA supplementation affects regulation of the immune response in the ovaries.

2. DHEA supplementation has proven effective in women

DHEA (5-androsten-3β-ol-17-one) is a C19 androgenic steroid (Figure 1) that is secreted primarily by the adrenal zona reticularis. DHEA is synthesized by the steroidogenic enzyme P450c17 and partly by the ovary (*22*). The secretion of DHEA has a diurnal rhythm similar to that of cortisol (*23,24*). In humans, the intra-individual concentrations of DHEA and its sulphate, DHEAS, steadily decline with advancing age, unlike those of other androgenic steroids. The concentration peaks during the third decade of life, with a clear sex

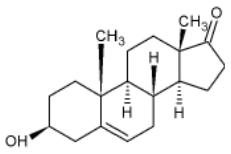

Figure 1. Chemical structure of DHEA.

difference since adult women have lower concentrations of DHEA than men (*25-27*). Given this characteristic of age-related decline, DHEA supplementation may help to improve age-related damage in human beings. To date, no studies have noted an apparent effect of DHEA in healthy males (*28*). Some double-blind placebo-controlled trials have demonstrated that DHEA does not markedly improve well-being or cognitive function in healthy elderly men and women over age 50 (*28,29*). However, DHEA was found to modulate immune function in postmenopausal women (*30*). DHEA is also reported to affect cardiovascular and immunological function differently in women and men (*31*).

2.1. *The effects of DHEA supplementation in women with DOR*

There are no set criteria for DOR thus far, but women with DOR share a poor ovarian response to stimulation as well as high cancellation rates and low pregnancy rates. A poor ovarian response in a previous IVF-embryo transfer (ET) cycle means that fewer oocytes were retrieved or that these oocytes were less mature follicles after high-dose gonadotropin stimulation. Different researchers have defined this process differently. Many studies have investigated the effects of DHEA supplementation on ovarian function. Twelve of those studies were analyzed in the current study (see Table 1). DHEA supplementation is usually oral and administered at 25 mg, three times a day, or 75-90 mg for the entire day, for 6 to 24 weeks. A previous case-control study showed that DHEA improved ovarian reserve and that it significantly increased antral follicle counts (AFCs), anti-Müllerian hormone (AMH) levels (*32-34*), numbers of fertilized oocytes, normal day 3 embryos, embryos transferred, and the average embryo score per oocyte (*35*) while significantly decreasing day 3 follicle-stimulating hormone (FSH) (*33*), fertilized aneuploid embryos (*36*), and miscarriage rates (*37*) (all p-values < 0.05). Estradiol (E2) levels tripled according to two studies (*12,38*) but decreased according to a third (*34*). Several randomized prospective controlled studies investigated the effects of DHEA supplementation but their results were inconsistent. Some researchers obtained the same results as described earlier (*34,38-40*), but the number of oocytes retrieved and the fertilization rate remained inconsistent (*38,40,41*), whereas others failed to show that DHEA was effective at improving IVF outcomes (*40,41*). These studies,

Table 1. Efficacy of DHEA supplementation prior to IVF cycle

(Table continued on next page)

Ref.	Definition of DOR	Study type	Methods			Result (P value)	Conclusion
			Study object	Route of medication	Dose		
Casson *et al.* (*12*)	Poor response to high-dose gonadotropin stimulation (peak E2 < 500 pg/mL and mature follicle ≤ 2)	A series of case studies	5 women with unexplained infertility (under age 41, FSH < 20 mIU/mL)	Oral, twice a day for 2 months, prior to IUI	80 mg	↑ DHEAs, testosterone, responsiveness, peak E2, and E2/ampoule ratio (0.012). One achieved twin pregnancy. The E2 level tripled in all five cases. The number of oocytes doubled	It improves the response to ovarian stimulation after controlling for gonadotropin dose
Barad *et al.* (*35*)	FSH > 10 mIU/mL or E2 >75 pq/mL (275.3 pmol/L)	Case-control study	25 women with DOR and repeated IVF failure	Oral, three times a day, for 17 ± 2.13 weeks	25 mg	↑ fertilized oocytes (< 0.001), normal day3 embryos (< 0.001), embryos transferred (0.005) and average embryo score per oocyte (< 0.001)	Confirms the previously reported beneficial effects of DHEA supplementation on ovarian function in women with DOR
Gleicher *et al.* (*37*)	FSH > 10 mIU/ml or E2 > 75 pq/mL (275.3 pmol/L)	Case-control study	22 consecutive patients with DOR	Oral, three times a day	25 mg	↓ miscarriage rate at all ages, but most pronounced above age 35	Miscarriage rates after DHEA were not only lower in an average IVF population but were comparable with rates reported in normal fertile populations
Gleicher *et al.* (*36*)	abnormally elevated age-specific baseline FSH or abnormally low age-specific AMH	1:2 matched case control study	120 women with DOR	Oral, three times a day, for at least 4 weeks	25 mg	↓ number (= 0.029) and percentage (< 0.001) of aneuploid embryos	Beneficial DHEA effects on DOR patients are the likely consequence of lower embryo aneuploidy
Gleicher *et al.* (*32*)	AMH concentrations were evaluated as a reflection of ovarian reserve	Retrospective cross-sectional and longitudinal analysis	15 women with DOR	Oral, three times a day, for 73 ± 27 days	25 mg	↑ AMH concentrations (= 0.002) and women age < 38 responded more than women who were older. AMH improved pregnancy rates longitudinally by 60% (< 0.0002), and IVF, by 23.64%, compared with those not treated (= 0.001)	DHEA supplementation significantly improved ovarian reserve in parallel with longer DHEA use and improvement was more pronounced in younger women
Weissman *et al.* (*89*)	Poor ovarian response in previous IVF-ET cycles (high-dose gonadotropin stimulation: < 5 oocytes retrieved, ≤ 3 follicles of 16 mm or larger each on the day of cycle cancellation, serum E2 level < 500 pg/mL on the day of hCG administration)	Case-control study	41 women (age ≤ 40 years) with DOR were divided into two groups: age < 35 or ≥ 35	Oral, once a day during the follicular phase in IVF	75 mg	↑ progesterone on day 5 of stimulation (< 0.0001); increased progesterone on the day of hCG administration (< 0.0001); Similar number of retrieved and fertilized oocytes	DHEA administration during IVF cycles in women with DOR causes a significant elevation of progesterone levels without an apparent deleterious effect on cycle outcome
Yilmaz *et al.* (*33*)	AFC < 5 or AMH < 1.1 ng/mL and a previous poor ovarian response	Case-sectional study	280 women (mean age 30.97 ± 5.76 years) were divided randomly into two groups: 104 women in the DHEA group and 104 women in the control group	Oral, three times a day prior to assisted reproductive technology for at least 6 weeks	25 mg	Significant differences were seen in both groups after DHEA supplementation: ↑ AFC (0.001), AMH (0.002) and inhibin B (0.001), ↓ day 3 FSH (0.001) and estradiol (0.001).	DHEA supplementation is an effective option for patients with DOR as an alternative to oocyte donation prior to assisted reproduction

Abbreviations: ↑, increased; ↓, decreased; DHEA, dehydroepiandrosterone; DOR, diminished ovarian reserve; POR, poor ovarian reserve; E2, estradiol; AMH, anti-Müllerian hormone; FSH, follicle stimulating hormone; LH, luteinizing hormone; IVF, *in vitro* fertilization; IUI, intrauterine insemination; IVF-ET, *in vitro* fertilization-embryo transfer; AFC, antral follicle count; POI, premature ovarian insufficiency; IVF-ICSI, *in vitro* fertilization-intracytoplasmic sperm injection; BMP-15, bone morphogenetic protein-15.

Table 1. Efficacy of DHEA supplementation prior to IVF cycle

(Table continued)

Ref.	Definition of DOR	Study type	Methods			Result (P value)	Conclusion
			Study object	Route of medication	Dose		
Kara *et al.* (*41*)	POR: serum AMH < 1 ng/mL or serum FSH > 15 IU/L and AFC < 4 on day 2 of the menstrual cycle.	Randomized, prospective controlled study	280 women (mean age 30.97 ± 5.76 years) were divided randomly into two groups: 104 women in the DHEA group and 104 women in the control group	Oral, once a day prior to IVF-ICSI	75 mg	The number of oocytes retrieved and the fertilization rate are slightly higher in the study group. The pregnancy rate is higher in the control group. No significant difference can be observed	Failed to show that DHEA supplementation enhances IVF-ICSI outcomes in women with poor ovarian reserve
Zhang *et al.* (*38*)	Fulfills any of the following: (1) day 3 FSH level ≥ 10 nIU/L or FSH/LH > 3:2; (2) AFC < 5; or (3) a previous poor ovarian response to ovarian stimulation: retrieval of fewer than five oocytes or cycle cancellation due to poor response to ovarian stimulation	Randomized, prospective controlled study	95 women with DOR were divided randomly into two groups: 42 in the DHEA group and 53 in the control group.	Oral, once a day for 3 consecutive menstrual cycles before entering IVF cycle	75 mg	The DHEA group had a significant increase in the serum level of AMH (0.015), FSH (0.036) and E2 (0.002), BMP-15 in follicular fluid samples (0.000), and the accumulated score of embryos (0.033)	Confirms the beneficial effect of DHEA for infertility patients with DOR
Poli *et al.* (*40*)		Experimental prospective, pre-post study	29 women with DOR or a poor response in a prior IVF cycle	Oral, once a day for 8 weeks before stimulation with FSH in IVF cycle.	75 mg	Significant increase in the number of the retrieved oocytes (< 0.01) and the oocyte quality (0.002). Significant decrease in cancelled IVF cycles (0.003)	Confirmed the beneficial effect of DHEA in patients who were poor responders to IVF treatments. DHEA appears to be an effective treatment for age related sub-fertility.
Tsui *et al.* (*34*)	POR: Individuals to whom the following apply: (1) FSH > 15 nIU/L or AMH < 1 ng/mL; (2) abnormally low AFC < 4 on day2 of their menstrual cycle; (3) an unsuccessful flexible daily GnRH antagonist in the first IVF cycle	Prospective study	10 women with POR	Oral, three times a day prior to next IVF cycle for 3 months (mean: 12.2 weeks)	30 mg	Significant increase in AFC (< 0.05), AMH (< 0.001), numbers of retrieved oocytes (< 0.01), fertilized oocytes (< 0.001), day 3 embryos (< 0.001), and transferred embryos (< 0.01). Significant decrease in Day 3 FSH and E2 (both < 0.001)	The potential benefits of DHEA supplementation in women with POR were suggested by biochemical parameters and IVF outcomes.
Tartagni *et al.* (*39*)	Out of the normal range: (1) Day 3 FSH < 10 IU/L; (2) AMH:2.8~6.8 ng/L; (3) inhibin > 45 pg/mL	Double blind, randomized, placebo-controlled study	109 infertile patients (ages 36-40 and failed in the first IVF cycle) were divided into 2 groups: (1) DHEA group and (2) control group.	Oral, once a day, from 8 weeks before next IVF cycle	75 mg	Significantly higher live birth rate (< 0.05) in the DHEA group and significantly higher miscarriage rate in the control group (< 0.05).	DHEA may significantly improve IVF outcomes in infertile women with advanced reproductive age and normal ovarian reserve.

Abbreviations: ↑, increased; ↓, decreased; DHEA, dehydroepiandrosterone; DOR, diminished ovarian reserve; POR, poor ovarian reserve; E2, estradiol; AMH, anti-Müllerian hormone; FSH, follicle stimulating hormone; LH, luteinizing hormone; IVF, *in vitro* fertilization; IUI, intrauterine insemination; IVF-ET, *in vitro* fertilization-embryo transfer; AFC, antral follicle count; POI, premature ovarian insufficiency; IVF-ICSI, *in vitro* fertilization-intracytoplasmic sperm injection; BMP-15, bone morphogenetic protein-15.

however, cannot be compared statistically since there were no set criteria to define DOR. Usually, DOR was defined as abnormally elevated age-specific baseline FSH levels and/or abnormally low AMH levels (*42-44*), elevated inhibin-B levels, and AFCs less than 4 to 5 (*33,34,38,41*).

2.2. *Immune function of DHEA*

Use of DHEA has been described in many areas and is mainly considered because of its immunoregulatory function. DHEA has an effect on human neuroendocrine cells and plays an important role in immune regulation, especially by balancing pro-inflammatory and anti-inflammatory signals. Humans develop inflammation with age, which involves the up-regulation of certain pro-inflammatory cytokines, such as interleukin (IL)-1, IL-6, tumor necrosis factor (TNF)-α, IL-12, interferon (IFN)-α, and IFN-β. In old age, these cytokines negatively impact various systems in the body (*45-47*). This leads to an unbalanced relationship between pro-inflammatory cytokines and anti-inflammatory cytokines (IL-4, IL-6, IL-13, IL-10) (*48*). DHEA is part of the hypothalamus-pituitary-adrenal (HPA) axis. When the HPA axis is activated, both cortisol and DHEA are released. Cortisol has an anti-inflammatory effect, whereas DHEA appears to have an opposing effect. As DHEA levels decline with age, the molar ratio of cortisol to DHEAS increases and may interact with weakened immune function (*49,50*). Elderly bereaved participants showed decreased production of neutrophil reactive oxygen species and an increased cortisol to DHEAS ratio (*10*). DHEA supplementation has a positive effect on immunity in the elderly. Treatment with 20 mg/kg DHEA for 8 weeks reversed antioxidant parameters, such as decreased superoxide dismutase activity in the brain and heart, decreased inducible nitric oxide synthase mRNA levels, and increased heme oxygenase mRNA levels, in aged rats (*51*). Buoso *et al*. found that cortisol acted in a dose-related manner *in vitro* and *in vivo* on human guanine nucleotide binding protein and the beta polypeptide 2 like 1 (GNB2 L1) promoter repressor, which reduced receptor for Activated C Kinase 1(RACK-1) mRNA and protein expression. Prolonged DHEA exposure counteracted the effects of cortisol and restored RACK-1 levels and cytokine production (assessed with lipopolysaccharide (LPS)-induced TNF-α release); this most likely occurred as a result of interfering with glucocorticoid receptor binding to the glucocorticoid responsive element (GRE) sequence (*52*). Furthermore, DHEA supplementation has been proven to be effective in treating other diseases and improving organ function and survival. However, these mechanisms are not yet fully understood. Over the past few years, an increasing number of researchers have turned their attention to the effects of DHEA on regulation of the immune response, but these effects have been produced in non-human mammals. In aged baboons, researchers found increased serum C-reactive protein and increased cytokine release from unstimulated peripheral blood mononuclear cells. Supplementary DHEA improved outcomes in a murine polymicrobial sepsis and trauma model by restoring TNF-α in the liver and lungs after 48 hours and attenuating it in the liver after 96 hours, much like a time- and organ-dependent modulator (*53*). DHEA supplementation also leads to a restoration of splenocyte proliferation, a decrease in the rate of cellular apoptosis of splenocytes, and an attenuation of increased IL-6 levels (*54*). DHEA also restored peripheral blood mononuclear cell (PBMC) function and increased the ability of human PBMCs patients with depressed immune function to release pro-inflammatory cytokines (IL-1β, IL-6, and TNF-α) following major abdominal surgery (*55*).

Table 2. Types of autoimmune abnormalities

Type of auto-antibody	Containing
Antinuclear antibody	–
Anti-phospholipid antibody	lupus anticoagulant, anti-phosphatidylserine, anti-cardiolipin, β2-glycoprotein (IgG, IgM, IgA)
Anti-thyroid antibodies	anti-thyroglobulin, anti-thyroid peroxidase
Anti-adrenal antibodies	anti-21-hydroxylase
Anti-ovarian antibodies	non-specific
Total immunoglobulins	IgG, IgM, IgA, IgE

3. DHEA and the immune response in the ovaries

The level of the immune response in the ovaries changes with age along with the ovarian reserve. There is substantial interaction between the immune system and the ovaries as immune cells are associated with regulation at every level of the hypothalamus-pituitary-ovarian axis by regulating growth and regression of both follicles and the corpus luteum (*56-58*). In adult ovaries, activated myeloid dendritic cells (MDC) also play a role in follicular development and atresia, as well as differentiation of the corpus luteum. MDC and T cells massively infiltrate the corpus luteum, resulting in parenchymal and vascular regression, which then leads to the demise of the corpus luteum (*59*). DHEA improves the ovarian reserve of women with age-related DOR women with POI even though POI is more closely related to ovarian immune disorders. Young women who have a history or family history of autoimmunity are at risk for POI (*60,61*). There are many types of autoimmune abnormalities (Table 2). There are three different types of autoimmune ovarian insufficiency: autoimmune ovarian insufficiency associated with adrenal autoimmunity, autoimmune

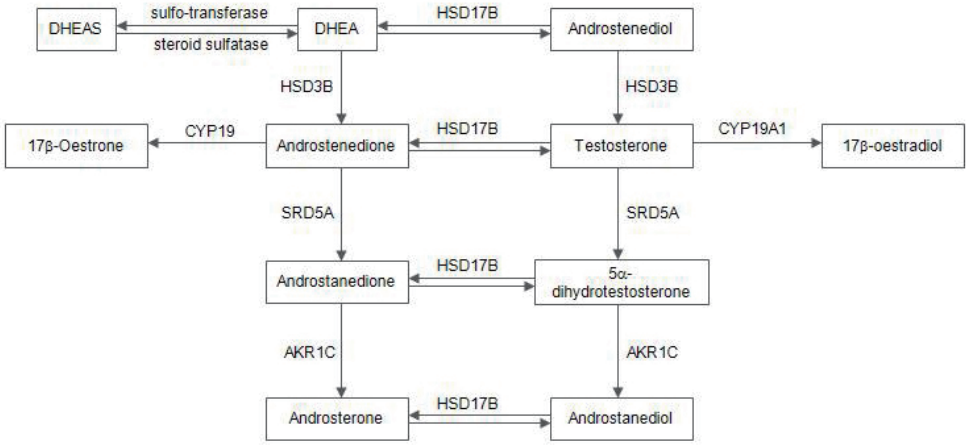

Figure 2. Path for conversion of DHEA to other downstream steroids. Abbreviations: DHEA, dehydroepiandrosterone; DHEAS, dehydroepiandrosterone sulphate; HSD17B,17β-hydroxysteroid dehydrogenase isoenzymes; HSD3B, 3β-hydrogenase isoenzymes; CYP19A1, P450 aromatase; SRD5A, 5α-reductase isoenzymes; AKR1C, 3α-hydroxysteroid dehydrogenase isoenzymes.

ovarian insufficiency associated with non-adrenal autoimmunity, and isolated idiopathic POI (iPOI) (*62*); adrenal autoimmunity is the most prevalent (*2,63*). Researchers tested for triple CGG repeats on both alleles of the fragile X mental retardation 1 (FMR1) gene and assessed autoimmune status (including an antiphospholipid antibody panel, an antinuclear antibody panel, total immunoglobulin levels, thyroid antibodies, and antiadrenal antibodies), and then they found that abnormal autoimmune function, including expansions in triple CGG repeats on the FMR1 gene, increased the risk for POI (*64,65*).

Although the effects of DHEA supplementation in women with DOR are readily evident, the mechanism behind these effects remains unclear. Given the complex immune function of DHEA and ovarian immune disorders in women with DOR, some researchers have begun to explore the immune function of DHEA in women with DOR. However, the research reports to date on this topic are extremely limited. Only a few studies have been conducted and their results are summarized below.

3.1. *Conversion to other steroids*

No certain specific receptor for DHEA has been found to date, and some theories suggest that DHEA may function once steroidogenic enzymes convert it to other downstream steroids, especially sex steroids such as estrone and androgens (Figure 2). Small structural changes in androgens result in markedly different biological effects. Steroidogenic enzymes have tissue-specific patterns of expression; thus, DHEA may have a special function. These steroids interact critically with immune function. Estrone can shift the female immune system to a Th2-type response in the luteal phase, whereas postmenopausal women often exhibit enhanced Th1 cytokines (*66*). As mentioned previously, DHEA can restore PBMC function and increase the ability of human PBMCs to release pro-inflammatory cytokines after surgery *via* the estrogen receptor; this immunomodulatory effect of DHEA appears to be connected to estrogen receptors (*55*). Although total androgen concentrations were not associated with pregnancy during DHEA supplementation in women with POI, interaction between DHEA and total and free testosterone also significantly affected pregnancy rates at the start of an IVF cycle (*67*). Total testosterone is significantly lower in women with POI or abnormal FMR1 genotypes (*68*). The efficiency of androgen conversion from DHEA to testosterone and the amplitude of testosterone gain are related to pregnancy rates. Conversion is usually more pronounced in young women and women with selected FMR1 genotypes/subgenotypes (*69*). DHEA and testosterone also suppressed canavalin A (Con A)-induced proliferation of thymocytes *in vitro*, and DHEA is less potent than testosterone, which means that the balance between the two steroids can alter immune homeostasis (*70*). Testosterone and estradiol levels vary widely after DHEA administration, and the testosterone to estradiol ratio increased significantly in seven healthy nonobese postmenopausal women (*71*).

When steroidogenic enzymes convert DHEA to other steroids, those enzymes have a substantial effect on the immune response. Although women with POI have a poor ovarian follicle pool compared to healthy fertile women, women with POI and steroidogenic cell autoimmunity (SCA-POI), which involves circulating autoantibodies directed against steroidogenic enzymes such as 21-α-hydroxylase, 17-β-hydroxylase, and side-chain cleavage enzyme (P450sccAb) (*72-76*), have a better ovarian reserve than women with iPOI and postmenopausal women. Steroid sulphatase is controlled by an x-linked gene. Women have twice the amount of steroid sulphatase in macrophages. The

macrophages enter peripheral lymphoid organs through afferent lymphatic drainage (*77,78*). IL-4, which is a typical Th2 cytokine, increases the expression of 3-beta-hydroxysteroid dehydrogenase type 2 (HSD3B2) mRNA, and thus may lead to the increased production of estrogen from DHEA (*79*).

3.2. *Balance of the Th1 and Th2 immune response*

Cytokines have an extremely important place in the immune response. They can influence communication between T cells, macrophages, and other immune cells. Numerous studies in mice and humans have deduced the presence of T helper (Th) cells based on the profile of cytokine secretion. The Th1-type immune response is thought to be associated with IgG2a production, which is driven by cytokines such as IFN-γ, IL-2, TNF-α, and IL-12, whereas the Th2-type immune response involves IgE production driven by specific cytokines (IL-4, IL-5, IL-10, and IL-13) (*80,81*). DHEA restores the cell-mediated immune response of pro-inflammatory cytokines (IL-1, IL-6, TNF-α, and IL-18). Mice treated with DHEA exhibited increased production of cytokines such as serum TNF-α, IL-6, IL-12p70, and IFN-γ (*82,83*). DHEA supplementation also increases vascular cell adhesion molecule 1 (VCAM-1) and intercellular cell adhesion molecule 1 (ICAM-1) in the granulosa cell layer of cysts and the theca cell layer of all follicles and cysts when DHEA androgenization induces the formation of cysts (*83*). DHEA may improve ovarian function in women with poor ovarian response by activating anti-apoptotic processes in cumulus cells. These processes most likely involve the upregulation of genes related to extracellular matrix (ECM) formation and downregulating genes related to cell development, differentiation, and apoptosis (*84*). In other areas, DHEA supplementation has been reported to have an effect on regulation of the Th1/Th2 response. In ovalbumin-sensitized asthmatic female mice, Th2-associated cytokines and chemokines were inhibited after DHEA administration, which led to hyper-responsiveness (*85*). DHEA decreased the release of anti-inflammatory cytokines (IL-2 and IL-10, which are also Th2-associated cytokines) and it reduced the expression of the activation marker CD69 on CD4+ T cells (*20*). All of these effects may bring about an enhanced Th1 response and a weakened Th2 response and lead to a new balance in the Th1/Th2 response.

3.3. *Balance between CD4+/CD8+ T cells*

DHEA also improves immune function by regulating the proliferation of and balance between different types of lymphocytes. During the culturing of T lymphocytes from BALB/c mice *in vitro*, DHEA did not change the viability of T lymphocytes, but it did increase oxidative stress by reducing antioxidant molecules, such as glutathione (GSH) (*86*). Burdick *et al*. conducted a study and found that oral administration of DHEAs in young pigs increased *in vitro* lymphocyte proliferation following immunization and that it increased the *in vivo* response of immunization against keyhole limpet haemocyanin (KLH), thus increasing the neutrophil to lymphocyte ratio and increasing the concentration of IgG (*21*). DHEA effects opposite those of cortisol; thus, the cortisol to DHEA ratio may influence the differentiation of T cells. Extrathymic (DP) CD4+/CD8+ T cells positively correlated with circulating levels of TNF-α and with the cortisol/DHEAs ratio (*87*). Flow cytometry showed that DHEA treatment in mice significantly increased the CD4+ lymphocyte population and decreased the CD8+ lymphocyte population, thus modulating the CD4+/CD8+ lymphocyte balance in both ovarian tissue and retroperitoneal lymph nodes (*82*). This may be due to the selective T lymphocyte infiltration of ovarian tissue (*88*).

4. Conclusion

DHEA attenuates diminished ovarian reserve and helps to obtain better results in IVF cycles. DHEA may modulate ovarian immunity through its conversion to other downstream steroids, by balancing the Th1/Th2 immune response, or by modulating the types and behavior of T lymphocytes. The mechanism underlying the immune effects of DHEA on ovarian tissue needs to be studied further.

Acknowledgements

This work was supported by the National Natural Science Foundation of China (Grant No. 31571196; L Wang; Grant No. 81401171; X-M Qiu), the Shanghai Municipal Science and Technology Commission (2015 Science and Technology Project to Guide Medicine Project No. 15401932200; L Wang), the FY2008 JSPS Postdoctoral Fellowship for Foreign Researchers (P08471; L Wang), the National Natural Science Foundation of China (Grant No. 30801502; L Wang), the Shanghai Pujiang Program (No.11PJ1401900; L Wang), the Program for Outstanding Leaders in Medicine (D-J Li), and the Development Project of Shanghai Peak Disciplines-Integrated Chinese and Western Medicine.

References

1. Monniaux D, Clement F, Dalbies-Tran R, Estienne A, Fabre S, Mansanet C, Monget P. The ovarian reserve of primordial follicles and the dynamic reserve of antral growing follicles: What is the link? Biol Reprod. 2014; 90:85.
2. Silva CA, Yamakami LY, Aikawa NE, Araujo DB, Carvalho JF, Bonfa E. Autoimmune primary ovarian insufficiency. Autoimmun Rev. 2014; 13:427-430.

3. Gurtcheff SE, Klein NA. Diminished ovarian reserve and Infertility. Clinical obstetrics and genecology. 2011; 54:666-674.
4. Ubaldi FM, Rienzi L, Ferrero S, Baroni E, Sapienza F, Cobellis L, Greco E. Management of poor responders in IVF. Reprod Biomed Online. 2005; 10:235-246.
5. Karande VC. Managing and predicting low response to standard *in vitro* fertilization therapy: A review of the options. Treat Endocrinol. 2003; 2:257-272.
6. Loutradis D, Vomvolaki E, Drakakis P. Poor responder protocols for in-vitro fertilization: Options and results. Curr Opin Obstet Gynecol. 2008; 20:374-378.
7. Caglar Aytac P, Kilicdag EB, Haydardedeoglu B, Simsek E, Cok T, Parlakgumus HA. Can calcium ionophore "use" in patients with diminished ovarian reserve increase fertilization and pregnancy rates? A randomized, controlled study. Fertil Steril. 2015; 104:1168-1174.
8. Mannic T, Viguie J, Rossier MF. *In vivo* and *in vitro* evidences of dehydroepiandrosterone protective role on the cardiovascular system. Int J Endocrinol Metab. 2015; 13:e24660.
9. Wang L, Hao Q, Wang YD, Wang WJ, Li DJ. Protective effects of dehydroepiandrosterone on atherosclerosis in ovariectomized rabbits *via* alleviating inflammatory injury in endothelial cells. Atherosclerosis. 2011; 214:47-57.
10. Vitlic A, Khanfer R, Lord JM, Carroll D, Phillips AC. Bereavement reduces neutrophil oxidative burst only in older adults: Role of the HPA axis and immunesenescence. Immun Ageing. 2014; 11:13.
11. Starka L, Duskova M, Hill M. Dehydroepiandrosterone: A neuroactive steroid. J Steroid Biochem Mol Biol. 2015; 145:254-260.
12. Casson PR, Lindsay MS, pisarska MD, Carson SA, Buster JE. Dehydroepiandrosterone supplementation augments ovarian stimulation in poor responders: A case series. Hum Reprod. 2000; 15:2129-2132.
13. Narkwichean A, Maalouf W, Campbell BK, jayaprakasan K. Efficacy of dehydroepiandrosterone to improve ovarian response in women with diminished ovarian reserve: A meta-analysis. Reprod Biol Endocrinol. 2013; 11:44.
14. Narkwichean A, Jayaprakasan K, Maalouf WE, Hernandez-Medrano JH, Pincott-Allen C, Campbell BK. Effects of dehydroepiandrosterone on *in vivo* ovine follicular development. Hum Reprod. 2014; 29:146-154.
15. Hassa H, Aydin Y, Ozatik O, Erol K, Ozatik Y. Effects of dehydroepiandrosterone (DHEA) on follicular dynamics in a diminished ovarian reserve *in vivo* model. Syst Biol Reprod Med. 2015; 61:117-121.
16. Hazeldine J, Arlt W, Lord JM. Dehydroepiandrosterone as a regulator of immune cell function. J Steroid Biochem Mol Biol. 2010; 120:127-136.
17. McNelis JC, Manolopoulos KN, Gathercole LL, Bujalska IJ, Stewart PM, Tomlinson JW, Arlt W. Dehydroepiandrosterone exerts antiglucocorticoid action on human preadipocyte proliferation, differentiation, and glucose uptake. Am J Physiol Endocrinol Metab. 2013; 305:E1134-1144.
18. Lazaridis I, Charalampopoulos I, Alexaki VI, Avlonitis N, Pediaditakis I, Efstathopoulos P, Calogeropoulou T, Castanas E, Gravanis A. Neurosteroid dehydroepiandrosterone interacts with nerve growth factor (NGF) receptors, preventing neuronal apoptosis. PLoS Biol. 2011; 9:e1001051.
19. Camporez JP, Akamine EH, Davel AP, Franci CR, Rossoni LV, Carvalho CR. Dehydroepiandrosterone protects against oxidative stress-induced endothelial dysfunction in ovariectomized rats. J Physiol. 2011; 589:2585-2596.
20. Pratschke S, von Dossow-Hanfstingl V, Dietz J, Schneider CP, Tufman A, Albertsmeier M, Winter H, Angele MK. Dehydroepiandrosterone modulates T-cell response after major abdominal surgery. J Surg Res. 2014; 189:117-125.
21. Burdick NC, Dominguez JA, Welsh TH, Jr., Laurenz JC. Oral administration of dehydroepiandrosterone-sulfate (DHEAS) increases *in vitro* lymphocyte function and improves *in vivo* response of pigs to immunization against keyhole limpet hemocyanin (KLH) and ovalbumin. Int Immunopharmacol. 2009; 9:1342-1346.
22. Burger HG. Androgen production in women. Fertil Steril. 2002; 77 (Suppl 4):S3-S5.
Arlt W. Dehydroepiandrosterone and ageing. Best Pract Res Clin Endocrinol Metab. 2004; 18:363-380.
24. Liu CH, Laughlin GA, Fischer UG, Yen SS. Marked attenuation of ultradian and circadian rhythms of dehydroepiandrosterone in postmenopausal women: Evidence for a reduced 17,20-desmolase enzymatic activity. J Clin Endocrinol Metab. 1990; 71:900-906.
25. Orentreich N, Brind JL, Rizer RL, Vogelman JH. Age changes and sex differences in serum dehydroepiandrosterone sulfate concentrations throughout adulthood. J Clin Endocrinol Metab. 1984; 59:551-555.
26. Palmert MR, Hayden DL, Mansfield MJ, Crigler JF, Jr., Crowley WF, Jr., Chandler DW, Boepple PA. The longitudinal study of adrenal maturation during gonadal suppression: Evidence that adrenarche is a gradual process. J Clin Endocrinol Metab. 2001; 86:4536-4542.
27. Reiter EO, Fuldauer VG, Root AW. Secretion of the adrenal androgen, dehydroepiandrosterone sulfate, during normal infancy, childhood, and adolescence, in sick infants, and in children with endocrinologic abnormalities. J Pediatr. 1977; 90:766-770.
28. Arlt W, Callies F, Koehler I, Vlijmen JCV, Fassnacht M, Starsburger CJ, Seibel MJ, Huebler D, Ernst M, Oettel M, Reincke M, Schulte HM, Allolio B. Dehydroepiandrosterone supplementation in healthy men with an age-related decline of dehydroepiandrosterone secretion. J Clin Endocrinol Metab. 2001; 86:4686-4692.
29. Grimley Evans J, Malouf R, Huppert F, van Niekerk JK. Dehydroepiandrosterone (DHEA) supplementation for cognitive function in healthy elderly people (Review). Cochrane Database Syst Rev. 2006; 4:CD006221.
30. Casson PR, Andersen RN, Herrod HG, Stentz FB, Straughn AB, Abraham GE, Buster JE. Oral dehydroepiandrosterone in physiologic doses modulates immune function in postmenopausal women. Am J Obstet Gynecol. 1993; 169:1536-1539.
31. Angele MK, Pratschke S, Hubbard WJ, Chaudry IH. Gender differences in sepsis: Cardiovascular and immunological aspects. Virulence. 2014; 5:12-19.
32. Gleicher N, Weghofer A, Barad DH. Improvement in diminished ovarian reserve after dehydroepiandrosterone supplementation. Reprod Biomed Online. 2010; 21:360-365.
33. Yilmaz N, Uygur D, Inal H, Gorkem U, Cicek N, Mollamahmutoglu L. Dehydroepiandrosterone supplementation improves predictive markers for diminished ovarian reserve: Serum AMH, inhibin B and

antral follicle count. Eur J Obstet Gynecol Reprod Biol. 2013; 169:257-260.
34. Tsui KH, Lin LT, Chang R, Huang BS, Cheng JT, Wang PH. Effects of dehydroepiandrosterone supplementation on women with poor ovarian response: A preliminary report and review. Taiwan J Obstet Gynecol. 2015; 54:131-136.
35. Barad D, Gleicher N. Effect of dehydroepiandrosterone on oocyte and embryo yields, embryo grade and cell number in IVF. Hum Reprod. 2006; 21:2845-2849.
36. Gleicher N, Weghofer A, Barad DH. Dehydroepiandrosterone (DHEA) reduces embryo aneuploidy: direct evidence from preimplantation genetic screening (PGS). Reprod Biol Endocrinol. 2010; 8:140.
37. Gleicher N, Ryan E, Weghofer A, Blanco-Mejia S, Barad DH. Miscarriage rates after dehydroepiandrosterone (DHEA) supplementation in women with diminished ovarian reserve: A case control study. Reprod Biol Endocrinol. 2009; 7:108.
38. Zhang HH, Xu PY, Wu J, Zou WW, Xu XM, Cao XY, Wei LZ. Dehydroepiandrosterone improves follicular fluid bone morphogenetic protein-15 and accumulated embryo score of infertility patients with diminished ovarian reserve undergoing *in vitro* fertilization: A randomized controlled trial. J Ovarian Res. 2014; 7:93.
39. Tartagni M, Cicinelli MV, Baldini D, Tartagni MV, Alrasheed H, DeSalvia MA, Loverro G, Montagnani M. Dehydroepiandrosterone decreases the age-related decline of the *in vitro* fertilization outcome in women younger than 40 years old. Reprod Biol Endocrinol. 2015; 13:18.
40. Poli E, Manfe S, Capuzzo D, Gava S, Vigano F, Coronella ML, Gangemi M. DHEA pre-treated patients, poor responders to a first IVF (ICSI) cycle: Clinical results. Clin Exp Obstet Gynecol. 2014; 41:5-9.
41. Kara M, Aydin T, Aran T, Turktekin N, Ozdemir B. Does dehydroepiandrosterone supplementation really affect IVF-ICSI outcome in women with poor ovarian reserve? Eur J Obstet Gynecol Reprod Biol. 2014; 173:63-65.
42. Barad DH, Weghofer A, Gleicher N. Age-specific levels for basal follicle-stimulating hormone assessment of ovarian function. Obstet Gynecol. 2007; 109:1404-1410.
43. Barad DH, Weghofer A, Gleicher N. Utility of age-specific serum anti-Mullerian hormone concentrations. Reprod Biomed Online. 2011; 22:284-291.
44. Fang T, Su Z, Wang L, Yuan P, Li R, Ouyang N, Zheng L, Wang W. Predictive value of age-specific FSH levels for IVF-ET outcome in women with normal ovarian function. Reprod Biol Endocrinol. 2015; 13:63.
45. McFarlane D, Wolf RF, McDaniel KA, White GL. Age-associated alteration in innate immune response in captive baboons. J Gerontol A Biol Sci Med Sci. 2011; 66:1309-1317.
46. Fagiolo U, Cossarizza A, Scala E, Fanales-Belasio E, Ortolani C, Cozzi E, Monti D, Franceschi C, Paganelli R. Increased cytokine production in mononuclear cells of healthy elderly people. Eur J Immunol. 1993; 23:2375-2378.
47. Franceschi C, Monti D, Sansoni P, Cossarizza A. The immunology of exceptional individuals: The lesson of centenarians. Immunol Today. 1995; 16:12-16.
48. Lio D, Scola L, Crivello A, Colonna-Romano G, Candore G, Bonafe M, Cavallone L, Marchegiani F, Olivieri F, Franceschi C, Caruso C. Inflammation, genetics, and longevity: Further studies on the protective effects in men of IL-10 -1082 promoter SNP and its interaction with TNF-alpha -308 promoter SNP. J Med Genet. 2003; 40:296-299.
49. Giunta S. Exploring the complex relations between inflammation and aging (inflamm-aging): Anti-inflamm-aging remodelling of inflamm-aging, from robustness to frailty. Inflamm Res. 2008; 57:558-563.
50. Butcher SK, Killampalli V, Lascelles D, Wang K, Alpar EK, Lord JM. Raised cortisol:DHEAS ratios in the elderly after injury: Potential impact upon neutrophil function and immunity. Aging Cell. 2005; 4:319-324.
51. Yin FJ, Kang J, Han NN, Ma HT. Effect of dehydroepiandrosterone treatment on hormone levels and antioxidant parameters in aged rats. Genet Mol Res. 2015; 14:11300-11311.
52. Buoso E, Lanni C, Molteni E, Rousset F, Corsini E, Racchi M. Opposing effects of cortisol and dehydroepiandrosterone on the expression of the receptor for Activated C Kinase 1: Implications in immunosenescence. Exp Gerontol. 2011; 46:877-883.
53. Barkhausen T, Hildebrand F, Krettek C, van Griensven M. DHEA-dependent and organ-specific regulation of TNF-α mRNA expression in a murine polymicrobial sepsis and trauma model. Critical Care. 2009; 13:R114.
54. Schmitz D, Kobbe P, Wegner A, Hammes F, Oberbeck R. Dehydroepiandrosterone during sepsis: Does the timing of administration influence the effectiveness. J Surg Res. 2010; 163:e73-77.
55. Frantz MC, Prix NJ, Wichmann MW, van den Engel NK, Hernandez-Richter T, Faist E, Chaudry IH, Jauch K-W, Angele MK. Dehydroepiandrosterone restores depressed peripheral blood mononuclear cell function following major abdominal surgery *via* the estrogen receptors. Critical Care Medicine. 2005; 33:1779-1786.
56. Vinatier D, Dufour P, Tordjeman-Rizzi N, Prolongeau JF, Depret-Moser S, Monnier JC. Immunological aspects of ovarian function: Role of the cytokines. Eur J Obstet Gynecol Reprod Biol. 1995; 63:155-168.
57. Chryssikopoulos A. The relationship between the immune and endocrine systems. Ann N Y Acad Sci. 1997; 816:83-93.
58. Pate JL. Involvement of immune cells in regulation of ovarian function. J Reprod Fertil Suppl. 1995; 49:365-377.
59. Bukovsky A, Caudle MR, Carson RJ, Gaytán F, Huleihel M, Kruse A, Schatten H, Telleria CM. Immune physiology in tissue regeneration and aging, tumor growth, and regenerative medicine. Aging (Albany NY). 2009; 1:157-181.
60. Gleicher N, Weghofer A, Barad DH. Cutting edge assessment of the impact of autoimmunity on female reproductive success. J Autoimmun. 2012; 38:J74-J80.
61. Cervera R, Balasch J. Bidirectional effects on autoimmunity and reproduction. Hum Reprod Update. 2008; 14:359-366.
62. Carp HJ, Selmi C, Shoenfeld Y. The autoimmune bases of infertility and pregnancy loss. J Autoimmun. 2012; 38:J266-274.
63. Gleicher N, Weghofer A, Kushnir VA, Shohat-Tal A, Lazzaroni E, Lee HJ, Barad DH. Is androgen production in association with immune system activation potential evidence for existence of a functional adrenal/ovarian autoimmune system in women? Reprod Biol Endocrinol. 2013; 11:58.
64. Gleicher N, Weghofer A, Oktay K, Barad DH. Is the

immunological noise of abnormal autoimmunity an independent risk factor for premature ovarian aging? Menopause. 2009; 16:760-764.
65. Gleicher N, Weghofer A, Barad DH. A pilot study of premature ovarian senescence: II. Different genotype and phenotype for genetic and autoimmune etiologies. Fertil Steril. 2009; 91:1707-1711.
66. Giron-Gonzalez JA, Moral FJ, Elvira J, Garcia-Gil D, Guerrero F, Gavilan I, Escobar L. Consistent production of a higher TH1:TH2 cytokine ratio by stimulated T cells in men compared with women. Eur J Endocrinol. 2000; 143:31-36.
67. Weghofer A, Kim A, Barad DH, Gleicher N. The impact of androgen metabolism and FMR1 genotypes on pregnancy potential in women with dehydroepiandrosterone (DHEA) supplementation. Hum Reprod. 2012; 27:3287-3293.
68. Gleicher N, Kim A, Weghofer A, Kushnir VA, Shohat-Tal A, Lazzaroni E, Lee HJ, Barad DH. Hypoandrogenism in association with diminished functional ovarian reserve. Hum Reprod. 2013; 28:1084-1091.
69. Gleicher N, Kim A, Weghofer A, Shohat-Tal A, Lazzaroni E, Lee HJ, Barad DH. Starting and resulting testosterone levels after androgen supplementation determine at all ages *in vitro* fertilization (IVF) pregnancy rates in women with diminished ovarian reserve (DOR). J Assist Reprod Genet. 2013; 30:49-62.
70. Yao G, Shang XJ. A comparison of modulation of proliferation of thymocyte by testosterone, dehydroisoandrosterone and androstenedione *in vitro*. Arch Androl. 2005; 51:257-265.
71. Caufriez A, Leproult R, L'Hermite-Baleriaux M, Kerkhofs M, Copinschi G. Effects of a 3-week dehydroepiandrosterone administration on sleep, sex steroids and multiple 24-h hormonal profiles in postmenopausal women: A pilot study. Clin Endocrinol (Oxf). 2013; 79:716-724.
72. Hoek A, Schoemaker J, Drexhage HA. Premature ovarian failure and ovarian autoimmunity. Endocr Rev. 1997; 18:107-134.
73. Bakalov VK, Anasti JN, Calis KA, Vanderhoof VH, Premkumar A, Chen S, Furmaniak J, Smith BR, Merino MJ, Nelson LM. Autoimmune oophoritis as a mechanism of follicular dysfunction in women with 46,XX spontaneous premature ovarian failure. Fertil Steril. 2005; 84:958-965.
74. Chen S, Sawicka J, Betterle C, Powell M, Prentice L, Volpato M, Rees Smith B, Furmaniak J. Autoantibodies to steroidogenic enzymes in autoimmune polyglandular syndrome, Addison's disease, and premature ovarian failure. J Clin Endocrinol Metab. 1996; 81:1871-1876.
75. Betterle C, Dal Pra C, Mantero F, Zanchetta R. Autoimmune adrenal insufficiency and autoimmune polyendocrine syndromes: Autoantibodies, autoantigens, and their applicability in diagnosis and disease prediction. Endocr Rev. 2002; 23:327-364.
76. Falorni A, Laureti S, Candeloro P, Perrino S, Coronella C, Bizzarro A, Bellastella A, Santeusanio F, De Bellis A. Steroid-cell autoantibodies are preferentially expressed in women with premature ovarian failure who have adrenal autoimmunity. Fertil Steril. 2002; 78:270-279.
77. Daynes RA, Araneo BA, Dowell TA, Huang K, Dudley D. Regulation of murine lymphokine production *in vivo*. III. The lymphoid tissue microenvironment exerts regulatory influences over T helper cell function. J Exp Med. 1990; 171:979-996.
78. Namazi MR. Hypothesis: Paradoxical absence of cellular immuno-deficiency in X-linked recessive ichthyosis and its explanation. J Dermatol Sci. 2003; 32:166-167.
79. Urata Y, Osuga Y, Akiyama I, Nagai M, Izumi G, Takamura M, Hasegawa A, Harada M, Hirata T, Hirota Y, Yoshino O, Koga K, Kozuma S. Interleukin-4 and prostaglandin E2 synergistically up-regulate 3beta-hydroxysteroid dehydrogenase type 2 in endometrioma stromal cells. J Clin Endocrinol Metab. 2013; 98:1583-1590.
80. Belardelli F. Role of interferons and other cytokines in the regulation of the immune response. APMIS. 1995; 103:161-179.
81. Kasakura S. A role for T-helper type 1 and type 2 cytokines in the pathogenesis of various human diseases. Rinsho Byori. 1998; 46:915-921.
82. Sander V, Luchetti CG, Solano ME, Elia E, Di Girolamo G, Gonzalez C, Motta AB. Role of the N, N'-dimethylbiguanide metformin in the treatment of female prepuberal BALB/c mice hyperandrogenized with dehydroepiandrosterone. Reproduction. 2006; 131:591-602.
83. Solano ME, Sander VA, Ho H, Motta AB, Arck PC. Systemic inflammation, cellular influx and up-regulation of ovarian VCAM-1 expression in a mouse model of polycystic ovary syndrome (PCOS). J Reprod Immunol. 2011; 92:33-44.
84. Tsui KH, Lin LT, Horng HC, Chang R, Huang BS, Cheng JT, Wang PH. Gene expression of cumulus cells in women with poor ovarian response after dehydroepiandrosterone supplementation. Taiwan J Obstet Gynecol. 2014; 53:559-565.
85. Liou CJ, Huang WC. Dehydroepiandrosterone suppresses eosinophil infiltration and airway hyperresponsiveness *via* modulation of chemokines and Th2 cytokines in ovalbumin-sensitized mice. J Clin Immunol. 2011; 31:656-665.
86. Solano ME, Sander V, Wald MR, Motta AB. Dehydroepiandrosterone and metformin regulate proliferation of murine T lymphocytes. Clin Exp Immunol. 2008; 153:289-296.
87. Perez AR, Morrot A, Berbert LR, Terra-Granado E, Savino W. Extrathymic CD4+CD8+ lymphocytes in Chagas disease: Possible relationship with an immunoendocrine imbalance. Ann N Y Acad Sci. 2012; 1262:27-36.
88. Luchetti CG, Solano ME, Sander V, Arcos ML, Gonzalez C, Di Girolamo G, Chiocchio S, Cremaschi G, Motta AB. Effects of dehydroepiandrosterone on ovarian cystogenesis and immune function. J Reprod Immunol. 2004; 64:59-74.
89. Weissman A, Horowitz E, Ravhon A, Golan A, Levran D. Dehydroepiandrosterone supplementation increases baseline follicular phase progesterone levels. Gynecol Endocrinol. 2011; 27:1014-1017.

(Received November 16, 2015; Revised December 17, 2015; Accepted December 27, 2015)

Original Article

DOI: 10.5582/bst.2015.01134

Polyphosphate-induced matrix metalloproteinase-3-mediated differentiation in rat dental pulp fibroblast-like cells

Taiki Hiyama[1], Nobuaki Ozeki[1,*], Naoko Hase[1], Hideyuki Yamaguchi[1], Rie Kawai[1], Ayami Kondo[2], Makio Mogi[2], Kazuhiko Nakata[1]

[1] *Department of Endodontics, School of Dentistry, Aichi Gakuin University, Nagoya, Aichi, Japan;*
[2] *Department of Medicinal Biochemistry, School of Pharmacy, Aichi Gakuin University, Nagoya, Aichi, Japan.*

Summary **Inorganic polyphosphate [Poly(P)] induces differentiation of osteoblastic cells. In this study, matrix metalloproteinase (MMP)-3 small interfering RNA (siRNA) was transfected into purified rat dental pulp fibroblast-like cells (DPFCs) to investigate whether MMP-3 activity induced by Poly(P) is associated with cell differentiation into osteogenic cells. Real-time quantitative polymerase chain reaction, western blotting, and an MMP-3 activity assay were used in this study. Poly(P) enhanced expression of mature odontoblast markers dentin sialophosphoprotein (DSPP) and dentin matrix protein (DMP)-1 in DPFCs. These cells also developed an osteogenic phenotype with increased expression of osteocalcin (OC) and osteopontin (OP), high alkaline phosphatase (ALP) activity, and an increased calcification capacity. Poly(P) induced the expression of MMP-3 mRNA and protein, and increased MMP-3 activity. MMP-3 siRNA potently suppressed the expression of osteogenic biomarkers ALP, OC, OP, DSPP, and DMP-1, and blocked osteogenic calcification. Taken together, Poly(P)-induced MMP-3 regulates differentiation of osteogenic cells from DPFCs.**

Keywords: Dental pulp, osteogenic cells, dentin sialophosphoprotein, dentin matrix protein-1

1. Introduction

Inorganic polyphosphate [Poly(P)] is a linear polymer consisting of tens to hundreds of orthophosphate residues linked by high-energy phosphoanhydride bonds. In mammals, Poly(P) is found in erythrocytes and cells of the brain, heart, lung, and liver (*1-4*). The most researched and well-known role of Poly(P) is in the promotion of intracellular calcification (*5*). Because Poly(P) induces alkaline phosphate (ALP) activity and up-regulates osteopontin (OP) and osteocalcin (OC) gene expression (*6*), Poly(P) is thought to play an important role in the maturation of bone-related immature cells, and may be involved in the construction of bone tissue by osteoblasts.

In addition to blood vessels and nerves, fibroblasts are a significant component of dental pulp tissue (*7*) and thus might represent a novel therapeutic target for treating pulpitis. However, the effect of Poly(P) regulation of differentiation on dental pulp fibroblast-like cells (DPFCs) has not been well defined.

Matrix metalloproteinase (MMP)-3 and interstitial collagenase (MMP-1) are produced by fibroblasts in response to increased levels of inflammatory cytokines in dental pulp injury and diseases such as periodontitis and rheumatoid arthritis (*8,9*). MMP-3 has been implicated in the joint and soft-tissue destruction associated with these conditions, where it participates in the inflammatory response (*10-14*). MMP-3 synthesis is tightly controlled *in vivo* (*13,15*). Our previous study reported that proinflammatory cytokine-induced MMP-3 actually accelerates wound healing following dental pulp injury (*16-18*) and promotes cell proliferation (*17,19,20*).

Recently, roles of Poly(P) have been suggested in apoptosis and modulation of the mineralization process in bone tissue (*21,22*). We previously reported that Poly(P) induces MMP-3-mediated proliferation of odontoblast-like cells derived from induced pluripotent stem cells (*23*). Although we previously reported that

*Address correspondence to:
Dr. Nobuaki Ozeki, Department of Endodontics, School of Dentistry, Aichi Gakuin University, 2-11 Suemori-dori, Chikusa-ku, Nagoya, Aichi 464-8651, Japan.
E-mail: ozeki@g.ag.ac.jp

Poly(P)-induced MMP-3-mediated proliferation of rat DPFCs is mediated by a Wnt5 signaling cascade (*24*), it is unknown whether Poly(P) is associated with differentiation. Therefore, we investigated the physiological effect of Poly(P) on DPFC differentiation *in vitro*. We reveal a novel role of Poly(P) in the regulation of MMP-3 activity during the differentiation of osteogenic cells from DPFCs.

2. Materials and Methods

2.1. *Materials*

Type-65 Poly(P) with an average chain length of 65 phosphate residues was prepared from sodium tripolyphosphate (Taihei Chemical Industrial Co., Ltd., Osaka, Japan). Concentrations of Poly(P) are shown in terms of phosphate residues (*25*). As a control, sodium phosphate buffer (pH 6.9) was used instead of Poly(P).

2.2. *Cell culture*

The study protocol (No. 63) was reviewed and approved by the Animal Experimentation Committee, School of Dentistry, Aichi Gakuin University, Japan. DPFCs were isolated from rat incisors and cultured using a previously described protocol (*20*). The proportion of platelet-derived growth factor receptor (PDGFR)-α positive cells in the total fibroblast-like cell population is a measure of the purity of DPFCs (*24*). Therefore, using flow cytometry, we evaluated the ratio of PDGFR-α-positive cells as a percentage of the total differentiated cells to determine the purity of the differentiated cell population. Our DPFC cultures showed 98.64 ± 5.2% homogeneity (% total, $n = 3$). In all experiments, DPFCs were used at passages 2-5. Cells were seeded into six-well tissue culture plates at a density of 1×10^5 cells/cm^2. To expose the cells to Poly(P), the culture medium was replaced with alpha-minimal essential medium containing 10% fetal bovine serum and Poly(P), followed by 7 days of culture.

2.3. *Functional assay for assessment of the osteogenic phenotype*

To assess the phenotype of the cultured cells, we measured ALP activity and calcification (as a marker of differentiation). ALP activity was determined using an ALP Staining Kit (Primary Cell Co., Ltd., Hokkaido, Japan). Mineralization from the Poly(P)-treated cells was quantified using an Alizarin red S (ARS) assay (Sigma-Aldrich, St. Louis, MO, USA). ARS staining was quantified using a previously reported method (*26*) and photographed using a BZ-9000 microscope (Keyence, Osaka, Japan) and/or an IN Cell Analyzer 2000 (GE Healthcare UK Ltd, Buckinghamshire, England).

2.4. *Real-time quantitative polymerase chain reaction (qRT-PCR) analysis*

qRT-PCR was performed for all samples and standards in triplicate with approximately 25 ng RNA, 0.25 mL Quantitect RT Mix (Qiagen Inc., Valencia, CA, USA), and 1.25 mL of 20× Primer/Probe Mix (rat ALP [*ALPL*]: Rn00575319_g1; rat OC [*BGLAP*]: Rn00566386_g1; rat OP [*SPP1*]: Rn01449972_m1; rat DSPP [*DSPP*]: Rn02132391_s1; rat DMP-1 [*DMP-1*]: Rn01450120_m1; rat *MMP-3*: Rn00591740_m1; human *MMP-1* (rat available): Hs00899658_m1; rat *MMP-2*: Rn01538170_m1; rat *MMP-9*: Rn00579162_m1; rat *MMP-13*: Rn01448194_m1). The standard curve method was used to determine the relative quantification of gene expression with glyceraldehyde-3-phosphate dehydrogenase (GAPDH) and 18S rRNA as controls. Analysis was performed by the delta-delta Ct method.

2.5. *Western blot analysis*

Cells were cultured for 6 h with or without Poly(P) and then lysed using cell lysis buffer (Cell Signaling Technology Japan, K.K., Tokyo, Japan). Protein lysates were separated on SDS-polyacrylamide gels (12%) in preparation for western blot analysis using anti-ALP, -OC, -OP, -MMP-3, -DMP-1, and -β-tubulin polyclonal antibodies (sc-271431, sc-30044, sc-10593, sc-6839, sc-5538, sc-13595, sc-6840, sc-30073, and sc-9935, respectively; Santa Cruz Biotechnology, Inc., Santa Cruz, CA, USA). Visualization of blotted protein bands was performed using a Multi Gauge-Ver3.X (Fujifilm, Tokyo, Japan).

2.6. *Measurement of MMP-3 activity*

The protocol for measurement of MMP-3 activity has been described previously (*27,28*) and is now a commercially available MMP-3 activity assay kit (SensoLyte™ 520 MMP-3 assay kit; AnaSpec, San Jose, CA, USA).

2.7. *Silencing of the MMP-3 gene by small interfering RNA (siRNA) transfection*

Commercially available MMP-3 siRNA (sc-61874, Santa Cruz Biotechnology, Inc.) was transfected into cultured cells using an siRNA reagent system (sc-45064, Santa Cruz Biotechnology, Inc.) according to the manufacturer's protocol. GAPDH siRNA and a control siRNA without known homology to any vertebrate sequence (Thermo Scientific, Lafayette, CO, USA) were used as positive and negative controls, respectively.

2.8. *Statistical analysis*

Data presented in bar graphs are the means ± standard

deviation (S.D.) of four to six independent experiments. Statistical significance was assessed using the Mann-Whitney *U*-test. A *p*-value of < 0.05 was considered statistically significant.

3. Results

3.1. *Poly(P) induces osteogenic differentiation of DPFCs*

We previously analyzed the effect of Poly(P) on cell proliferation of DPFCs, and found that 0.1 mM Poly(P) is an optimal concentration to enhance the cell growth, whereas > 0.2 mM Poly(P) results in potent inhibition of cell proliferation (*24*).

To examine whether Poly(P) induced osteogenic characteristics in DPFCs, the cells were cultured in the presence of 0.1 mM Poly(P) for 7 days. Both qRT-PCR and western blotting revealed higher expression of osteogenic differentiation markers *ALPL*(ALP), *BGLAP*(OC), *SPP1*(OP), *DSPP*, and *DMP-1* (Figure 1A-a, b).

The majority of Poly(P)-treated DPFCs showed strong ALP expression, whereas control cells had undetectable ALP expression (Figure 1B-b). Extensive deposits of calcified matrix were observed in Poly(P)-treated DPFC cultures, whereas calcified matrix was not apparent in control cell cultures (Figure 1C-b). Consistently, Poly(P) treatment induced a marked increase in ARS signals (Figure 1C-a, b). Taken together, Poly(P) induced osteogenic cells from DPFCs.

3.2. *Poly(P) induces expression of MMP-3 mRNA and MMP-3 activity in DPFCs*

MMP-3 induction by 0.1 mM Poly(P) was assessed using qRT-PCR to measure changes in MMP-3 mRNA expression. The levels of MMP-3 mRNA expression in Poly(P)-treated cells were significantly increased ($p < 0.05$) at days 3, 5, and 7 of culture (Figure 2A). Furthermore, MMP-3 activity was significantly increased ($p < 0.01$) at days 3, 5, and 7 following treatment of DPFCs with Poly(P) for 24 h (Figure 2C).

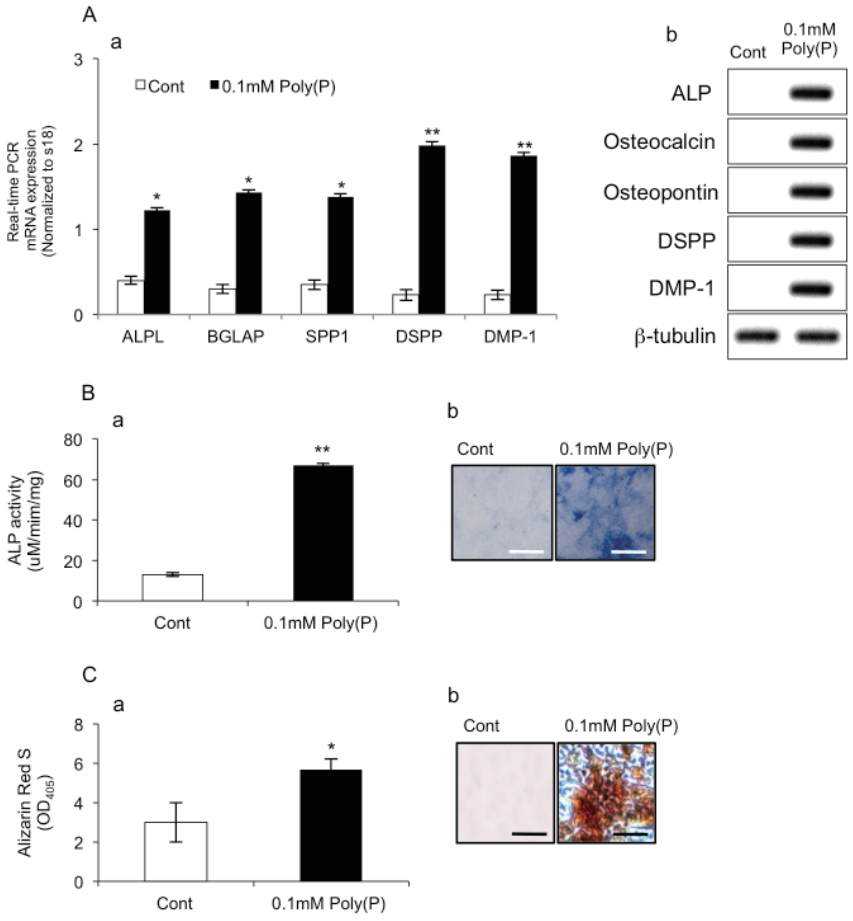

Figure 1. Expression of differentiation markers during osteogenic differentiation induced by Poly(P). (A-a) DPFCs were treated with Poly(P for 7 days. Expression of osteogenic differentiation markers was assessed by qRT-PCR, including ALPL, BGLAP, SPP1, DSPP, and DMP-1. (*$p < 0.05$, **$p < 0.01$ *vs*. control). Data are presented as means ± S.D. and are representative of at least three independent experiments. Similar changes in the protein expression levels of these markers were observed in western blot analyses **(A-b)**. ALP activity was measured in DPFCs treated with or without Poly(P). **(B-a,b)** ALP activity was measured by absorbance at 405 nm and normalized against total protein (**$p < 0.01$ *vs*. control). Scale bar: 100 μm. **(C-a,b)** ARS staining of DPFCs treated with Poly(P) (*$p < 0.05$ *vs*. control). Scale bar: 100 μm.

Bone-associated cells also express other MMP proteins including MMP-1, MMP-2, MMP-9, and MMP-13 (*29-31*). However, we found no significant changes in their expression levels in DPFCs treated with 0.1 mM Poly(P) (Figure 2B).

MMP-3 activity is precisely regulated at the post-translational level as a precursor zymogen and by endogenous tissue inhibitors of metalloproteinases (TIMPs) (*32*). Although TIMP-2 and TIMP-3 are known to be induced by cytokines (*32*), we found that TIMP-1, TIMP-2, and TIMP-3 proteins were constitutively expressed in all experimental conditions (data not shown).

3.3. *siRNA silencing of MMP-3 blocks osteogenic differentiation*

To examine whether the up-regulation of MMP-3 expression was associated with osteogenic differentiation, DPFCs were transfected with MMP-3 siRNA or a control scrambled siRNA, and then treated with Poly(P) as described above. Transfection of MMP-3 siRNA abrogated the induction of osteogenic differentiation markers ALPL, BGLAP, SPP1, DSPP, and DMP-1 ($p < 0.05$, Figure 3A). Similar changes in the protein levels of each marker were observed in western blot analyses (Figure 3B). Furthermore, MMP-3 siRNA blocked

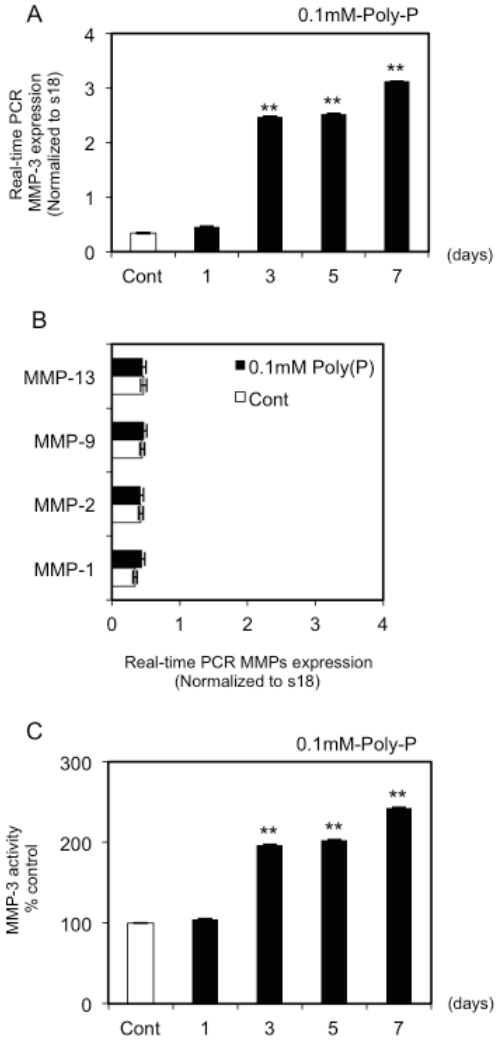

Figure 2. Evaluation of Poly(P)-induced MMP-3 mRNA expression and MMP-3 activity in DPFCs. (A) qRT-PCR analysis of Poly(P)-induced MMP-3 mRNA in DPFCs at 24 h. **(B)** Expression of other MMP mRNAs and proteins in DPFCs. DPFCs were treated with 0.1 mM Poly(P) prior to qRT-PCR analysis of MMP-1, MMP-2, MMP-9, and MMP-13 mRNA expression compared with the control (18S rRNA). Data are the means ± S.D. of four independent experiments. **(C)** Measurement of active MMP-3 released from cultured DPFCs following treatment with 0.1 mM Poly(P). Cells were incubated in serum-free medium in the absence or presence of 0.1 mM Poly(P) for 24 h. Data are the means ± S.D. of at least three independent experiments (**$p < 0.01$).

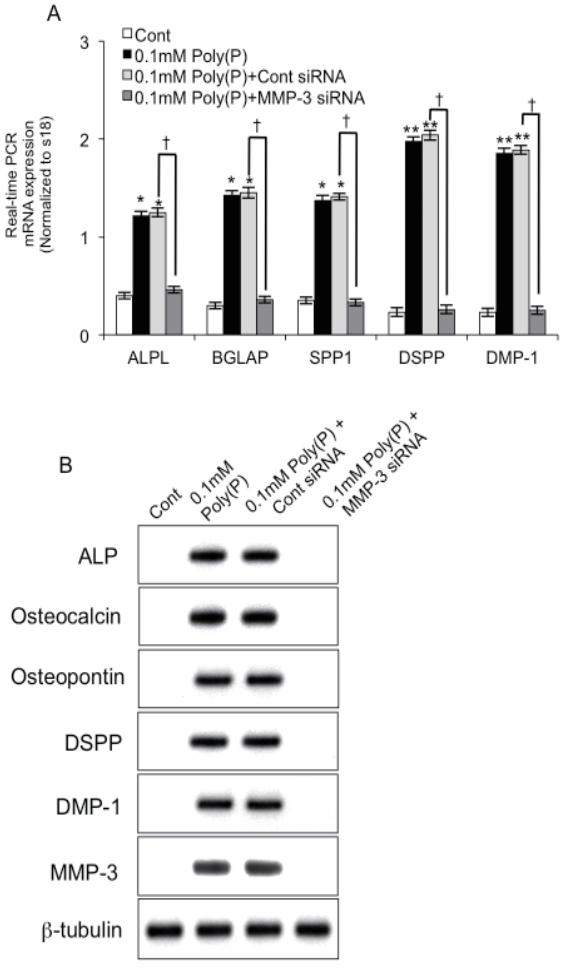

Figure 3. Effect of siRNA silencing on induction of osteogenic markers. (A) The expression of osteogenic marker mRNAs (ALPL, BGLAP, SPP1, DSPP, and DMP-1) in Poly(P)-treated DPFCs was assessed by qRT-PCR following culture in the presence of MMP-3 siRNA. **(B)** Western blot analysis of osteogenic marker protein expression in these cells at 24 h after siRNA transfection. Poly(P)-treated DPFCs were treated with MMP-3 siRNA, and then expression of ALP, OC, OP, DSPP, DMP-1, and MMP-3 proteins was measured. No significant cross-reactivity with other proteins was observed for the antibodies used in the analyses. Images are representative of at least three independent experiments.

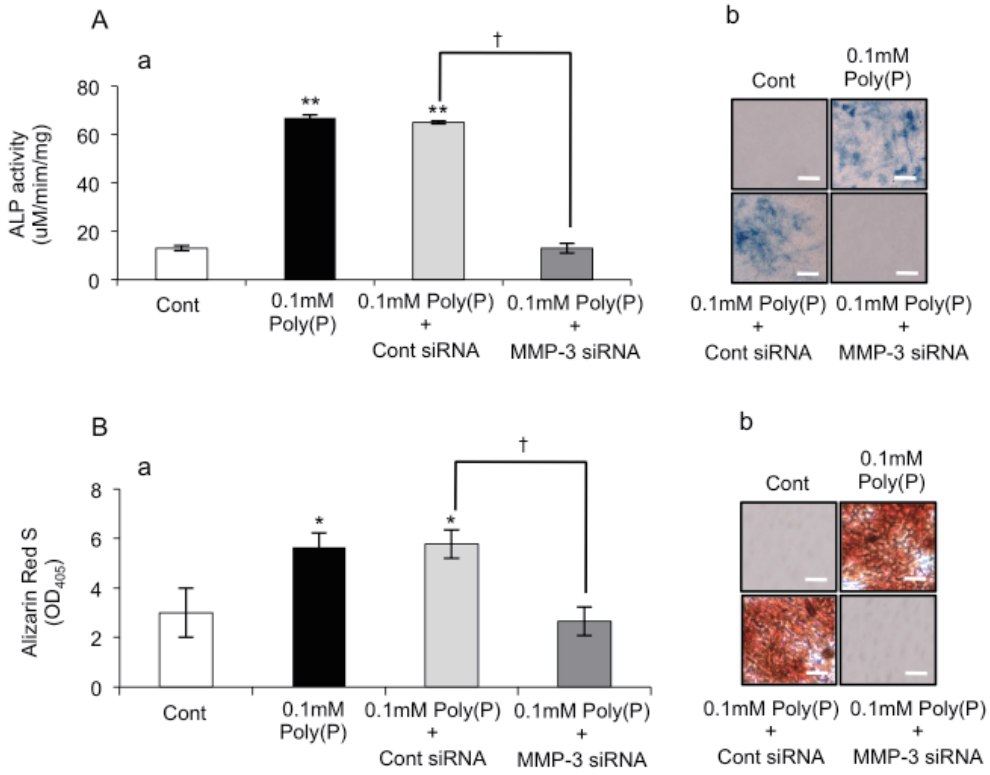

Figure 4. siRNA silencing of MMP-3 blocks osteogenic differentiation. (A-a,b) Effect of MMP-3 siRNA on the functional activities of DPFCs. ALP activity was measured in control and MMP-3-depleted DPFCs treated with 0.1 mM Poly(P). Data are presented as the means ± S.D. ($n = 4$) normalized against total protein, (**$p < 0.01$ *vs*. control; †$p < 0.05$ as indicated). Scale bar: 100 μm. **(B-a,b)** Effect of MMP-3 siRNA on the mineralization capacity of DPCs. Cells were prepared and cell mineralization was assessed by ARS staining with quantification performed by measuring absorbance at 405 nm. Data are the means ± S.D. ($n = 4$). *$p < 0.05$ *vs*. control; †$p < 0.05$ as indicated. Scale bar: 100 μm.

induction of ALP activity in Poly(P)-treated cells ($p < 0.01$, Figure 4A-a, b). Similarly, the induction of calcification was markedly suppressed ($p < 0.05$) by Poly(P) treatment of MMP-3-depleted cells (Figure 4B-a, b). Collectively, these data show that expression of MMP-3 is required for osteogenic-specific functions in DPFCs.

4. Discussion

This study indicated that Poly(P)-treated DPFCs can be a novel *in vitro* model of dental pulp regeneration. Poly(P) at a concentration of 0.1 mM induced MMP-3 expression in DPFCs (Figure 2A) and led to enhanced DPFC differentiation into osteogenic cells (Figure 1A–C), although we were unable to precisely determine how many DPFCs had differentiated. However, phenotypic characterization based on calcification and the levels of ALPL (ALP), BGLAP (OC), SPP1 (OP), DSPP, and DMP-1 suggested that a large proportion of the DPFC population differentiated into osteogenic cells (Figure 1A-a, b).

We have previously demonstrated that the inflammatory cytokine interleukin-1β or a cytokine mixture induces MMP-3-regulated cell proliferation and suppresses apoptosis in rat DPFCs (*19,20*). Moreover, we previously reported that Poly(P)-induced, MMP-3-mediated proliferation in rat DPFCs is mediated by a Wnt5 signaling cascade (*24*). Because we had no definite data on Poly(P)-induced MMP-3 in terms of IGF-1/PI3K/Akt and MAPK signaling pathways (*33,34*) in osteogenic differentiation, it remains to be shown. This study is the first report of Poly(P)-induced, MMP-3-mediated responses in the differentiation of DPFCs. Considering the effect of MMP-3 on osteogenic cell differentiation, the present findings suggest that targeting the *MMP-3* gene in these osteogenic cells may have a utility in the treatment of suppurative pulpitis. Additionally, Poly(P)-treated DPFCs could serve as an effective model to explore the pathophysiological mechanisms of wound healing. Furthermore, our current evidence suggests that Poly(P)-induced MMP-3 has previously unrecognized physiological functions in wound healing and dental pulp tissue regeneration.

We showed that Poly(P)-induced cells acquired osteogenic-specific functions following differentiation from DPFCs. Poly(P)-treated DPFCs appeared to be predominantly odontoblasts and osteoblasts. A major concern is that we were unable to identify the differentiated cells as odontoblasts because these cells also expressed specific osteoblastic markers including OC and OP. We speculate that DPFCs contain a small population of dental pulp stem cells. Therefore,

osteogenic cells may be predominantly derived from dental pulp stem cells, which remains to be elucidated.

The findings presented here support our previous reports (*19,20*) and indicate that MMP-3 may have a previously unrecognized physiological function in wound healing and tissue regeneration. Because Poly(P) induces MMP-3-regulated DPFC differentiation into osteogenic cells, the use of Poly(P) represents a potentially superior therapeutic approach for treatment of dental pulp injury instead of applying pulp-capping materials.

Acknowledgements

This work was supported by a Grant-in-Aid for Scientific Research (A) (Grant No. 25253101 to SY), a Grant-in-Aid-for Scientific Research (C) (Grant No. 26462905 to KN), a Grant-in-Aid-for Scientific Research (C) (Grant No. 26462904 to NO), and a Grant-in-Aid-for Young Scientists (B) (Grant No. 15K20418 to NH) from the Ministry of Education, Culture, Sports, Science and Technology of Japan.

References

1. Kornberg A, Rao NN, Ault-Riche D. Inorganic polyphosphate: A molecule of many functions. Annu Rev Biochem. 1999; 68:89-125.
2. Kumble KD, Kornberg A. Inorganic polyphosphate in mammalian cells and tissues. J Biol Chem. 1995; 270:5818-5822.
3. Leyhausen G, Lorenz B, Zhu H, Geurtsen W, Bohnensack R, Muller WE, Schroder HC. Inorganic polyphosphate in human osteoblast-like cells. J Bone Miner Res. 1998; 13:803-812.
4. Schroder HC, Kurz L, Muller WE, Lorenz B. Polyphosphate in bone. Biochemistry (Mosc). 2000; 65:296-303.
5. Shiba T, Nishimura D, Kawazoe Y, Onodera Y, Tsutsumi K, Nakamura R, Ohshiro M. Modulation of mitogenic activity of fibroblast growth factors by inorganic polyphosphate. J Biol Chem. 2003; 278:26788-26792.
6. Kawazoe Y, Shiba T, Nakamura R, Mizuno A, Tsutsumi K, Uematsu T, Yamaoka M, Shindoh M, Kohgo T. Induction of calcification in MC3T3-E1 cells by inorganic polyphosphate. J Dent Res. 2004; 83:613-618.
7. Teles JC. [Study on the dentin-pulp complex]. Rev Bras Odontol. 1967; 25:305-310.
8. Birkedal-Hansen H. Role of matrix metalloproteinases in human periodontal diseases. J Periodontol. 1993; 64:474-484.
9. Paula-Silva FW, da Silva LA, Kapila YL. Matrix metalloproteinase expression in teeth with apical periodontitis is differentially modulated by the modality of root canal treatment. J Endod. 2010; 36:231-237.
10. Araujo AA, Souza TO, Moura LM, Brito GA, Aragao KS, Araujo LS, Medeiros CA, Alves MS, Araujo RF, Jr. Effect of telmisartan on levels of IL-1, TNF-alpha, down-regulated COX-2, MMP-2, MMP-9 and RANKL/RANK in an experimental periodontitis model. J Clin Periodontol. 2013; 40:1104-1111.
11. de Araujo Junior RF, Souza TO, de Medeiros CA, de Souza LB, Freitas Mde L, de Lucena HF, do Socorro Costa Feitosa Alves M, de Araujo AA. Carvedilol decrease IL-1beta and TNF-alpha, inhibits MMP-2, MMP-9, COX-2, and RANKL expression, and up-regulates OPG in a rat model of periodontitis. PLoS One. 2013; 8:e66391.
12. Emingil G, Han B, Gurkan A, Berdeli A, Tervahartiala T, Salo T, Pussinen PJ, Kose T, Atilla G, Sorsa T. Matrix metalloproteinase (MMP)-8 and tissue inhibitor of MMP-1 (TIMP-1) gene polymorphisms in generalized aggressive periodontitis: Gingival crevicular fluid MMP-8 and TIMP-1 levels and outcome of periodontal therapy. J Periodontol. 2014; 85:1070-1080.
13. Tian J, Chen JW, Gao JS, Li L, Xie X. Resveratrol inhibits TNF-alpha-induced IL-1beta, MMP-3 production in human rheumatoid arthritis fibroblast-like synoviocytes *via* modulation of PI3kinase/Akt pathway. Rheumatol Int. 2013; 33:1829-1835.
14. Tseng WY, Huang YS, Chiang NY, Chou YP, Wu YJ, Luo SF, Kuo CF, Lin KM, Lin HH. Increased soluble CD4 in serum of rheumatoid arthritis patients is generated by matrix metalloproteinase (MMP)-like proteinases. PLoS One. 2013; 8:e63963.
15. Azuma Y, Kosaka K, Kashimata M. Phospholipase D-dependent and -independent p38MAPK activation pathways are required for superoxide production and chemotactic induction, respectively, in rat neutrophils stimulated by fMLP. Eur J Pharmacol. 2007; 568:260-268.
16. Eba H, Murasawa Y, Iohara K, Isogai Z, Nakamura H, Nakamura H, Nakashima M. The anti-inflammatory effects of matrix metalloproteinase-3 on irreversible pulpitis of mature erupted teeth. PLoS One. 2012; 7:e52523.
17. Hiyama T, Ozeki N, Mogi M, Yamaguchi H, Kawai R, Nakata K, Kondo A, Nakamura H. Matrix metalloproteinase-3 in odontoblastic cells derived from ips cells: Unique proliferation response as odontoblastic cells derived from ES cells. PLoS One. 2013; 8:e83563.
18. Zheng L, Amano K, Iohara K, Ito M, Imabayashi K, Into T, Matsushita K, Nakamura H, Nakashima M. Matrix metalloproteinase-3 accelerates wound healing following dental pulp injury. Am J Pathol. 2009; 175:1905-1914.
19. Ozeki N, Yamaguchi H, Hiyama T, Kawai R, Nakata K, Mogi M, Nakamura H. IL-1beta-induced matrix metalloproteinase-3 regulates cell proliferation in rat dental pulp cells. Oral Dis. 2015; 21:97-105.
20. Yamaguchi H, Ozeki N, Kawai R, Tanaka T, Hiyama T, Nakata K, Mogi M, Nakamura H. Proinflammatory cytokines induce stromelysin-1-mediated cell proliferation in dental pulp fibroblast-like cells. J Endod. 2014; 40:89-94.
21. Kawano MM. Inorganic polyphosphate induces apoptosis specifically in human plasma cells. Haematologica. 2006; 91:1154A.
22. Orriss IR, Key ML, Brandao-Burch A, Patel JJ, Burnstock G, Arnett TR. The regulation of osteoblast function and bone mineralisation by extracellular nucleotides: The role of p2x receptors. Bone. 2012; 51:389-400.
23. Ozeki N, Hase N, Yamaguchi H, Hiyama T, Kawai R, Kondo A, Nakata K, Mogi M. Polyphosphate induces matrix metalloproteinase-3-mediated proliferation of odontoblast-like cells derived from induced pluripotent

stem cells. Exp Cell Res. 2015; 333:303-315.
24. Ozeki N, Yamaguchi H, Hase N, Hiyama T, Kawai R, Kondo A, Nakata K, Mogi M. Polyphosphate-induced matrix metalloproteinase-3-mediated proliferation in rat dental pulp fibroblast-like cells is mediated by a Wnt5 signaling cascade. Biosci Trends. 2015; 9:160-168.
25. Tsutsumi K, Saito N, Kawazoe Y, Ooi HK, Shiba T. Morphogenetic study on the maturation of osteoblastic cell as induced by inorganic polyphosphate. PLoS One. 2014; 9:e86834.
26. Gregory CA, Gunn WG, Peister A, Prockop DJ. An Alizarin red-based assay of mineralization by adherent cells in culture: Comparison with cetylpyridinium chloride extraction. Anal Biochem. 2004; 329:77-84.
27. Candelario-Jalil E, Taheri S, Yang Y, Sood R, Grossetete M, Estrada EY, Fiebich BL, Rosenberg GA. Cyclooxygenase inhibition limits blood-brain barrier disruption following intracerebral injection of tumor necrosis factor-alpha in the rat. J Pharmacol Exp Ther. 2007; 323:488-498.
28. Koyama Y, Tanaka K. Endothelins stimulate the production of stromelysin-1 in cultured rat astrocytes. Biochem Biophys Res Commun. 2008; 371:659-663.
29. Hayami T, Kapila YL, Kapila S. MMP-1 (collagenase-1) and MMP-13 (collagenase-3) differentially regulate markers of osteoblastic differentiation in osteogenic cells. Matrix Biol. 2008; 27:682-692.
30. Huang CY, Pelaez D, Dominguez-Bendala J, Garcia-Godoy F, Cheung HS. Plasticity of stem cells derived from adult periodontal ligament. Regen Med. 2009; 4:809-821.
31. Xu J, Wang W, Kapila Y, Lotz J, Kapila S. Multiple differentiation capacity of STRO-1+/CD146+ PDL mesenchymal progenitor cells. Stem Cells Dev. 2009; 18:487-496.
32. Visse R, Nagase H. Matrix metalloproteinases and tissue inhibitors of metalloproteinases: Structure, function, and biochemistry. Circ Res. 2003; 92:827-839.
33. Hassanian SM, Dinarvand P, Smith SA, Rezaie AR. Inorganic polyphosphate elicits pro-inflammatory responses through activation of the mammalian target of rapamycin complexes 1 and 2 in vascular endothelial cells. J Thromb Haemost. 2015; 13:860-871.
34. Wang Z, Li X, Li Z, Yang L, Sasaki Y, Wang S, Zhou L, Araki S, Mezawa M, Takai H, Ogata Y. Effects of inorganic polyphosphate on bone sialoprotein gene expression. Gene. 2010; 452:79-86.

(Received October 8, 2015; Revised December 9, 2015; Accepted December 20, 2015)

Original Article

DOI: 10.5582/bst.2015.01168

Lipopolysaccharide-induced serotonin transporter up-regulation involves PKG-I and p38MAPK activation partially through A3 adenosine receptor

Rui Zhao[1], Shoubao Wang[1], Zhonglin Huang[2], Li Zhang[1], Xiuying Yang[1], Xiaoyu Bai[1], Dan Zhou[1], Zhizhen Qin[1], Guanhua Du[1,*]

[1] *Beijing Key Laboratory of Drug Target and Screening Research, Institute of Materia Medica, Chinese Academy of Medical Sciences & Peking Union Medical College, Beijing, China;*
[2] *School of Pharmacy, Xinxiang Medical University, Xinxiang, Henan, China.*

Summary **Serotonin transporter (SERT) is a critical determinant of synaptic serotonin (5-hydroxytryptamine, 5-HT) inactivation which plays a critical role in the pathology of depression and other mood disorders. Lipopolysaccharide (LPS), a potent activator of the inflammatory system, has been reported to cause depression symptoms by the modulation of SERT *in vivo* and *in vitro*. This study is aimed to investigate the underlying mechanism of LPS-induced SERT modulation. The 4-(4-(dimethylamino) styryl)-N-methylpyridinium iodide (ASP) assay was used to detect dynamic 5-HT uptake as read out of SERT activities in RBL-2H3 cells, and cytosol Ca^{2+} concentrations ($[Ca^{2+}]i$) and nitric oxide (NO) were examined. Using specific cyclic GMP-dependent protein kinase type I (PKG-I), p38 mitogen-activated protein kinases (p38MAPK) and A3 adenosine receptor (A3AR) inhibitors, SERT expression was evaluated by western blot and immunofluorescence analysis. Results showed that 24 h treatment with LPS stimulated 5-HT transport and up-regulate plasma membrane distribution of SERT in RBL-2H3 cells. LPS treatment increased NO and $[Ca^{2+}]i$, and led to significant increases in levels of phosphorylated calcium/calmodulin-dependent protein kinase type II (CaMK-II), inducible NOS (iNOS) and PKG-I as well as active p38 MAPK. Moreover, PKG-I inhibitor KT5823 or p38MAPK inhibitor SB203580 respectively impaired SERT activation and transposition to plasma membrane by LPS. Notably, A3 adenosine receptor inhibitor MRS1191 also hindered SERT stimulation by LPS. In conclusion, LPS-induced 5-HT uptake and transposition to plasma membrane of SERT in RBL-2H3 cells involves CaMK-II/iNOS/PKG-I and p38 MAPK activation, which may be partially mediated by A3 adenosine receptor activation. This finding provides a novel insight into the interrelationship between LPS and depression.**

Keywords: Serotonin transport (SERT), lipopolysaccharide, cyclic GMP-dependent protein kinase type I (PKG-I), p38 mitogen-activated protein kinases (p38MAPK), A3 adenosine receptor

1. Introduction

Serotonin (5-hydroxytryptamine, 5-HT) is a neurotransmitter which plays a critical role in the pathology of depression following its binding to specific 5-HT receptors and their downstream signalling cascade (*1*). The serotonin transporter (SERT) is a critical determinant of synaptic 5-HT inactivation and an important target molecule for the antidepressant drugs including selective serotonin reuptake inhibitors (SSRIs) (*2,3*). When these drugs bind to the SERT, they inhibit its function, thereby blocking 5-HT uptake from the synapse and consequently enhancing synaptic 5-HT concentration. Their delayed effect in remission of patients suggests that it is not simple rapid blockade *per se*, but rather additional mechanisms regulating

**Address correspondence to:*
Dr. Guan-hua Du, Institute of Materia Medica, Chinese Academy of Medical Sciences & Peking Union Medical College, 1 Xiannongtan Street, Beijing 100050, China.
E-mail: dugh@imm.ac.cn

SERT function that may underlie the eventual clinical improvement after prolonged exposure to antidepressant drugs (*4*). Although the entire mechanism responsible has not been elucidated, SERT is subject to multiple posttranslational regulations that can rapidly alter 5-HT uptake and clearance rates. Specific cell surface receptors as well as pathways activating protein kinase C (PKC), protein kinase G (PKG) and p38 mitogen activated protein kinase (p38MAPK) regulating SERT trafficking and catalytic function are now well established and received greater attention (*5*). Zhu *et al*. revealed two PKG-dependent pathways supporting rapid SERT regulation by A3 adenosine receptor (A3AR), one leading to enhanced SERT surface trafficking, and a separate, p38 MAPK-dependent process augmenting SERT intrinsic activity, demonstrating mechanistic links between the A3AR and SERT (*6*). Remarkably, disease-associated alterations in SERT not only implicate SERT activity but also impact SERT regulatory pathways.

Although the etiology of depression is complex and remains unknown, there is a growing body of evidence that depressed subjects display an elevation of pro-inflammatory cytokines, and inflammation plays an important role in the development of depression (*7*). Viral and bacterial infections that stimulate the production of pro-inflammatory cytokines can produce symptoms of depression (*8*). The antidepressant-sensitive SERT can be regulated by pro-inflammatory cytokine signaling. Zhu and co-workers have shown that the inflammatory cytokines interleukin-1β (IL-1β) and tumor necrosis factor-α (TNF-α) produce rapid catalytic activation of SERT in cultured 5-HT neurons-derived RN46A cells and mouse nerve terminal preparations *in vitro* (*9*). Lipopolysaccharide (LPS) is a component of Gram-negative bacteria outer membrane, which acts as a potent activator of the inflammatory system. It is reported that LPS induces depression symptoms associated with elevations of serum IL-1β in subjects without a psychiatric history (*10*). It has been demonstrated that LPS binds to toll-like receptor 4 (TRL4) leading to the rapid systemic release of pro-inflammatory cytokines and induces anhedonia in rats and mice (*11*). Most remarkably, Zhu *et al*. found that peripheral activation of the innate immune system with LPS leads to a rapid (1 h) stimulation of central nervous system (CNS) SERT activity, accompanied by an acceleration of 5-HT clearance rate and alterations in SERT-dependent behaviors (*12*). In contrast, another study on the human enterocyte-like Caco-2 cell line have shown that LPS treatment diminished SERT activity and SERT protein level on brush border membrane, and the LPS effect might be due to an alteration of the intracellular traffic of SERT partially mediated by protein kinase C (PKC) activation (*13*). Therefore, more investigation is needed to provide more information about the effects of LPS on SERT activity and expression.

Using cells derived from rodent mast cells RBL-2H3, the aim of this work was to study the effect of LPS on SERT activity and expression and to determine the intracellular mechanism underlying this effect. Many studies have demonstrated RBL-2H3 cells expressing serotonin synthesis and transporter systems as an ideal model for elucidating the regulatory mechanisms relating to SERT (*14-16*). Consistent with previous reports, results obtained in our laboratory have shown that the fluorescent styryl dye ASP assay enables the detection of dynamic transport activities of SERT and is amenable for measuring 5-HT uptake (*17-21*).The results obtained from the present study showed that LPS treatment enhances 5-HT uptake in RBL-2H3 cells in a dose-dependent manner. LPS-induced up-regulation of 5-HT uptake results from the increase in surface-expressed SERT protein, which might be partially mediated by PKG-I and p38MAPK activation following A3 adenosine receptor activation. This finding may contribute to a better understanding of the involvement of the LPS in the pathology and modeling of depression.

2. Materials and Methods

2.1. *Reagents and antibodies*

ASP (4-(4-(dimethylamino) styryl)-N-methylpyridinium iodide) and Fluo-3/AM were obtained from Invitrogen (Carlsbad, CA, USA); SB203580 and KT5823 were obtained from the Beyotime Institute of Biotechnology (Jiangsu, China). LPS and MRS1191 were obtained from Sigma Chemical Company (St Louis, MO, USA). Primary antibodies against SERT and PKG-I were purchased from Santa Cruz Biotechnology Inc. (Santa Cruz, CA, USA), and those against phosphor-p38MAPK, iNOS were purchased from Cell Signaling Technology (Danvers, MA, USA).

2.2. *Cell culture*

RBL-2H3 cells were purchased from the China Center for Type Culture Collection (CCTCC; Wuhan, China). RBL-2H3 cells were maintained in nucleoside free Minimum Essential Medium (MEM) α containing 15% fetal bovine serum and were grown into monolayers. Cells were plated on polystyrene tissue culture dishes at densities of 3-10 × 10^5 cells/mL. After 12 h incubation, cells were replaced with fresh serum-free media. After 4 h, RBL-2H3 cells were incubated in fresh media containing 0.75, 1.5, 3 μg/mL LPS or 0.1% DMSO (as vehicle control) with or without pre-treatment with MRS1191, SB203580 or KT5823.

Primary neuron cultures were prepared from E18 Sprague Dawley rat pups. Animals were treated in accordance with the National Institute of Health Guidelines for the Care and Use of Laboratory Animals. Briefly, tissues were harvested on ice and were washed in D-Hanks Balanced Salt Solution containing 100

IU/mL penicillin, and 100 μg/mL streptomycin, and then mechanically dissociated using trituration and trypsinization. Cells were then seeded onto poly-D-lysine-coated 6-well plates at 2×10^6 cells/well in DMEM/F12 media containing B27, L-glutamine, 100 IU/mL penicillin, and 100 μg/mL streptomycin. Neuron cultures were typically grown for 7-10 days.

2.3. *Assay for 5-HT uptake*

5-HT transport activities were measured using ASP assay on RBL-2H3 cells. Briefly, cells from 80% confluent culture flasks were harvested using 0.25% trypsin and were seeded (35,000 cells per well) into 96-well plates and cultured for 24 h in nucleoside free MEM α containing 15% fetal bovine serum. After 20 h, the media was replaced with serum free media and cells were cultured for 4 h prior to assays. ASP (Invitrogen) dissolved in DMSO was added (final concentration, 1 mM) and incubated in the dark at 37°C for 60 min. Unincorporated ASP was removed by washing (3 times with PBS) and 5-HT transporter activity was quantified according to fluorescence intensities (λex, 475 nm; λem, 605 nm) using a SpectraMax M5 Microplate Reader (Sunnyvale, CA, USA).

2.4. *Detection of cytosol Ca^{2+} using Fluo-3/AM*

Detection of intracellular calcium in RBL-2H3 cells was performed using the fluorescent indicator Fluo-3/AM. All images were acquired on a Leica TCS SP5 imaging system mounted on a microscope and an argon ion laser (458-514 nm). Image processing and quantification was carried out using the mean fluorescence intensities of sections acquired.

2.5. *NO assay*

NO levels were measured with the Griess method using a nitrite detection kit (Beyotime, Jiangsu, China) according to the manufacturer's instructions. Briefly, 100 μL of medium or standard $NaNO_2$ was mixed with 100 μL of Griess reagent in a 96-well plate. After 15 min, optical density was read using a SpectraMax M5 Microplate Reader at 540 nm. Results were calculated for statistical analysis by a standard curve using $NaNO_2$.

2.6. *RT-PCR*

Total RNA was extracted from cells cultured under different experimental conditions. The extracted RNA (1 μg) was used as a template for first-strand cDNA synthesis using oligo (dT) primers and a modified M-MLV reverse transcriptase (Carlsbad, CA, Invitrogen). Negative amplification control was performed in the absence of reverse transcriptase. One-tenth of the resultant cDNA was used for human TLR4 and human SERT PCR amplification with human β-actin as an internal control. Real-time quantitative polymerase chain reaction (RT-PCR) was performed with the Bio-rad CFX real-time PCR system and β-actin was used as the reference gene. Gene expression was determined using the $2^{-\Delta\Delta CT}$ method with the following custom designed primers: for β-actin, 5'-AGATCCTGACCGAGCGTGGC-3' and 5'-CCAGGGAGGAAGAGGATGCG-3'; for SERT, 5'-GGTGTGGGTAGATGCCGCCG-3' and 5'-GCTGGGGCCTGCGTCTTTGG-3'.

2.7. *Western blot analysis*

For surface-localized SERT, the Cell Surface Protein Isolation Kit (Thermo Scientific, Pierce, #89881, Waltham, MA, USA) was used for biotinylation and the isolation of cell surface proteins for western blot analysis. Equal amounts of protein (30 μg) were separated on 12% polyacrylamide gels. Proteins were then transferred to 0.45-μm polyvinylidene difluoride (PVDF) membranes using a Bio-Rad Laboratories Mini Protein system. After treating PVDF membranes with blocking buffer TBS/0.1% Tween20 (TBST) containing 3% BSA for 2 h at 37°C, membranes were incubated overnight at 4°C in TBS buffer containing 3% BSA and primary antibodies against active p38MAPK (1:1000), SERT (1:100), PKG-I (1:100), iNOS (1:1000). Membranes were washed 3 times for 10 min in TBST, and were then incubated for 1 h at 37°C with a secondary horseradish peroxidase (HRP)-conjugated antibody at a dilution of 1:1000 in blocking buffer. Finally, membranes were washed extensively in TBST and photographic images were taken after illumination using an enhanced chemiluminescence (ECL) detection reagent. The densitometric analyses of autoradiograms were performed using quantity one software (Bio-Rad Laboratories Inc., Hercules, CA, USA), and data were expressed relative to internal control protein expression.

2.8. *Immunofluorescence staining of SERT*

Cells were seeded at 5,000 cells per well into 96-well black wall clear bottom plates to receive different experimental treatments. Cells were then fixed in 1× PBS containing 4% paraformaldehyde for 30 min, and were subsequently washed three times with 1× PBS. Fixed cells were then blocked in 1× PBS containing 3% BSA for 10 min. Primary antibodies against SERT and phospho-p38MAPK were applied overnight at 4°C. Cells were then washed three times in PBS and were incubated with fluorescent secondary antibodies at 37°C for 2 h in the dark. Finally, Hoechst 33342 (Molecular Probes) was added (final concentration, 1 μg/mL) for the final 10 min, cells were washed three times in PBS, and then PBS containing 50% glycerol was added. Images were acquired and analyzed using a Cellomics ArrayScan®

VTI Imaging Platform (Thermo Fisher Scientific Inc., Waltham, MA, USA).

2.9. *Statistical analysis*

All experiments were replicated a minimum of three times. Subsequently, raw data was normalized and exported into GraphPad Prism (GraphPad Software Inc. San Diego, CA, USA) to generate figures. Differences were identified using one- and two-way analysis of variance (ANOVA) with subsequent Dunnett's comparisons and Student *t*-test. Differences were considered significant when $p < 0.05$.

3. Results

3.1. *LPS enhanced 5-HT uptake in RBL-2H3 cells in a dose-dependant manner*

To examine the effects of LPS on 5-HT uptake, the fluorescent styryl dye ASP was used to detect dynamic transport activities of SERT, and ASP fluorescent intensities in RBL-2H3 cells were monitored after 24 h treatment with LPS. As shown, treatment with 1.5, 3 μg/mL LPS significantly elevated 5-HT transport indicated by increased ASP fluorescence, as readout of SERT activity, in RBL-2H3 cells (Figure 1A), suggesting that

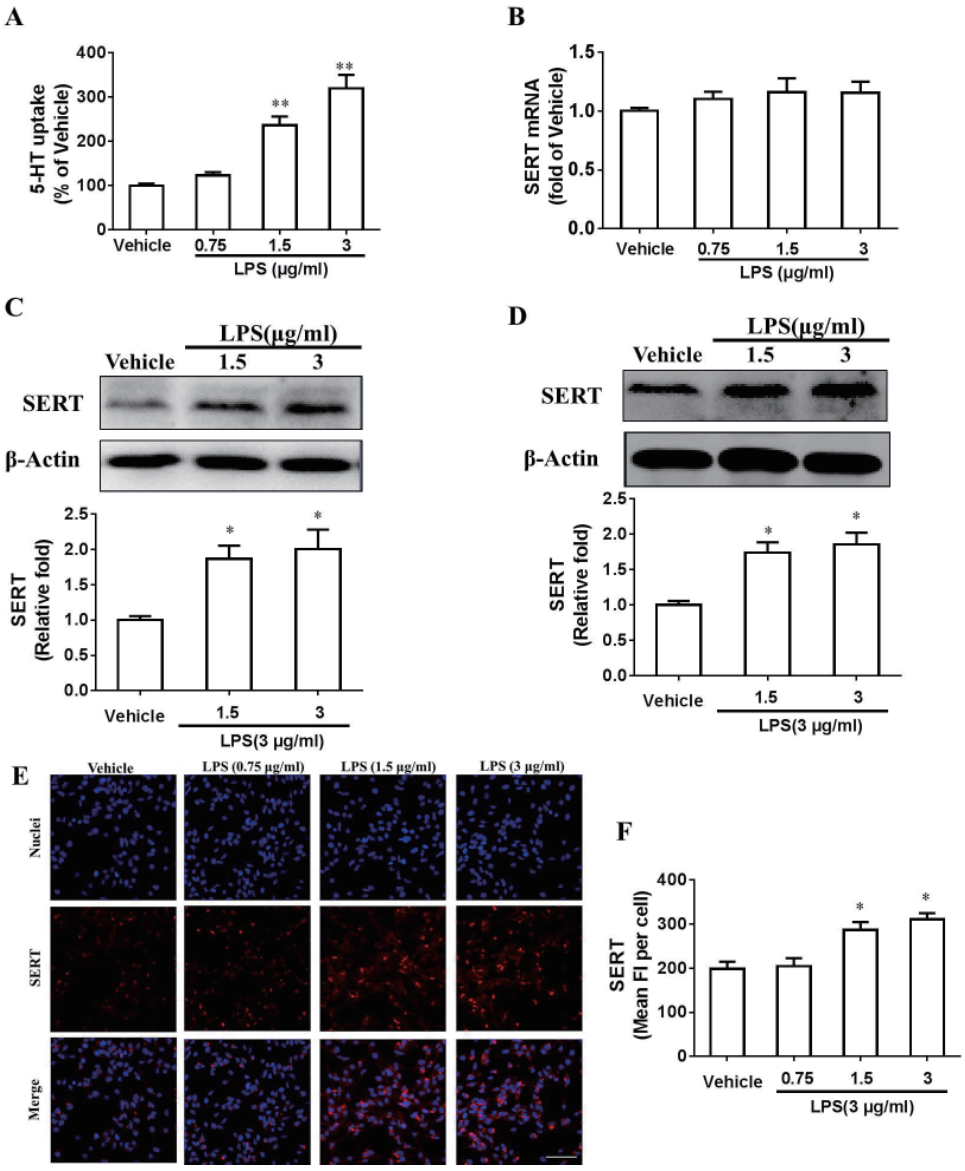

Figure 1. LPS enhanced 5-HT uptake and the level of surface-expressed SERT. (A) RBL-2H3 cells (3.5×10^5 cells/well) were seeded in 96-well microplate and treated with LPS at the indicated concentrations for 24 h before examination. LPS enhanced 5-HT uptake indicated by ASP fluorescence intensity monitored. **(B)** The mRNA level of SERT was analyzed by real-time PCR following LPS treatment. **(C)** The protein content of SERT in RBL-2H3 cells was analyzed following LPS treatment. A Thermo Scientific Pierce Cell Surface Protein Isolation Kit (#89881) was used to biotinylate and isolate cell surface proteins for western blot analysis. **(D)** The protein content of SERT in isolated E18 primary rat cortical neurons was analyzed by western blot following 24 h LPS treatment. **(E, F)** The protein content of SERT in RBL-2H3 cells was confirmed by immunofluorescence analyse following 24 h LPS treatment. Scale bar, 40 μm. Values are expressed as the mean of at least three experiments ± S.E.M; $^*p < 0.05$, $^{**}p < 0.01$ compared to vehicle.

LPS caused dramatic alteration in 5-HT uptake into RBL-2H3 cells in a dose-dependent manner.

3.2. *LPS elevated the level of surface-expressed SERT in RBL-2H3 cells and isolated E18 primary rat cortical neurons*

The observation of increased 5-HT uptake by LPS treatment in RBL-2H3 cells prompted us to investigate whether LPS induced the alteration in the level of SERT expression. Thus, the transcript level of SERT was determined using quantitative PCR analysis, and the results showed that treatment with LPS did not affect SERT mRNA level compared to vehicle treatment (Figure 1B). Furthermore, western blot analysis on the whole lysate of RBL-2H3 cells demonstrated that LPS did not influence total protein level of SERT, however, level of SERT protein in plasma membrane subfraction prepared from RBL-2H3 cells remarkably increased (Figure 1C). Immunofluorescence analysis using specific SERT antibody showed the protein content of plasma membrane-localized SERT in RBL-2H3 cells significantly increased with mean FI per cell of 286 ± 31 and 311± 46 following 24 h LPS treatment compared to 198 ± 23 of vehicle treatment (Figures 1E and 1F). Moreover, we isolated E18 primary rat cortical neurons to further examine the increase in SERT protein level induced by LPS. Representative blot images

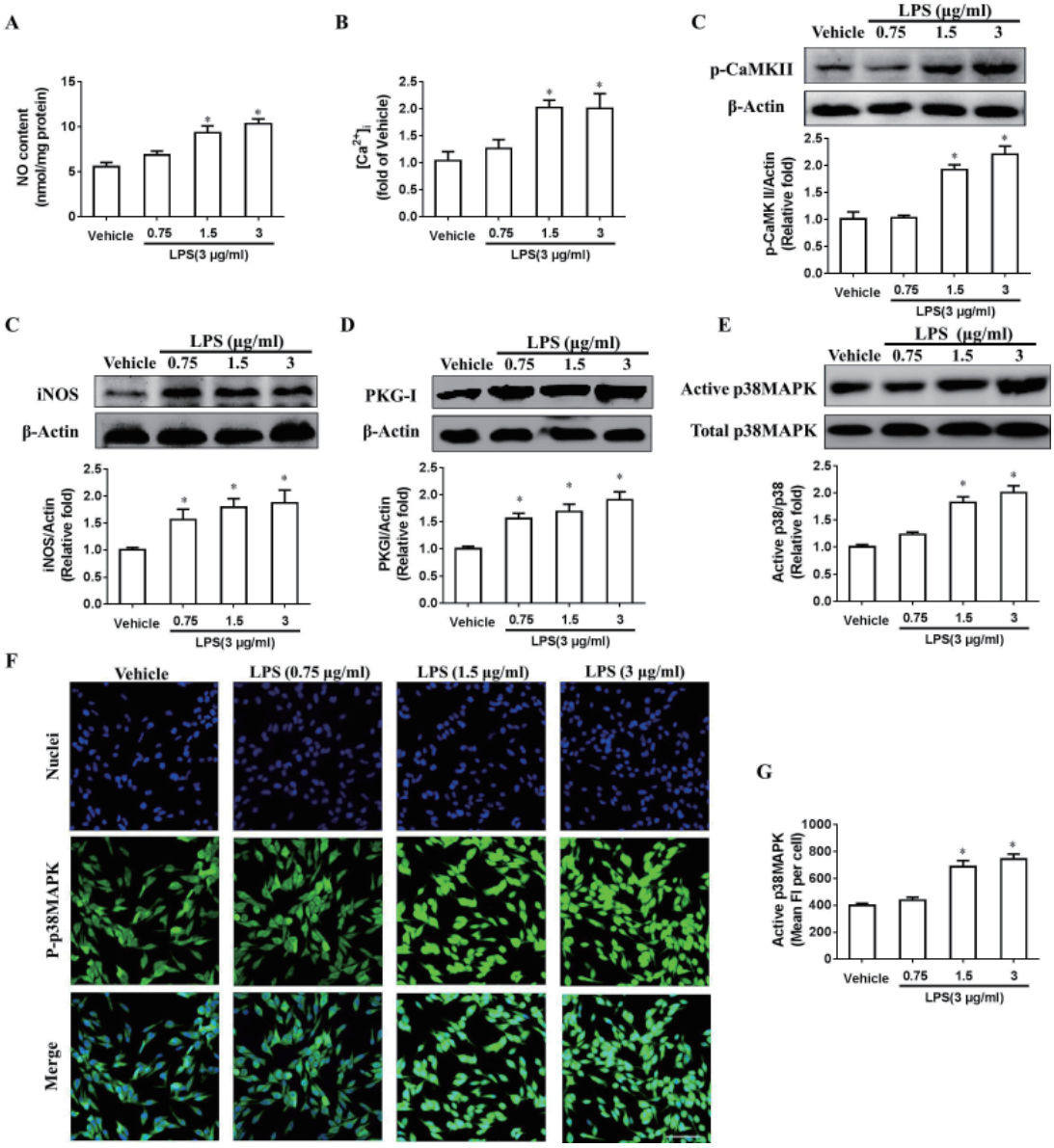

Figure 2. LPS elevated NO content and the level of cytosol calcium, and stimulated CaMK-II/iNOS/PKG-I signaling pathway and p38MAPK in RBL-2H3 cells. RBL-2H3 cells (3.5×10^5 cells/well) were seeded in 96-well microplate and treated with LPS at the indicated concentrations for 24 h before examination. **(A)** LPS elevated NO content examined by Griess method. **(B)** The level of cytosol calcium was determined using Fluo-3/AM following LPS treatment. The phosphorylation of CaMK-II **(C)**, protein level of iNOS **(D)**, PKG-I **(E)** and active p38MAPK **(F)** in RBL-2H3 cells was analyzed by western blot following 24 h LPS treatment. **(G, H)** The activation of p38MAPK in RBL-2H3 cells was examined by immunofluorescence analysis following 24 h LPS treatment. Scale bar, 40 μm. Values are expressed as the mean of at least three experiments ± S.E.M; $^{*}p < 0.05$, $^{**}p < 0.01$ compared to vehicle.

demonstrated that 1.5 and 3 μg/mL LPS treatment significantly boosted the expression of surface-expressed protein SERT (Figure 1D). Taken together, these data indicate that although LPS did not affect the total SERT expression, but notably induced the elevation in the plasma membrane distribution of SERT.

3.3. *LPS Increased Ca^{2+} and NO followed by PKG-I/p38MAPK pathway activation*

Increasing evidence indicates that SERT-mediated 5-HT clearance is controlled by multiple pathways that regulate both plasma membrane expression and catalytic activity of SERT (*18*). Recent studies demonstrate that the up-regulation of SERT activity by serine/threonine kinases, PKG-I and p38MAPK-linked pathways contains increased SERT activation and membrane distribution (*22*). Thus, Ca^{2+}-CaMK- II/iNOS-NO/PKG-I and p38MAPK pathway received more attention as one of the most widely studied regulatory mechanisms. In the current study, NO level was firstly determined using Griess method after 24 h treatment with LPS.

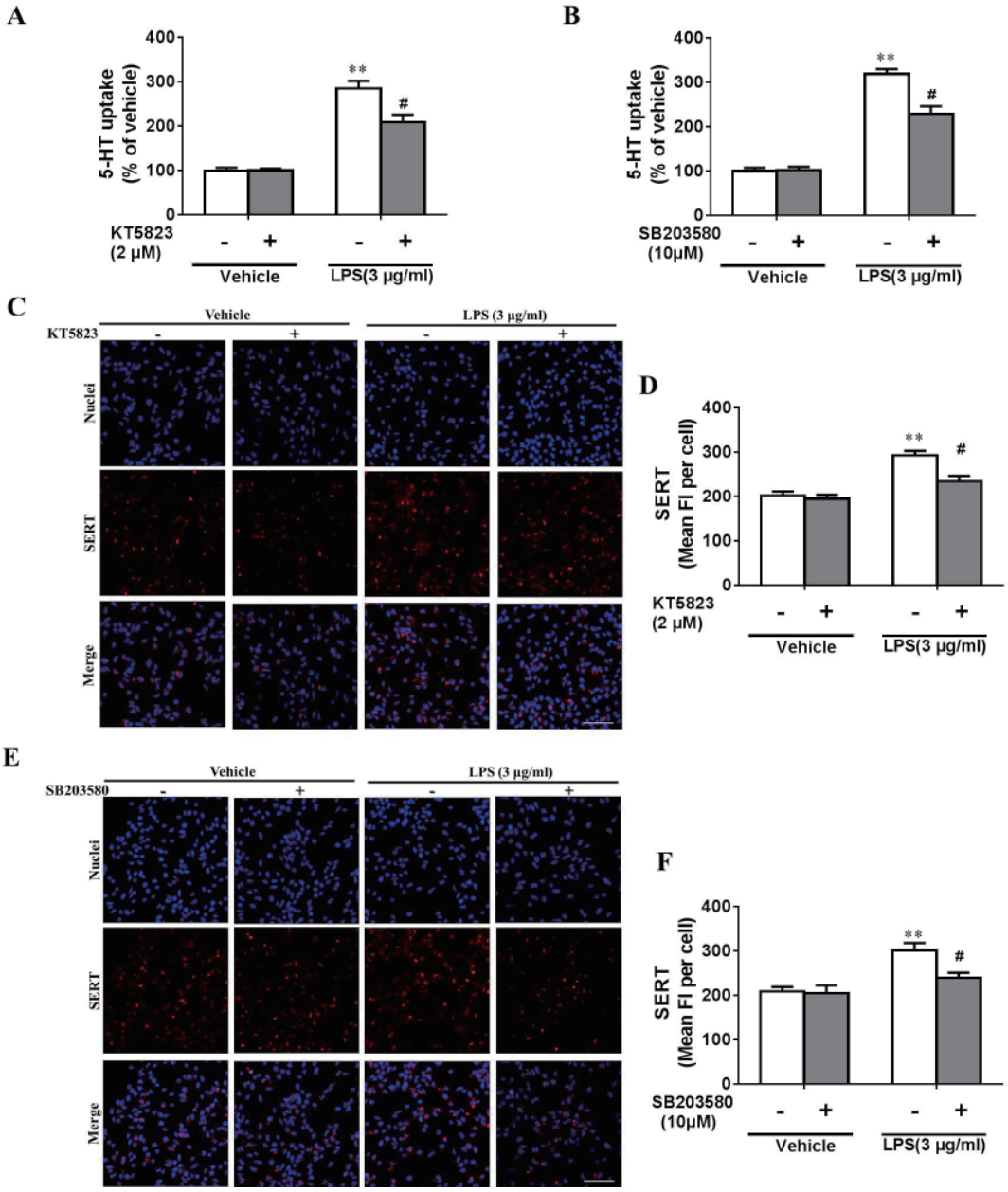

Figure 3. LPS-induced 5-HT uptake and surface-expressed SERT in RBL-2H3 cells was hindered by inhibition of PKG-I or p38MAPK. RBL-2H3 cells (3.5×10^5 cells/well) were seeded in 96-well microplate and treated with 3 μg/mL LPS for 24 h following 6 h pre-treatment with PKG-I inhibitor KT5823 (2 μM) treatment or p38MAPK inhibitor SB203580 (10 μM). **(A-B)** Change in 5-HT uptake was determined using ASP assay. **(C-D)** Representative immunofluorescence images and quantification of SERT expression following 24 h LPS treatment in the presence of PKG-I inhibitor KT5823. **(E-F)** Representative immunofluorescence images and quantification of SERT expression following 24 h LPS treatment in the presence of p38MAPK inhibitor SB203580. Scale bar, 40 μm. Values are expressed as the mean of at least three experiments ± S.E.M; $^{*}p < 0.05$, $^{**}p < 0.01$ compared to vehicle; $^{\#}p < 0.05$ compared to LPS 3 μg/mL treatment.

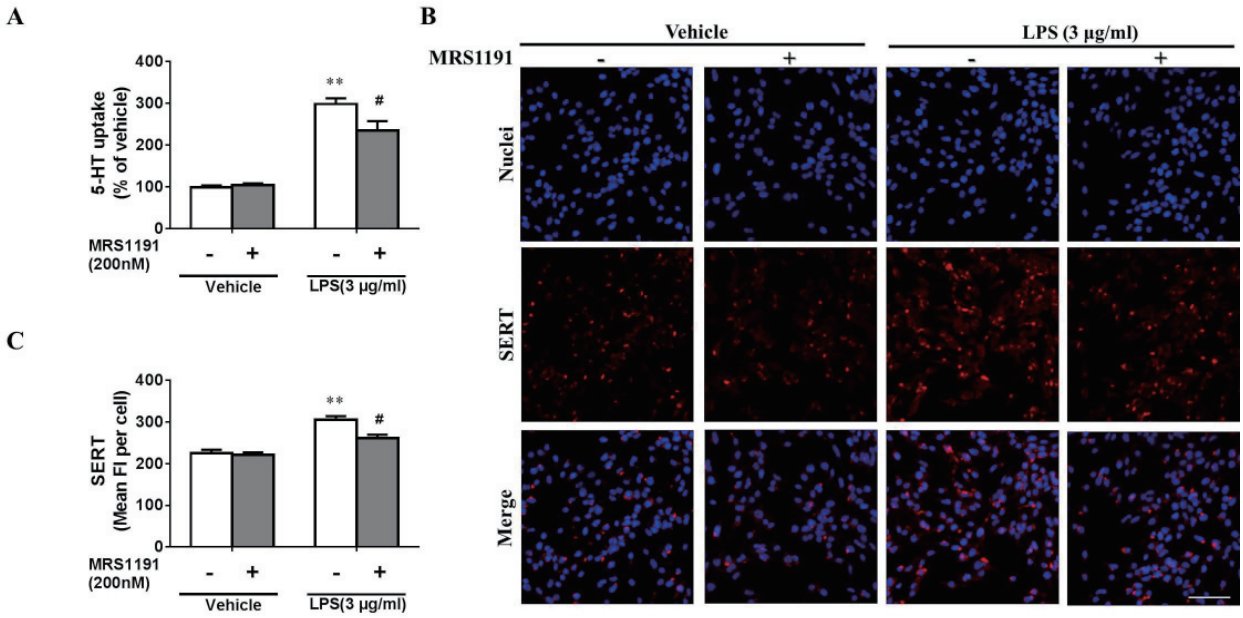

Figure 4. A3AR antagonism inhibited LPS-induced 5-HT uptake and surface-expressed SERT in RBL-2H3 cells. RBL-2H3 cells (3.5×10^5 cells/well) were seeded in 96-well microplate and treated with 3 μg/mL LPS for 24 h in the presence or absence of A3AR antagonist MRS1191 (200 nM). **(A)** Change in 5-HT uptake was determined using ASP assay. **(B-C)** Representative immunofluorescence images and quantification of SERT expression. Scale bar, 40 μm. Values are expressed as the mean of at least three experiments ± S.E.M; $^{*}p < 0.05$, $^{**}p < 0.01$ compared to vehicle; $^{\#}p < 0.05$ compared to LPS 3 μg/mL treatment.

The results showed that NO levels in RBL-2H3 cells significantly increased when treated with 1.5 and 3 μg/mL LPS (nmol/mg protein: 9.36 ± 0.79 and 10.34 ± 0.65) (Figure 2A). Subsequently, the fluorescent staining using Fluo-3/AM demonstrated that intracellular Ca^{2+} concentration ([Ca^{2+}] i) in RBL-2H3 cells was lifted by LPS treatment up to 2-fold of that in vehicle treated cells (Figure 2B). Western blot analysis indicated that phosphorylated CaMK-II, protein level of iNOS and PKG-I as well as active p38MAPK were markedly elevated (Figures 2C-2E). Consistent with the data shown above, immunofluorescence staining using anti-phosphorylated p38MAPK further confirmed the almost 1.6-fold increase in the level of active p38MAPK by LPS treatment (Figures 2F and 2G). Taken together, these data suggest that Ca^{2+}-CaMK-II/iNOS-NO/PKG-I and p38MAPK signaling might be implicated in the up-regulation of SERT by LPS.

3.4. *The Effect of PKG-I or p38MAPK inhibition on LPS-induced 5-HT uptake and SERT expression in RBL-2H3 cells*

To clarify the involvement of PKG-I or p38MAPK in LPS-induced 5-HT uptake and SERT expression, here, PKG-I inhibitor KT5823 or p38MAPK inhibitor SB203580 was respectively pretreated to RBL-2H3 cells to investigate their influences on LPS profile. The assay for 5-HT uptake using ASP transport demonstrated that PKG-I inhibitor KT5823 (2 μM) or p38MAPK inhibitor SB203580 (10 μM) pretreatment did not notably affected the 5-HT uptake, however, 3 μg/mL LPS-induced increase in the 5-HT uptake was remarkably impaired in the presence of the two inhibitors (Figures 3A and 3B). The immunofluorescence assay labeling SERT indicated that as compared to control treatment with just 3 μg/mL LPS, the protein level of SERT in the surface of RBL-2H3 cells markedly declined when treated with 2 μM PKG-I inhibitor KT5823 followed by 3 μg/mL LPS treatment for extra 24 h (Figures 3C and 3D). The fluorescence intensities of surface-localized SERT in RBL-2H3 cells co-treated with 3 μg/mL LPS and 10 μM p38MAPK inhibitor SB203580 also significantly fell into decline. Therefore, these results suggest that PKG-I and p38MAPK activation play a crucial role in the LPS-induced 5-HT uptake and SERT expression in RBL-2H3 cells.

3.5. *Effect of Adenosine 3A Receptor (A3AR) antagonism on LPS-induced 5-HT uptake and SERT expression in RBL-2H3 cells*

It is reported that the activation of A3AR results in increased 5-HT uptake in RBL-2H3 cells and that A3AR regulates serotonin transport *via* NO and cyclic guanosine monophosphate (cGMP) (*22,23*). Thus, it is necessary to dig out the role of A3AR in the LPS-induced 5-HT uptake and SERT expression. RBL-2H3 cells were pre-treated with an A3AR antagonist MRS1191 (200 nM) for 6 h, followed by treatment with 3 μg/mL LPS. After 24 h of incubation, the change in the 5-HT uptake was assessed as described previously, and we observed that the addition of MRS1191 notably disrupted the effects exerted by 3 μg/mL LPS (Figure

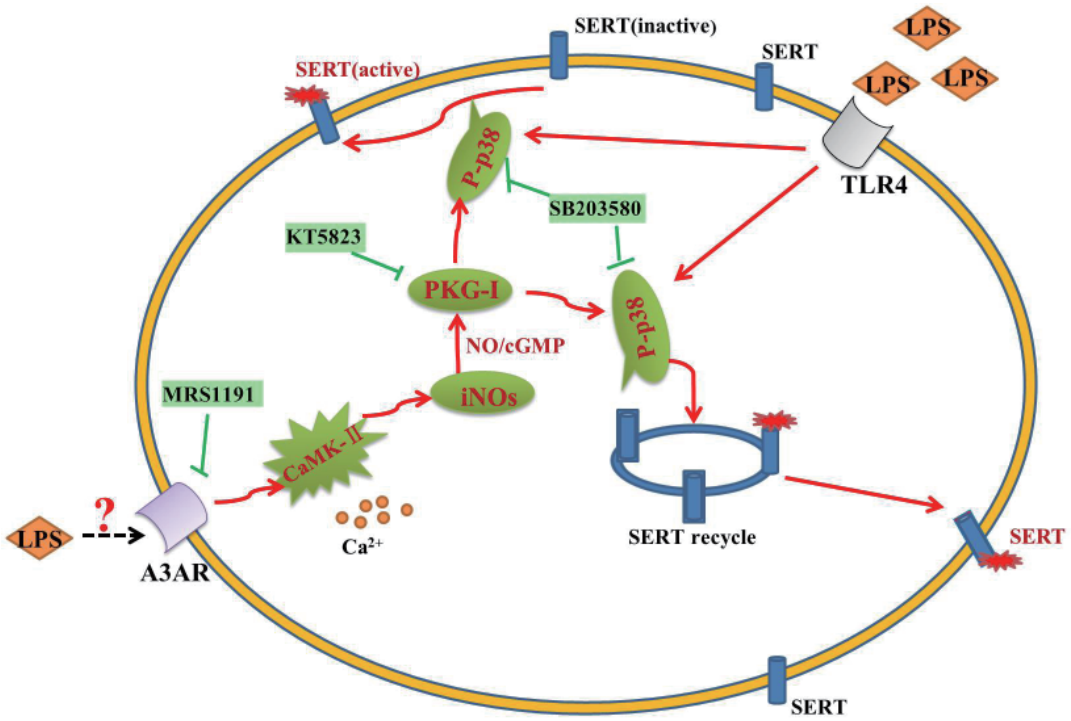

Figure 5. The schematic pathway involved in LPS-induced 5-HT uptake and surface-expressed SERT in RBL-2H3 cells.

4A). Immunofluorescence assay also showed that there was no remarkable difference between vehicle and MRS1191 treatment, however, level of surface-expressed SERT was significantly higher (316 ± 27) of 3 μg/mL LPS treatment than that of co-treatment with 200 nM MRS1191 and 3 μg/mL LPS (245 ± 31) (Figures 4B and 4C), indicating that the activation of A3AR was implicated in LPS-induced upregulation of 5-HT uptake and SERT expression in RBL-2H3 cells.

4. Discussion

In the present study, we showed that 24 h treatments with LPS significantly increased the 5-HT uptake and plasma membrane expression of SERT in a rat basophilic leukemia cell line RBL-2H3 cell. Moreover, elevation in NO content and intracellular Ca^{2+} concentrations was observed following LPS treatment. Mechanismatic investigation showed that LPS induced CaMK-II/iNOS/PKG-I and p38MAPK signaling pathways, leading to an increase in the activation and plasma membrane distribution of SERT. Furthermore, the effects of LPS on SERT were impaired by the presence of A3AR antagonist MRS1191.

In our experiments, we found that LPS significantly increased the 5-HT uptake and upregulated the protein level of SERT in RBL-2H3 cell, as contrast to the previous report on the human enterocyte-like Caco-2 cell line (*13*). Although Caco-2 expresses the human SERT, this cell line lacks in serotonin synthesis and discretion. Comparatively, rat basophilic mast cells RBL-2H3 express not only transporter systems but also serotonin synthesis, and are regarded more relative to the physiology of 5-HT neurons. Miller and Hoffman first provided evidence of adenosine receptor (AR) regulation of SERT using this cell line (*22*). Kim *et al*. investigated the molecular mechanisms of antidepressant drugs that sertraline up-regulates tryptophan hydroxylase expression and serotonin synthesis in RBL-2H3 cells (*24*). These studies proved RBL-2H3 cells as an ideal model for studying the SERT. In addition, SERT is also widely expressed in the front cortexes of the brain and the hippocampus which are closely associated with the pathogenesis of depression (*23,25*), so we verified the effects of LPS in isolated E18 primary rat cortical neurons and gained the same observation.

It is believed that lipopolysaccharide activity is mediated by TLR 4 activation and a cascade of intracellular reactions which involves different signalling pathways including p38 MAPK, protein kinase A (PKA) and PKC (*26*). It has been reported that interleukin-1β (IL-1β) and TNF-α stimulation of SERT activity *in vitro* is mediated through the activation of p38 MAPK (*9*). Since LPS tightly correlates to these pro-inflammatory cytokines, we examined the requirement for p38 MAPK in SERT modulation exerted by LPS using treatment with p38 MAPK inhibitor SB203580. The observation that active p38 MAPK increased with LPS treatment and the SERT up-regulation by LPS was impaired by treatment with SB203580 indicates that p38 MAPK may act as an activator of SERT function.

Increasing evidences indicate that SERT are tightly controlled by multiple signaling pathways including

G-protein coupled receptors-linked pathways and various kinases as well as their substrates (*27-31*). Recently, Miller *et al*. showed that the activation of A3AR results in increased 5-HT uptake in RBL-2H3 cells and that A3AR regulates serotonin transport *via* NO and cGMP (*22*). Some *in vitro* studies have revealed multiple second messengers or second messenger-linked kinases participate in acute SERT regulation (*32*). Experiments with synaptosomes and cell lines demonstrate that SERT activity decreases after depletion of intracellular Ca^{2+}, treatment with calmodulin inhibitors and phorbol esters (*33,34*). PKA, PKC and PKG activation have also been demonstrated to impose post-translational regulation on SERT by phosphorylation, possibly reflecting the heterologous context of SERT expression. Zhu *et al*. have reported that involvement of A3AR in serotonin transporter trafficking and activation in RBL-2H3 cells and SERT stimulation by A3AR requires activation of PKG by a phospholipase C, Ca^{2+}, NOS and cGMP-dependent mechanism (14,27). In the present study, we provided evidence that Ca^{2+}-CaMK-II/iNOS/PKG-I signaling pathways contribute to up-regulation of SERT in RBL-2H3 cells by LPS. This effect maybe partially mediated through activates A3AR by LPS (Figure 5). Although the potential mechanism by which LPS enhances activates A3AR in RBL-2H3 cells remains unclear, this finding offers a novel insight into the modulation of SERT. Moreover, many researches are still needed to clarify the interaction between A3AR and LPS.

In conclusion, the present experiments demonstrate that LPS enhances the 5-HT uptake and transposition from cytosol to plasma membrane of SERT in RBL-2H3 cells, and the underlying mechanism involves CaMK-II/iNOS/PKG-I and p38 MAPK activation following calcium flux, which may be partially mediated by A3AR activation. LPS-induced alteration possibly provides a powerful tool to model the pathology of depression and the discovery of new antidepressant.

Acknowledgements

This work was supported by grants from the National Science and Technology Major Project (2013ZX09102106, 2013ZX09103001-008, 2012ZX09103101-078) and the National Natural Science Foundation of China (81202538).

References

1. Sharp T, Cowen PJ. 5-HT and depression: Is the glass half-full. Curr Opin Pharmacol. 2011; 11:45-51.
2. Stahl SM, Lee-Zimmerman C, Cartwright S, Morrissette DA. Serotonergic drugs for depression and beyond. Curr Drug Targets. 2013; 14:578-585.
3. Blier P, de Montigny C. Current advances and trends in the treatment of depression. Trends Pharmacol Sci. 1994; 15:220-226.
4. Lau T, Horschitz S, Berger S, Bartsch D, Schloss P. Antidepressant-induced internalization of the serotonin transporter in serotonergic neurons. FASEB J. 2008; 22:1702-1714.
5. Steiner JA, Carneiro AM, Blakely RD. Going with the flow: Trafficking-dependent and -independent regulation of serotonin transport. Traffic. 2008; 9:1393-1402.
6. Zhu CB, Lindler KM, Campbell NG, Sutcliffe JS, Hewlett WA, Blakely RD. Colocalization and regulated physical association of presynaptic serotonin transporters with A(3) adenosine receptors. Mol Pharmacol. 2011; 80:458-465.
7. Li W, Ling S, Yang Y, Hu Z, Davies H, Fang M. Systematic hypothesis for post-stroke depression caused inflammation and neurotransmission and resultant on possible treatments. Neuro Endocrinol Lett. 2014; 35:104-109.
8. Dantzer R, O'Connor JC, Freund GG, Johnson RW, Kelley KW. From inflammation to sickness and depression: When the immune system subjugates the brain. Nat Rev Neurosci. 2008; 9:46-56.
9. Zhu CB, Blakely RD, Hewlett WA. The proinflammatory cytokines interleukin-1beta and tumor necrosis factor-alpha activate serotonin transporters. Neuropsychopharmacology. 2006; 31:2121-2131.
10. Leonard B, Maes M. Mechanistic explanations how cell-mediated immune activation, inflammation and oxidative and nitrosative stress pathways and their sequels and concomitants play a role in the pathophysiology of unipolar depression. Neurosci Biobehav Rev. 2012; 36:764-785.
11. Van Heesch F, Prins J, Konsman JP, Westphal KG, Olivier B, Kraneveld AD, Korte SM. Lipopolysaccharide-induced anhedonia is abolished in male serotonin transporter knockout rats: An intracranial self-stimulation study. Brain Behav Immun. 2013; 29:98-103.
12. Zhu CB, Lindler KM, Owens AW, Daws LC, Blakely RD, Hewlett WA. Interleukin-1 receptor activation by systemic lipopolysaccharide induces behavioral despair linked to MAPK regulation of CNS serotonin transporters. Neuropsychopharmacology. 2010; 35:2510-2520.
13. Mendoza C, Matheus N, Iceta R, Mesonero JE, Alcalde AI. Lipopolysaccharide induces alteration of serotonin transporter in human intestinal epithelial cells. Innate Immun. 2009; 15:243-250.
14. Zhu CB, Steiner JA, Munn JL, Daws LC, Hewlett WA, Blakely RD. Rapid stimulation of presynaptic serotonin transport by A(3) adenosine receptors. J Pharmacol Exp Ther. 2007; 322:332-340.
15. Harville BA, Dreyfus LA. Release of serotonin from RBL-2H3 cells by the Escherichia coli peptide toxin STb. Peptides. 1996; 17:363-366.
16. Hoffman BJ, Mezey E, Brownstein MJ. Cloning of a serotonin transporter affected by antidepressants. Science. 1991; 254:579-580.
17. Baik SY, Jung KH, Choi MR, Yang BH, Kim SH, Lee JS, Oh DY,Choi IG,Chung H,Chai YG.Fluoxetine-induced up-regulation of 14-3-3zeta and tryptophan hydroxylase levels in RBL-2H3 cells. Neurosci Lett. 2005; 374:53-57.
18. Fowler A, Seifert N, Acker V, Woehrle T, Kilpert C, de Saizieu A. A nonradioactive high-throughput/high-content assay for measurement of the human serotonin reuptake transporter function *in vitro*. J Biomol Screen.

2006; 11:1027-1034.
19. Jorgensen S, Nielsen EO, Peters D, Dyhring T. Validation of a fluorescence-based high-throughput assay for the measurement of neurotransmitter transporter uptake activity. J Neurosci Methods. 2008; 169:168-176.
20. Fowler A, Seifert N, Acker V, Woehrle T, Kilpert C, de Saizieu A. A nonradioactive high-throughput/high-content assay for measurement of the human serotonin reuptake transporter function *in vitro*. J Biomol Screen. 2006; 11:1027-1034.
21. Oz M, Libby T, Kivell B, Jaligam V, Ramamoorthy S, Shippenberg TS. Real-time, spatially resolved analysis of serotonin transporter activity and regulation using the fluorescent substrate, ASP+. J Neurochem. 2010; 114:1019-1029.
22. Miller KJ, Hoffman BJ. Adenosine A3 receptors regulate serotonin transport *via* nitric oxide and cGMP. J Biol Chem. 1994; 269:27351-27356.
23. Ramkumar V, Stiles GL, Beaven MA, Ali H. The A3 adenosine receptor is the unique adenosine receptor which facilitates release of allergic mediators in mast cells. J Biol Chem. 1993; 268:16887-16890.
24. Kim SW, Park SY, Hwang O. Up-regulation of tryptophan hydroxylase expression and serotonin synthesis by sertraline. Mol Pharmacol. 2002; 61:778-785.
25. Hoffman BJ, Hansson SR, Mezey E, Palkovits M. Localization and dynamic regulation of biogenic amine transporters in the mammalian central nervous system. Front Neuroendocrinol. 1998; 19:187-231.
26. MacKenzie CJ, Paul A, Wilson S, de Martin R, Baker AH, Plevin R. Enhancement of lipopolysaccharide-stimulated JNK activity in rat aortic smooth muscle cells by pharmacological and adenovirus-mediated inhibition of inhibitory kappa B kinase signalling. Br J Pharmacol. 2003; 139:1041-1049.
27. Blakely RD, DeFelice LJ, Galli A. Biogenic amine neurotransmitter transporters: Just when you thought you knew them. Physiology (Bethesda). 2005; 20:225-231.
28. Zhu CB, Hewlett WA, Feoktistov I, Biaggioni I, Blakely RD. Adenosine receptor, protein kinase G, and p38 mitogen-activated protein kinase-dependent up-regulation of serotonin transporters involves both transporter trafficking and activation. Mol Pharmacol. 2004; 65:1462-1474.
29. Ramamoorthy S, Blakely RD. Phosphorylation and sequestration of serotonin transporters differentially modulated by psychostimulants. Science. 1999; 285:763-766.
30. Baganz NL, Lindler KM, Zhu CB, Smith JT, Robson MJ, Iwamoto H, Deneris ES,Hewlett WA,Blakely RD. A requirement of serotonergic p38alpha mitogen-activated protein kinase for peripheral immune system activation of CNS serotonin uptake and serotonin-linked behaviors. Transl Psychiatry. 2015; 5:e671.
31. Eaton MJ, Whittemore SR. Adrenocorticotropic hormone activation of adenylate cyclase in raphe neurons: Multiple regulatory pathways control serotonergic neuronal differentiation. J Neurobiol. 1995; 28:465-481.
32. Leenders AG, Sheng ZH. Modulation of neurotransmitter release by the second messenger-activated protein kinases: Implications for presynaptic plasticity. Pharmacol Ther. 2005; 105:69-84.
33. Ramamoorthy S, Giovanetti E, Qian Y, Blakely RD. Phosphorylation and regulation of antidepressant-sensitive serotonin transporters. J Biol Chem. 1998; 273:2458-2466.
34. Ansah TA, Ramamoorthy S, Montanez S, Daws LC, Blakely RD. Calcium-dependent inhibition of synaptosomal serotonin transport by the alpha 2-adrenoceptor agonist 5-bromo-N-[4,5-dihydro-1H-imidazol-2-yl]-6-quinoxalinamine (UK14304). J Pharmacol Exp Ther. 2003; 305:956-965.

(Received December 10, 2015; Revised December 17, 2015; Accepted December 21, 2015)

Original Article

DOI: 10.5582/bst.2015.01159

Knockdown of AT-rich interaction domain (ARID) 5B gene expression induced AMPKα2 activation in cardiac myocytes

Lisa Hirose-Yotsuya[1,*], Fumio Okamoto[1,2], Takahiro Yamakawa[1], Robert H. Whitson[1], Yoko Fujita-Yamaguchi[1,3], Keiichi Itakura[1]

[1] *Department of Molecular & Cellular Biology, Beckman Research Institute of City of Hope, Duarte, California, USA;*
[2] *Emergency Medicine and Cardiology of Takatsuki Red Cross Hospital, Osaka, Japan;*
[3] *Department of Diabetes Complications & Metabolism, Beckman Research Institute of City of Hope, Duarte, California, USA.*

Summary **This study demonstrated that ARID5B mRNA is present in mouse cardiomyocyte HL-1 cells, and that ARID5B siRNA constantly knocked down *ARID5B* gene expression to the 40% level of control. AMPKα2 protein was elevated in such ARID5B knockdown HL-1 cells, and this was accompanied by an increase in the level of phosphorylated AMPKα. Since AMPKα2 mRNA levels did not change in ARID5B knockdown cells, the stability of AMPKα2 protein was investigated using inhibitors for protein synthesis and proteasomal degradation. Treatment of HL-1 cells with either cycloheximide or MG132 caused an appreciable increase in the amount of AMPKα2 protein in ARID5B knockdown cells, which suggests that knockdown of ARID5B mRNA extends the half-life of AMPKα2 protein in HL-1 cells *via* yet unidentified mechanisms. As for the expected downstream consequences of AMPKα2 activation, we found thus far that glucose uptake, fatty acid uptake, or fatty acid oxidation remained unchanged in HL-1 cells after knockdown of ARID5B. Further studies are required to understand the mechanisms for ARID5B knockdown and resulting AMPKα2 activation, and also to identify which metabolic pathways are affected by AMPKα2 activation in these cells. In summary, this study provided the foundation for an *in vitro* cell culture system to study possible roles of ARID5B in cardiomyocytes.**

Keywords: Mrf-2, ARID5B, downregulation by siRNA, AMPKα2 activation, cardiac myocytes, HL-1 cells

1. Introduction

ARID5B (AT-rich interaction domain-containing protein 5B) was previously known as Mrf-2 (modulator recognition factor 2). It was identified in our laboratory in 1996 as a novel nuclear protein that binds to sequences upstream of the human cytomegalovirus major immediate-early enhancer/promoter and exerts repressor activity in undifferentiated human Tera-2 cells (*1*). Subsequent studies revealed the three-dimensional structure of the novel DNA-binding motif (ARID) of Mrf-2 and mechanisms of DNA recognition (*2-4*). The ARID family of DNA-binding proteins has grown since then to include fifteen proteins found in humans and most other vertebrate species, and six proteins found in *Drosophila* as well as proteins found in worms, fungi, plants and yeast (*5-8*). The ARID family is divided into six sub-families. In addition to a variety of roles as transcription factors in cell growth, differentiation, and development (*6*), a number of studies have suggested that proteins in most of the ARID sub-families are involved in cancer as tumor suppressors or promoters (*8*). A notable exception is the ARID5 sub-family which consists of two members, Mrf-1/ARID5A and Mrf-2/ARID5B (*7,8*). Mrf-2/ARID5B is expressed in various tissues including mouse cardiac and vascular tissues, where it seems to regulate smooth muscle cell differentiation and proliferation (*9*), lung, kidney, and brain as well as less abundantly in adrenal gland, spleen and thymus (*10*). Important roles of ARID5B in growth, immune, and sexual development have been

**Address correspondence to:*
Dr. Lisa Hirose-Yotsuya, Department of Molecular Metabolic Regulation, Diabetes Research Center, Research Institute National Center for Global Health and Medicine, 1-21-1 Toyama, Shinjuku-ku, Tokyo 162-8655, Japan (current address).
E-mail: ryotsuya@ri.ncgm.go.jp

suggested (*10*). While the role of ARID5B in cancer is still elusive, previous studies suggested that genetic variations in the *ARID5B* gene are associated with susceptibility to coronary atherosclerosis or type 2 diabetes in Japanese populations (*11,12*).

Targeted disruption of the ARID5B gene resulted in slower neonatal weight gains, high rates of mortality in neonates, and significant reductions in adult weight and adiposity (*13*). This suggested that ARID5B is essential for embryonic development and accumulation of lipids in postnatal life. Studies using mouse embryonic fibroblasts (MEFs) derived from *ARID5B*$^{-/-}$ embryos and *ARID5B*$^{+/+}$ littermate controls demonstrated that adipogenesis in *ARID5B*$^{-/-}$ MEFs was significantly lower than that in *ARID5B*$^{+/+}$ MEFs, but was restored when ARID5B was expressed in *ARID5B*$^{-/-}$ MEFs (*14*). Similarly, the expression of multiple adipogenic genes was inhibited following transient transfection of siRNA targeting ARID5B in 3T3-L1 cells (*14*). Since a role of ARID5B in the regulation of metabolism has been suggested (*11-13*), we investigated the potential involvement of ARID5B and AMP-activated protein kinase (AMPK) in the metabolism of cardiac myocytes.

AMPK has been known as a sensor and regulator of energy balance at the cellular level as well as at the whole body level by responding to hormonal and nutrient signals (*15-17*). Multiple AMPK subunit isoforms encoded by distinct genes were identified with two α subunits (α1 and α2), two β subunits (β1 and β2), and three γ subunits (γ1, γ2, and γ3) (*15,16*). The α subunit is a kinase which is activated by phosphorylation in response to an increase in the AMP:ATP ratio. Binding of AMP to the γ subunit of the AMPK αβγ complex induces conformational changes in the α subunit kinase leading to the critical Thr172 phosphorylation by its upstream kinases. Although the mechanisms of these signaling pathways are not fully understood, it has been well-documented that activation of AMPK in skeletal and cardiac muscles is induced by metabolic stress and whole-body energy status as well as the AMPK mimetic AICAR and diabetic drugs such as metformin (*15,18,19*).

Previous studies showed that AICAR increased glucose uptake in heart muscle, indicating that AMPK may be involved in GLUT4 translocation (*20*), and that AMPK and PI-3K/Akt had an additive effect on oxidative stress-mediated GLUT4 translocation in cardiac myocytes (*21*). Furthermore, mice lacking AMPKα2 or expressing dominant negative AMPKα2 inhibited the ischemia-induced stimulation of glucose uptake in cardiac myocytes (*22-24*). These studies strongly suggested that AMPKα2 plays an important role in regulating cardiac glucose metabolism and protecting the heart from metabolic stresses.

The current study tested the hypothesis that ARID5B plays a role in glucose metabolism *via* the AMPK signaling pathway in cardiac myocytes. We found that when siRNA was introduced to HL-1 cardiomyocytes, ARID5B mRNA was significantly reduced, and that the levels of both total and phosphorylated AMPKα2 subunit were significantly increased. The mechanism and functional consequences of the AMPKα2 activation induced by ARID5B knockdown in HL-1 cells were also investigated. Although not conclusive, this study provided a good model system for further studying the role of ARID5B knockdown in AMPKα2 signaling pathways.

2. Materials and Methods

2.1. *Materials*

Mouse HL-1 cardiomyocytes were provided by Dr. W. Claycomb (Louisiana State University Health Science Center, New Orleans, LA) (*25,26*). Claycomb medium, fetal bovine serum (FBS), penicillin-streptomycin, norepinephrine, L-glutamine, trypsin-EDTA, trypsin inhibitor, fibronectin, cytochalasin B, cycloheximide, and MG132 were purchased from Sigma-Aldrich. L-Ascorbic acid sodium salt was from Mallinckrodt. Opti-MEM and Lipofectamine® RNAiMAX Transfection Reagent were from Life technologies. Bacto gelatin, ON-TARGETplus Mouse ARID5B siRNA-SMART pool (siRNA), ON-TARGETplus Non-targeting Pool (control scramble RNA), Tris-HEPES gels, and 20× Tris-HEPES buffer for sodium dodecyl sulfate polyacrylamide gel electrophoresis (SDS-PAGE) were obtained from Thermo Fisher Scientific. Polyvinylidene difluoride (PVDF) membrane was from GE Healthcare Life Sciences. 10× TBS was from Bio-Rad. Non-fat milk was from Labscientific, Inc. HyGLO Chemiluminescent HRP Antibody Detection Reagent was from Denville Scientific Inc. 2-Deoxy-D-[^{3}H] glucose and [^{3}H]palmitic acid were from American Radiolabel Chemicals.

2.2. *Cell culture*

HL-1 cells were grown as monolayer cultures in flasks, dishes, and plates precoated with 2 μg/cm^2 fibronectin dissolved in 0.02% gelatin. HL-1 cells were maintained in Claycomb medium supplemented with 10% FBS, 2 mM L-glutamine, 0.1 mM norepinephrine (prepared freshly from 10 mM stock solution in 30 mM L-ascorbic acid), and 100 μg/mL penicillin-streptomycin. Cells were grown at 37˚C in an atmosphere of 5% CO_2. The medium was changed every other day.

2.3. *siRNA transfection*

The transfection procedure is summarized in Figure 1. We used a commercially-available mixture of four double-stranded siRNAs with the following sequences on the sense strand; 5'-acaauaacugugacgguaa-3',

5'-gugaugaguucgcgccaaa-3', 5'-cggagaagauccacgucaa-3', and 5'-gguccaugcuuaaacggau-3'. These siRNA's target exons 5, 4-plus- 5, 10, and 4, respectively of *ARID5B*. Cells were seeded in 24-well plates, 12-well plates, or 35 mm dishes (2.5×10^4 cells/cm^2), and transfected 24 h after seeding. At that time (40-50% confluence), the cells were incubated for 2-3 h in Claycomb medium without penicillin and streptomycin, then transfected with 50 nM siRNA or control scramble RNA using Lipofectamine® RNAiMAX Transfection Reagent. After 24 h, the medium was replaced by Claycomb medium without penicillin and streptomycin. Cells were used for molecular and cellular experiments at 48 h post-transfection. To confirm the effect of siRNA, cells were lysed with 700 μL of Qiazol (Qiagen), and RNA was isolated with Qiagen RNeasy®. ARID5B mRNA level was determined by quantitative real-time PCR as described in section 2.4.

2.4. *Quantitative real-time PCR*

Total RNA samples (1 μg) were reverse-transcribed with High-Capacity cDNA Reverse Transcription Kit (Life technologies), and the resulting cDNA samples were amplified with the specific primer pairs for mouse ARID5B and Rpl19 as a control housekeeping gene using iQ SYBR Green Super Mix (Bio-Rad). The sequences of specific primer pairs used were as follows. ARID5B forward, 5'-agaaaaacgcccatcgagc-3'; reverse, 5'-ctcccaggattaccacctaac-3' and Rpl19 forward, 5'-agcctgtgactgtccattcc-3'; reverse, 5'-gcagtacccttcctcttcc-3'. The reaction was performed using the following temperature cycles, initial denaturation at 95˚C for 10 min followed by 40 cycles of amplification at 95˚C for 10 sec and 56˚C for 30 sec (ARID5B), or 40 cycles of amplification at 95˚C for 10 sec and 61˚C for 30 sec (Rpl19). The mRNA expression level was determined using the CFX96 real-time detection system (Bio-Rad). Relative gene expression was calculated using the ΔΔCT method.

2.5. *Western blotting analysis*

At 48 h post-transfection, cells were washed twice with ice-cold PBS and lysed using ice-cold cell lysis buffer (50 mM HEPES, pH 7.4, containing 2 mM Na_3VO_4, 10 mM $Na_4P_2O_7$, 10 mM NaF, 2 mM EDTA 2Na, 2 mM EGTA, and 0.2 mM PMSF). After incubation on a shaker for 15 min at 4˚C, cell lysates were centrifuged at 14,000 rpm at 4˚C for 15 min. Protein concentrations in the cleared lysates were measured by BCA assay (Thermo Fisher Scientific). Samples of 10-20 μg were subjected to SDS-PAGE using Tris-HEPES gels and then transferred to PVDF membranes. The membranes were blocked with 5% non-fat milk in TBST buffer (TBS containing 0.1% Tween 20) for 1 h at room temperature. After blocking, membranes were incubated at 4˚C overnight with the following primary antibodies; anti-phospho-AMPKα (1:1000, #2535) and anti-AMPKα (1:1000, #2603) from Cell Signaling Technology, anti-AMPKα2 (1:1000, ab97275) from Abcam, anti-EFTUD2 (1:2000, 10208-1-AP) from Proteintech, and anti-GAPDH (1:10000, AM4300) from Ambion. Subsequently, the membranes were washed 3 times with TBST for 5 min and incubated with HRP-conjugated anti-rabbit IgG (#170-6515, Bio-Rad) or HRP-conjugated anti-mouse IgG (sc-2005, Santa Cruz) for 1 h at room temperature. Then, the membranes were washed 4 times with TBS containing 0.1% Tween 20 and 0.1% Triton X-100 for 5 min at room temperature, then incubated with HyGLO Chemiluminescent HRP Antibody Detection Reagent. The membranes were exposed to X-ray film, and the protein bands on the films were quantified using Image J software.

2.6. *Analysis of AMPKα2 protein stability*

HL-1 cells in 35 mm dishes were tranfected with siRNA as described in 2.3, and at 48 h post-transfection, the growth medium was changed to medium containing 5 μg/mL cycloheximide (CHX) or 10 μM MG132, a proteasomal degradation inhibitor. Cells were harvested at different time points after CHX or MG132 treatment, and AMPKα2 and GAPDH protein levels were determined by Western blotting.

2.7. *Glucose and fatty acid uptake assays in HL-1 cells*

Cells were grown in 24-well plates and transfected with siRNA as described in section 2.3. Cells were washed with KRPH buffer (130 mM NaCl, 4.7 mM KCl, 1.24 mM $MgSO_4$, 2.5 mM $CaCl_2$, 1 mM HEPES, 2.5 mM NaH_2PO4) once at 48 h post-transfection. Then cells were incubated in 250 μL of fresh KRPH buffer for 15 min at 37˚C. For the glucose uptake assay, HL-1 cells were incubated with [^{3}H]2-deoxy-D-glucose (10 μM; 137.5 μCi/well) for 10 min at 37˚C. The incubation medium was aspirated, then the cells were washed four times with ice-cold PBS and solubilized by adding 100 μL of 0.5 M NaOH to each well. Aliquots of the cell extracts were transferred to vials for scintillation counting. In order to determine the level of non-specific background, cells in replicate wells were pre-treated with 20 μM cytochalasin B for 15 min at 37˚C, incubated with [^{3}H]2-deoxy-D-glucose, and processed in the same way. Aliquots of the same cell extracts were used for determining protein concentrations by BCA assay. Results were calculated as pmol of glucose uptake per min per mg of protein.

For fatty acid uptake assays, cells were incubated for 15 min at 37˚C in KRPH buffer, and [^{3}H] palmitic acid (40 μM; 10.5 μCi/well) was added to each well. After a 20 min-incubation at 37˚C, the medium was removed, the cells were washed 4 times with ice-cold

PBS, and solubilized with 100 μL of 0.5 M NaOH per well. The radioactivity in both the incubation medium and the cell lysate from each well were measured by scintillation counting. The percentage of fatty acid uptake was calculated by dividing ^{3}H in the cell lysate by total ^{3}H from both the cell lysate and incubation medium.

2.8. *Positron Emission Tomography (PET) for glucose uptake in the heart of ARID5B knockout mice*

Animal studies were approved by the City of Hope Animal Care and IACUC. Generation of the total body *ARID5B* knockout mice has been previously described (*13*). Mice were housed in a temperature-controlled environment with a 12 h light: 12 h dark cycle and allowed *ad libitum* access to standard chow and water.

Thirty two week-old male mice were used for these experiments. The ^{18}F-flurodeoxyglucose (^{18}F-FDG) radio-tracer was obtained from the City of Hope radio-pharmacy. The mice were imaged at the City of Hope Small Animal Imaging Core on two days: On the first day, two *ARID5B*$^{-/-}$ males and one *ARID5B*$^{+/+}$ male littermate control were imaged; on the second day, one *ARID5B*$^{-/-}$ male and two *ARID5B*$^{+/+}$ male littermate controls were imaged. The average weight for the *ARID5B*$^{-/-}$ males was 25.7 ± 4.0 grams; the average weight for the *ARID5B*$^{+/+}$ males was 41.3 ± 4.1 grams ($p < 0.05$). Prior to imaging, the mice were placed in individual cages with Sani-chip bedding, and fasted overnight (from 5:30 PM to 9:00 AM). The mice were placed in a cage with a warming light for 15 min prior to injection *via* the tail vein with 121-177 μCi of ^{18}F-FDG, and then moved to cages without warming lights for uptake periods of 58-60 min. Following the uptake period, tail regions of the mice were imaged for 2 min to insure that there was no extravasation of the tracer from the injection site. The mice were imaged for 10 min while under isoflurane anesthesia. Following the imaging scans, the mice were euthanized under isoflurane, and various organs and tissues were harvested. The tissue samples were weighed, and the ^{18}F in each sample was measured using a gamma counter. The CPM values were corrected for the radioactive decay that occurred in the interval following the injection. Imaging data were analyzed using the ASI-Pro software package. Specific uptake values in the heart were estimated as follows. The PET images were rotated so that a series of transverse optical sections of the heart could be analyzed. In each optical section both the heart plus the enclosed blood space and the blood space alone were analyzed by defining the appropriate regions of interest. The volume of heart tissue was calculated as the volume of heart-plus-blood minus the volume of blood alone. Similarly, the total DPM of ^{18}F per cc in the heart was as calculated by subtracting the blood space values from the heart-plus-blood space values. Specific uptake values are expressed as (DPM/cc tissue)/(injected dose in μCi/ml blood). The blood volume was calculated as 5.85% of total body weight.

2.9. *Statistics*

Data are expressed as mean ± SEM. Differences were evaluated by two-tailed Student *t* test. Statistical significance was set at $p < 0.05$.

3. Results

3.1. *ARID5B gene expression was reduced in HL-1 cardiomyocytes by siRNA*

The siRNA transfection protocol as schematically illustrated in Figure 1 was used throughout this study.

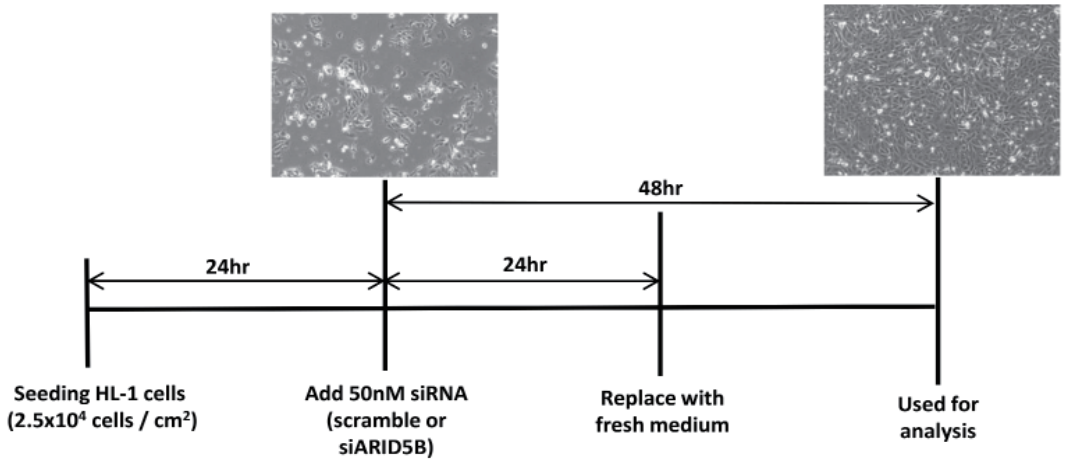

Figure 1. Schematic diagram of the siRNA transfection protocol used in this study. HL-1 cardiomyocytes were seeded in 24-well plates, 12-well plates, or 35 mm dishes with a density of 2.5×10^4 cells/cm^2. Cells were cultured for 24 h to reach 40-50% confluence (inset, left panel) before transfection of siRNA or control scramble RNA as described in Methods. At 24 h post-transfection (inset, right panel), the medium was replaced with fresh medium to allow HL-1 cells to recover. At 48 h post-transfection, cells were subjected to various analyses.

HL-1 cardiomyocytes were cultured for 24 h to allow them to attach to the plates (Figure 1 insets, left panel) before being treated with siRNA or scramble RNA for 24 h. The transfection medium was replaced with fresh culture medium and the resulting HL-1 cardiomyocytes were subjected to cellular and molecular analyses at 48 h post-transfection (Figure 1 insets, right panel).

In each experiment, the level of ARID5B expression in HL-1 cells was determined by quantitative real-time PCR. The results of nine independent experiments showed that the mRNA level in cells treated with ARID5B siRNA was always ~38% of the value for cells treated with control scramble RNA (Mean ± SE: 37.7 ± 2.1 %, $n = 9$, $p < 0.001$). Results of representative experiments are shown in Figures 2A, 3A, 4A, and 5A. This indicates not only that ARID5B mRNA is present in HL-1 cells, but also that siRNA efficiently knocked down gene expression.

3.2. *Both AMPKα2 protein and AMPKα phosphorylation levels were elevated by knockdown of ARID5B mRNA*

After confirming siRNA downregulated ARID5B mRNA (Figure 2A), we determined AMPKα protein levels by Western blotting. As seen in Figure 2B, Western blotting analysis of cell lysates with anti-AMPKα1 or anti-AMPKα2 antibody clearly showed that the AMPKα2 protein level was significantly increased in cells transfected with ARID5B siRNA, but that no change was observed in the AMPKα1 protein level (Figure 2B). Quantiation of immunostained bands from four experiments revealed an average increase of 1.4-fold (1.4 ± 0.15, $n = 4$, $p < 0.05$) in AMPKα2 protein level (Figure 2C, right panel) but no change in the AMPKα1 protein level (Figure 2C, left panel).

The phosphorylation status of T172 of AMPKα was also determined by Western blotting using anti-phospho AMPKα. This monoclonal antibody was produced by immunizing animals with a synthetic phospho-peptide corresponding to amino acid residues surrounding Thr172 of human AMPKα protein. Because this amino acid sequence is conserved between mouse and humans and between AMPKα1 and AMPKα2 in both species, the antibody recognizes phospho-Thr172 in both AMPKα1 and AMPKα2. Thus, in order to assess AMPKα phosphoylation, the levels of total AMPKα protein (AMPKα1 plus α2)

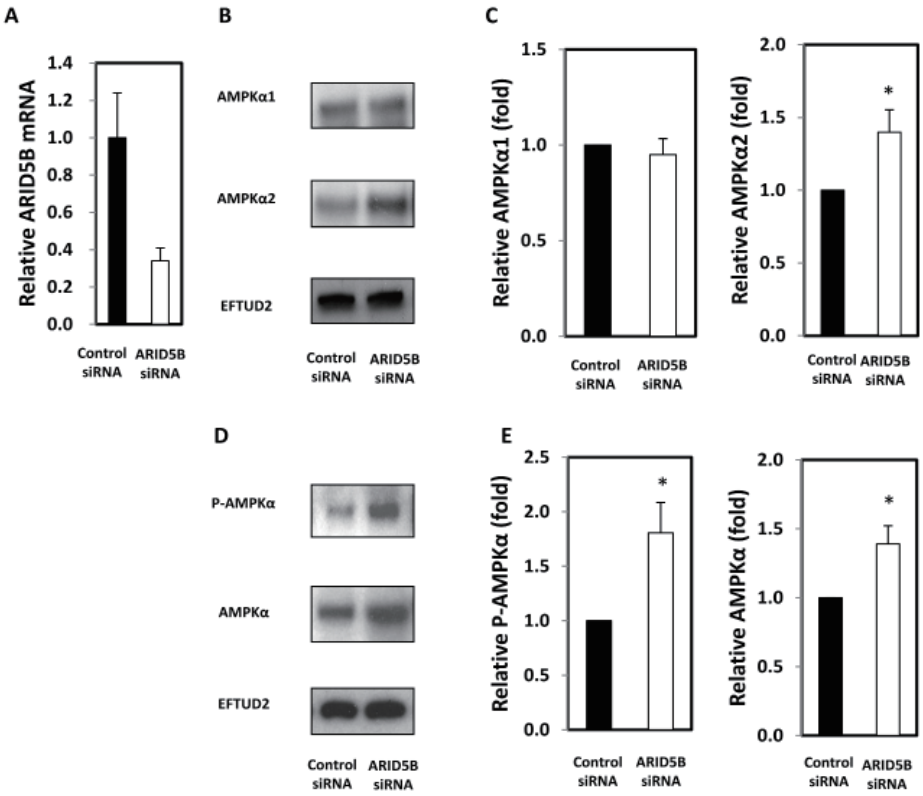

Figure 2. AMPK protein expression levels in control and ARID5B knockdown HL-1 cells. A: HL-1 cells were seeded in 12-well plates. siRNA efficiency was confirmed by qPCR at 48 h post-transfection. **B**: The levels of AMPK α1 and α2 proteins were examined by Western blotting with subunit-specific antibodies. Cell lysates (10-20 μg of protein per lane) were subjected to SDS-PAGE and immunoblotted as described in Methods. EFTUD2 was used as a loading control. A representative Western blotting result of four independent experiments is shown. **C**: Quantitation of AMPKα1 or α2 bands ($n = 4$; $^*p < 0.05$). **D**: Total AMPKα protein and total AMPKα phospho-protein levels were examined by Western blotting. Cell lysates (10 μg protein per lane) were subjected to SDS-PAGE and blotted with primary antibodies as described in Methods. EFTUD2 was used as a loading control. A representative result of four independent experiments is shown. **E**: Quantification of AMPKα or phospho-AMPKα bands as shown in **D** ($n = 4$; $^*p < 0.05$). In **A**, **C**, and **E**, shown are results from control (■) and ARID5B siRNA experiments (□).

and the combined levels of phosphorylated AMPKα1 plus α2 were measured by Western blotting. Figure 2D clearly shows an increase in the amount of total AMPKα protein. Since the experiments shown in Figures 2B and 2C indicate that AMPKα2 increases while AMPKα1 does not, it is clear that the increase in total AMPKα protein is due solely to the increase in AMPKα2. Figure 2E (right panel) revealed the increase in total AMPKα (1.4 ± 0.13 -fold, $n = 4$, $p < 0.05$), which is consistent with the increase in AMPKα2 shown in Figure 2C (right panel). Figure 2D and E clearly show that the increase in total phospho-AMPKα (1.8 ± 0.28 -fold, $n = 4$, $p < 0.05$) is also significant and even greater than the increase in total AMPKα. Although other possibilities must be considered, these results, taken together, strongly suggest that ARID5B knockdown resulted in the increase in AMPKα2 protein and in phospho-AMPKα2, which is indicative of AMPKα2 activation.

3.3. *Knockdown of ARID5B mRNA extended the half-life of AMPKα2 protein*

In order to understand the mechanisms by which ARID5B knockdown increases AMPKα2 levels, we first compared AMPKα2 mRNA levels in cells transfected with siRNA or control scramble RNA. The results showed no difference (data not shown), which suggested that ARID5B is not involved in transcriptional regulation of AMPKα2. Next, we investigated the stability of AMPKα2 protein. Cells transfected with siRNA or control scramble RNA (Figure 3A) were subjected to treatment with cycloheximide (CHX) or MG132, and their effects on inhibition of AMPKα2 protein synthesis or proteasomal degradation were measured. A representative result from two CHX experiments is shown in Figures 3B and 3C. In the absence of CHX, the level of AMPKα2 protein was elevated by ARID5B knockdown HL-1 cells by more than 2-fold (compare Figure 3B lanes 1 and 5). In the presence of CHX the level of AMPKα2 protein declined rapidly at 30 min, then recovered slowly over the next 2 h in the control cells (Figure 3B lanes 1-4). In contrast, the levels of AMPKα2 protein remained elevated in ARID5B knockdown cells for 1 h, even when compared to the levels of AMPKα2 protein in control cells in the absence of CHX (compare Figure 3B lanes 1 to lanes 6 and 7). These results suggest that AMPKα2 protein appears more stable when ARID5B mRNA level is reduced.

When cells were treated with 10 μM MG132, a slight increase in AMPKα2 protein was seen in the control cells after 4 and 8 h-incubation (Figures 3D and 3E). This indicated that AMPKα2 protein is being accumulated in HL-1 cells due to the inhibition of proteasome-mediated protein degradation as expected. In siRNA-transfected cells, a significant elevation of

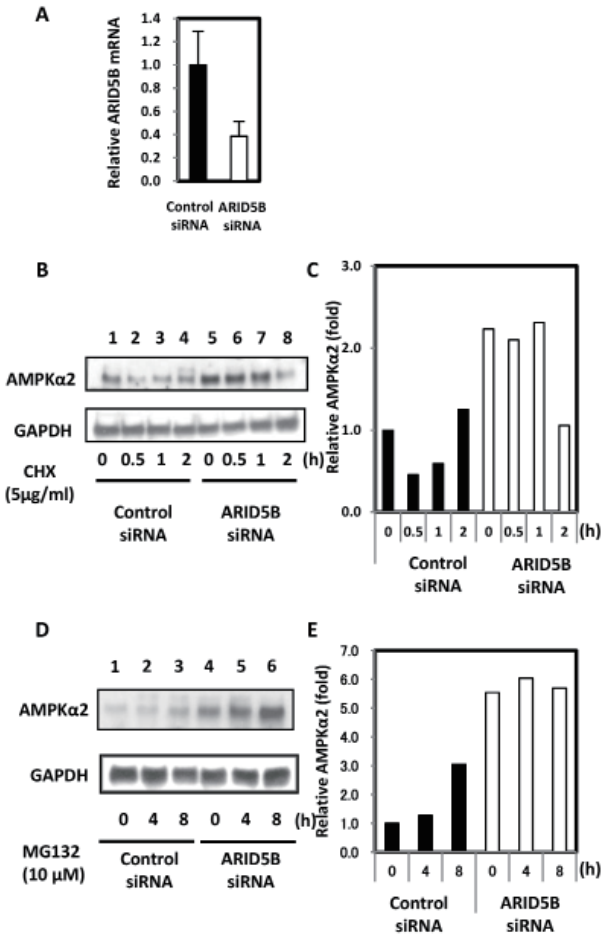

Figure 3. Knockdown of ARID5B increases the half-life of AMPK α2 protein. A representative result of two independent experiments is shown. **A**: HL-1 cells were seeded in 35 mm dishes. siRNA efficiency was confirmed by qPCR at 48 h post-transfection. **B**: At 48 h post-transfection, HL-1 cells were treated with cycloheximide (CHX) (5 μg/mL) for 0, 0.5, 1, or 2 h to block protein synthesis. Cell lysates were prepared and 20 μg protein per lane was immunoblotted with anti-AMPKα2 antibody. GAPDH was used as a loading control. **C**: Quantification of AMPKα2 bands as shown in **B**. **D**: At 48 h post-transfection, HL-1 cells were treated with 10 μM MG132 for 0, 4, or 8 h. Then cell lysates were prepared and 20 μg protein per lane was immunoblotted with anti-AMPKα2 antibody. GAPDH was used as a loading control. **E**: Quantification of AMPKα2 as shown in **D**. In **A**, **C**, and **E**, shown are results from control (■) and ARID5B siRNA experiments (□).

AMPKα2 protein (an average of 4-fold at 0 h) was observed, again confirming the results described in section 3.2. The effect of MG132 was also seen in an accumulation of AMPKα2 protein after 4 or 8 h-incubation but to a lesser extent (Figures 3D and 3E), which may indicate that the AMPKα2 protein expression had already saturated at 0 h of MG132 treatment in cells when ARID5B mRNA was knocked down.

The results shown in Figure 3 thus suggested that knockdown of ARID5B mRNA most likely extended the half-life of AMPKα2 protein. It remains to be answered how ARID5B controls the stability of AMPKα2 protein.

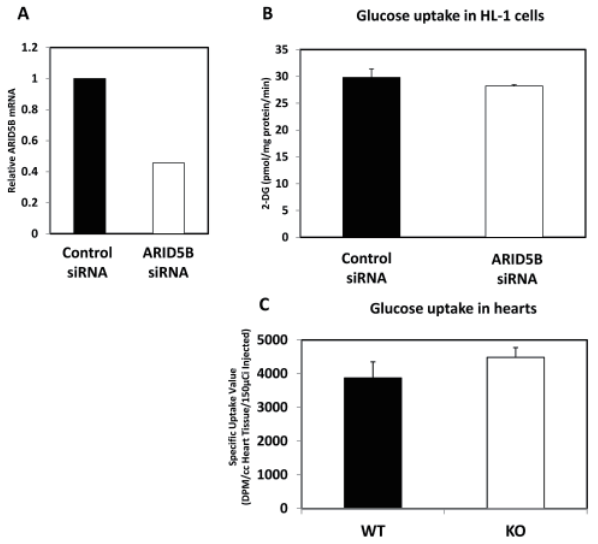

Figure 4. Glucose uptake in ARID5B knockdown HL-1 cells and in the hearts of wild-type and ARID5B knockout mice. A: HL-1 cells were seeded in 24-well plates. siRNA efficiency was confirmed by qPCR at 48 h post-transfection. RNA was isolated from three wells of a 24-well plate and the combined samples were analyzed for mRNA expression levels as described in Methods. **B**: At 48 h post-transfection, the cells were washed with KRPH buffer, and incubated with 2-deoxy-D-[^{3}H]glucose for 10 min. Then cells were lysed with 0.5 M NaOH and radioactivity in the cell lysate was measured by scintillation counting. Results were calculated as pmol of glucose uptake per min per mg of protein (n = 3 per each group). In **A** and **B**, shown are results from control (■) and ARID5B siRNA experiments (□).**C**: PET imaging of heart tissue in *ARID5B*$^{-/-}$ and *ARID5B*$^{+/+}$ male mice. Three mice each of genotype were injected with ^{18}F-flurodeoxyglucose and imaged after a 1 h uptake period. PET images of each heart were analyzed, and the specific uptake values were calculated as described in Methods. Shown are results from wild-type (WT) control (■) and ARID5B knockout (KO) experiments (□).

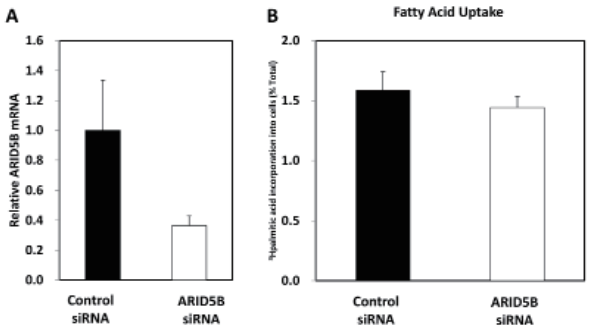

Figure 5. Fatty acid uptake in control and ARID5B knockdown HL-1 cells. A: HL-1 cells were seeded in 24-well plates. siRNA efficiency was confirmed by qPCR at 48 h post-transfection. **B**: HL-1 cells were seeded in 24-well plates and at 48 h post-transfection HL-1 cells were incubated for 15 min at 37˚C in KRPH buffer, then incubated with [^{3}H] palmitic acid for 20 min. Incubation medium was collected and the cells were lysed with 0.5 M NaOH. ^{3}H in the incubated medium and cell lysate was measured by scintillation counting. [^{3}H] palmitic acid incorporation into cells was calculated as described in Methods and is shown as percentage of total (n = 6 for control; n = 10 for ARID5B siRNA). Shown are results from control (■) and ARID5B siRNA experiments (□).

3.4. *Glucose uptake in ARID5B knockdown HL-1 cells and hearts of ARID5B knockout mice*

Next, we investigated possible physiological consequences of high levels of activated AMPKα2 protein which is considered to be a sensor and regulator of energy balance at the cellular level. Since AMPKα2 activation clearly occurs in the ARID5B knockdown cells, glucose uptake, one of possible physiological change, was measured in cells transfected with siRNA and control scramble RNA. The results, which are summarized in Figures 4A and 4B, did not show any significant differences in glucose uptake in those cells, however. Glucose uptake in HL-1 cardiomyocytes did respond to the AMPK mimetic AICAR which we used for control experiments. When added at 0.5 mM to the media 1 h prior to glucose uptake experiments, AICAR stimulated glucose uptake in non-treated and scramble RNA-treated cells increased 1.2 ± 0.13 (n = 3, p > 0.05) and 1.3 ± 0.03 (n = 3, p < 0.01)-fold, respectively. These effects, though small, positively demonstrated the correlation of glucose uptake and AMPK activation in HL-1 cells.

In order to investigate whether a decrease in ARID5B expression affects glucose uptake in live animals, positron emission tomography (PET) for glucose uptake in the hearts of wild-type and *ARID5B* knockout mice (n = 3) was performed. Although some tendency of a slight increase was observed in glucose uptake in the hearts of *ARID5B* knockout mice as compared to that in the hearts of wild type mice, the difference was not statically significant (Figure 4C).

3.5. *Fatty acid uptake in ARID5B knockdown HL-1 cells*

Generally speaking, the adult heart utilizes fatty acids as its main energy source (*27*). Thus, it can be speculated that fatty acid utilization may be affected by ARID5B knockdown. No difference in fatty acid uptake was, however, observed between control and ARID5B knockdown HL-1 cells (Figure 5).

4. Discussion

We demonstrated that siRNA efficiently knocked down *ARID5B* gene expression (to an average of 38% of control levels) in mouse cardiomyocyte HL-1 cells. AMPKα2 protein levels were elevated in ARID5B knockdown HL-1 cells, and this was accompanied by an increase in the phosphorylation of AMPKα2. Thus, in short, this study provided the foundation for an *in vitro* cell culture system to study possible roles of ARID5B in cardiomyocytes. This experimental *in vitro* cell culture may be useful in studying cardiac metabolism in pathophysiological conditions such as diabetic cardiomyopathy (*28*).

It has been well documented that activation of AMPK increases glucose uptake. Specifically, activation of AMPK *via* AICAR increased glucose uptake in

heart muscle (*20*) and in cardiac myocytes (*21*). Mice lacking AMPKα2 or expressing dominant negative AMPKα2 showed an inhibition of ischemia-induced stimulation of glucose uptake in cardiac muscle (*22-24*). In HL-1 cells it has been shown that insulin or the AMPK activator oligomycin stimulated glucose uptake by inducing translocation of GLUT4 (*30*). Adiponectin treatment also enhanced glucose and fatty acid uptake in HL-1 cells, and these effects were accompanied by increased AMPK phosphorylation (*31*). Based on previous reports, AMPKα2 activation in ARID5B knockdown HL-1 cells would be expected to result in increase in glucose and/or fatty acid uptake. When the functional consequences of the AMPKα2 activation induced by ARID5B knockdown in HL-1 cells were evaluated, however, under the culture conditions used in this study, we did not observe changes in glucose uptake (Figure 4), glycolysis (data not shown), fatty acid uptake (Figure 5), and fatty acid oxidation (data not shown). Further studies are obviously required to identify which metabolic pathways are affected by AMPKα2 activation in HL-1 cells.

Since AMPKα2 mRNA levels were not affected by ARID5B knockdown in HL-1 cells, the stability of AMPKα2 protein was investigated using an inhibitor of protein synthesis (CHX) and an inhibitor of the proteasome degradation pathway (MG132). AMPKα2 protein levels remained significantly elevated for an hour following CHX treatment in ARID5B knockdown HL-1 cells, while AMPKα2 protein levels fell dramatically in control cells. These results indicated that ARID5B knockdown extends the half-life of AMPKα2 protein in HL-1 cells. On the other hand, MG132 increased AMPKα2 protein levels three-fold in control cells, but had no effect in ARID5B knockdown HL-1 cells. It should be noted that the level of AMPKα2 protein in MG132-treated control cells was only half that of untreated ARID5B knockdown cells, even after eight hours of treatment. Wang *et al*. showed that calorie restriction (CR) increased the protein level of AMPKα2 and phosphorylation of AMPKα2 in skeletal muscle of wild-type mice, and that these changes in skeletal muscle contributed to an increase in whole body insulin sensitivity (*32*). CR did not increase insulin sensitivity in *AMPKα2*$^{-/-}$ mice. They also demonstrated that CR serum increased the stability of AMPKα2 protein in C2C12 myoblasts by inhibiting ubiquitnation of AMPKα2 (*32*). Another study showed that life-long CR elicits a myocardial phenotype that is profoundly protected against ischemia/reperfusion injury, and that AMPK activation may play an important role in this process (*33*). It has been suggested that ubiquitination of AMPK in the heart may play a significant role in the etiology of cardiac diseases, and that this process presents an attractive target for developing novel therapies (*34*). In this regard, our finding that ARID5B may de-stabilize AMPKα2 protein in cardiomyocytes is intriguing. Whether or not the regulation of AMPK by ubiquitination is involved in this phenomenon requires further investigation.

In summary, this study provided the foundation for an *in vitro* cell culture system to study possible roles of ARID5B in cardiomyocytes. Further studies are required to understand the link between ARID5B knockdown and resulting AMPKα2 activation and the possible involvement of the ubiquitin proteasome system in AMPKα2 activation.

Acknowledgements

We thank Drs. W. Claycomb and M. Lam of LSU Health Science Center for providing us with HL-1 cells and very helpful instructions on culture conditions. The author (L H.-Y.) also thanks members of Dr. Itakura's laboratory for their continuous support and encouragement, and for Drs. M. Matsumoto and M. Kasuga at Research Institute National Center for Global Health and Medicine for their support.

References

1. Huang TH, Oka T, Asai T, Okada T, Merrills BW, Gertson PN, Whitson RH, Itakura K. Repression by a differentiation-specific factor of the human cytomegalovirus enhancer. Nucleic Acids Res. 1996; 24:1695-1701.
2. Yuan YC, Whitson RH, Liu Q, Itakura K, Chen Y. A novel DNA-binding motif shares structural homology to DNA replication and repair nucleases and polymerases. Nature Structural Biology. 1998; 5:959-964.
3. Zhu L, Hu J, Lin D, Whitson R, Itakura K, Chen Y. Dynamics of the Mrf-2 DNA-binding domain free and in complex with DNA. Biochemistry. 2001; 40:9142-9150.
4. Whitson RH, Huang T, Itakura K. The novel Mrf-2 DNA-binding domain recognizes a five-base core sequence through major and minor-groove contacts. Biochem Biophys Res Commun. 1999; 258:326-331.
5. Kortschak RD, Tucker PW, Saint R. ARID proteins come in from the desert. Trends Biochem Sci. 2000; 25:294-299.
6. Wilsker D, Patsialou A, Dallas PB, Moran E. ARID proteins: A diverse family of DNA binding proteins implicated in the control of cell growth, differentiation, and development. Cell Growth Differ. 2002; 13:95-106.
7. Patsialou A, Wilsker D, Moran E. DNA-binding properties of ARID family proteins. NucleicAcids Res. 2005; 33:66-80.
8. Lin C, Song W, Bi X, Zhao J, Huang Z, Li Z, Zhou J, Cai J, Zhao H. Recent advances in the ARID family: Focusing on roles in human cancer. Onco Targets Ther. 2014; 7:315-324.
9. Watanabe M, Layne MD, Hsieh CM, Maemura K, Gray S, Lee ME, Jain MK. Regulation of smooth muscle cell differentiation by AT-rich interaction domain transcription factors Mrf2alpha and Mrf2beta. Circ Res. 2002; 91:382-389.
10. Lahoud MH, Ristevski S, Venter DJ, Jermiin LS, Bertoncello I, Zavarsek S, Hasthorpe S, Drago J, de Kretser D, Hertzog PJ, Kola I. Gene targeting of Desrt, a

novel ARID class DNA-binding protein, causes growth retardation and abnormal development of reproductive organs. Genome Res. 2001; 8:1327-1334.
11. Wang G, Watanabe M, Imai Y, Hara K, Manabe I, Maemura K, Horikoshi M, Kohro T, Amiya E, Sugiyama T, Fujita T, Kadowaki T, Yamazaki T, Nagai R. Genetic variations of Mrf-2/ARID5B confer risk of coronary atherosclerosis in the Japanese population. Int Heart J. 2008; 49:313-327.
12. Wang G, Watanabe M, Imai Y, Hara K, Manabe I, Maemura K, Horikoshi M, Ozeki A, Itoh C, Sugiyama T, Kadowaki T, Yamazaki T, Nagai R. Associations of variations in the MRF2/ARID5B gene with susceptibility to type 2 diabetes in the Japanese population. J Hum Genet. 2012; 57:727-733.
13. Whitson RH, Tsark W, Huang TH, Itakura K. Neonatal mortality and leanness in mice lacking the ARID transcription factor Mrf-2. Biochem Biophys Res Commun. 2003; 312:997-1004.
14. Yamakawa T, Whitson RH, Li SL, Itakura K. Modulator recognition factor-2 is required for adipogenesis in mouse embryo fibroblasts and 3T3-L1 cells. Mol Endocrinol. 2008; 22:441-453.
15. Steinberg GR, Kemp BE. AMPK in Health and Disease. Physiol Rev. 2009; 89:1025-1078.
16. Carling D. The AMP-activated protein kinase cascade – A unifying system for energy control. Trends Biochem Sci. 2004; 29:18-24.
17. Kahn BB, Alquier T, Carling D, Hardie DG. AMP-activated protein kinase: Ancient energy gauge provides clues to modern understanding of metabolism. Cell Metab. 2005; 1:15-25.
18. Merrill GF, Kurth EJ, Hardie DG, Winder WW. AICA riboside increases AMP-activated protein kinase, fatty acid oxidation, and glucose uptake in rat muscle. Am J Physiol. 1997; 273:E1107-12.
19. Zhou G, Myers R, Li Y, Chen Y, Shen X, Fenyk-Melody J, Wu M, Ventre J, Doebber T, Fujii N, Musi N, Hirshman MF, Goodyear LJ, Moller DE., Role of AMP-activated protein kinase in mechanism of metformin action. J Clin Invest. 2001; 108(8):1167-74.
20. Russell RR 3rd, Bergeron R, Shulman GI, Young LH. Translocation of myocardial GLUT-4 and increased glucose uptake through activation of AMPK by AICAR. Am J Physiol. 1999; 277:H643-649.
21. Horie T, Ono K, Nagao K, Nishi H, Kinoshita M, Kawamura T, Wada H, Shimatsu A, Kita T, Hasegawa K. Oxidative stress induces GLUT4 translocation by activation of PI3-K/Akt and dual AMPK kinase in cardiac myocytes. J Cell Physiol. 2008; 215:733-742.
22. Carvajal K, Zarrinpashneh E, Szarszoi O, Joubert F, Athea Y, Mateo P, Gillet B, Vaulont S, Viollet B, Bigard X, Bertrand L, Ventura-Clapier R, Hoerter JA. Dual cardiac contractile effects of the alpha2-AMPK deletion in low-flow ischemia and reperfusion. Am J Physiol Heart Circ Physiol. 2007; 292:H3136-H3147.
23. Russell RR 3rd, Li J, Coven DL, Pypaert M, Zechner C, Palmeri M, Giordano FJ, Mu J, Birnbaum MJ, Young LH. AMP-activated protein kinase mediates ischemic glucose uptake and prevents postischemic cardiac dysfunction, apoptosis, and injury. J Clin Invest. 2004; 114:495-503.
24. Xing Y, Musi N, Fujii N, Zou L, Luptak I, Hirshman MF, Goodyear LJ, Tian R. Glucose metabolism and energy homeostasis in mouse hearts overexpressing dominant negative alpha2 subunit of AMP-activated protein kinase. J Biol Chem. 2003; 278:28372-28377.
25. Claycomb WC, Lanson NA Jr, Stallworth BS, Egeland DB, Delcarpio JB, Bahinski A, Izzo NJ Jr. HL-1 cells: A cardiac muscle cell line that contracts and retains phenotypic characteristics of the adult cardiomyocyte. Proc. Natl. Acad. Sci. U S A. 1998; 95:2979-2984.
26. White SM, Constantin PE, Claycomb WC. Cardiac physiology at the cellular level: Use of cultured HL-1 cardiomyocytes for studies of cardiac muscle cell structure and function. Am J Physiol Heart Circ Physiol. 2004; 286:H823-829.
27. Kodde IF, van der Stok J, Smolenski RT, de Jong JW. Metabolic and genetic regulation of cardiac energy substrate preference. Comparative Biochemistry and Physiology Part A: Molecular & Integrative Physiology. 2007; 146:26-39.
28. An D, Rodrigues B. Role of changes in cardiac metabolism in development of diabetic cardiomyopathy. Am J Physiol Heart Circ Physiol. 2006; 291:H1489-506.
29. Palanivel R, Eguchi M, Shuralyova I, Coe I, Sweeney Gary. Distinct effects of short- and long-term leptin treatment on glucose and fatty acid uptake and metabolism in HL-1 cariomyocytes. Metabolism and Clinical Experimental. 2006; 55:1067-1075.
30. Schwenk RW, Dirkx E, Coumans WA, Bonen A, Klip A, Glatz JF, Luiken JJ. Requirement for distinct vesicle-associated membrane proteins in insulin- and AMP-activated protein kinase (AMPK)-induced translocation of GLUT4 and CD36 in cultured cardiomyocytes. Diabetologia. 2010; 53:2209–2219.
31. Piñeiro R, Iglesias MJ, Gallego R, Raghay K, Eiras S, Rubio J, Diéguez C, Gualillo O, González-Juanatey JR, Lago F. Adiponectin is synthesized and secreted by human and murine cardiomyocytes. FEBS Lett. 2005; 579:5163-5169.
32. Wang P, Zhang RY, Song J, Guan YF, Xu TY, Du H, Viollet B, Miao CY. Loss of AMP-activated protein kinase-α2 impairs the insulin-sensitizing effect of calorie restriction in skeletal muscle. Diabetes. 2012; 61:1051-1061.
33. Edwards AG, Donato AJ, Lesniewski LA, Gioscia RA, Seals DR, Moore RL. Life-long caloric restriction elicits pronounced protection of the aged myocardium: A role for AMPK. Mech Ageing Dev. 2010; 131:739-742.
34. Zungu M, Schisler JC, Essop MF, McCudden C, Patterson C, Willis MS. Regulation of AMPK by the ubiquitin proteasome system. Am J Pathol. 2011; 178:4-11.

(Received November 20, 2015; Revised December 20, 2015; Accepted December 20, 2015)

Original Article

DOI: 10.5582/bst.2015.01161

Overexpression of C35 in breast carcinomas is associated with tumor progression and lymphnode metastasis

Kun Yin[1,*], Zaihua Ba[2,*], Chenchen Li[1], Chao Xu[1], Guihua Zhao[1], Song Zhu[1], Ge Yan[1,]**

[1] *Shandong Academy of Medical Sciences, Shandong Institute of Parasitical Disease, Jining, Shandong, China;*
[2] *Jining Medical University, Jining, Shandong, China.*

Summary **To investigate C35 protein expression in breast carcinoma and to investigate its clinicopathological significance, a total of 68 cases of breast carcinoma and 20 cases of normal breast tissue samples were obtained from the clinic. Protein expression of C35, ER, PR and HER-2 were determined using immunohistochemistry. The correlations between C35 expression and clinicopathological parameters were analyzed on the basis of individual clinicopathologic records. Overexpression of C35 was detected in 56 of 68 (82.35%) breast carcinoma samples and only 3 of 20 (15%) normal breast tissue samples, and frequency of C35 expression was significantly associated with clinical Tumor Node Metastasis staging and Scarff-Bloom-Richardson grade ($p < 0.05$), but was not related to patients age, menstrual status and tumor diameter. C35 expression was positively related with the expression of HER-2 ($r = 0.207$), whereas negatively related with the expression of ER and PR. Further, C35 was prevalent in all four molecular subtypes of breast carcinoma with no significant difference of expression frequency. However, they have significant differences in lymphatic metastasis cases compared to the non-metastasis cases ($p < 0.05$). Since C35 protein was extensively expressed in all stages of breast carcinoma, and was closely associated with tumor progression and lymph node metastasis, it might be used as a reliable biomarker or therapeutic target for diagnosis and treatment.**

Keywords: C35, breast carcinoma, biomarker, expression, clinicopathologic correlation

1. Introduction

Breast carcinoma (BC) is the most common malignant cancer in women living in China at present. According to the statistics from the Fan *et a*l. report published in 2014, the incidence of BC in China is increasing rapidly, more than 1.6 million people were diagnosed and 1.2 million people died of BC each year, and the newly diagnosed cases account for 12.2% (*1*). The increasing incidence of BC is associated with the residents increasing socioeconomic status and unique reproductive patterns. Additionally, higher incidence and younger patients occur in high-income cities such as Beijing, Shanghai and Tianjin (*2*). Notably, delays in diagnosis and inherent subjectivity involved in histopathology lead to a more advanced stage of this disease, thus effective biomarkers are introduced into the clinic to improve tumor classification and diagnosis of this disease.

Currently, three molecular biomarkers progesterone (PR), estrogen (ER) receptors, and human epidermal growth factor receptor-2 (HER-2) are systematically assessed and applied in clinical practice (*3*). However, all these traditional biomarkers have suboptimal effects on the treatment of BC, since the disease is caused by the accumulation of multiple molecular alterations (*4*). C35 is a newly identified biomarker of BC, also termed C17orf37, is located within the minus region of human chromosome 17q12 bounded by the oncogene *ERBB2* and the growth factor receptor-bound protein 7 (*GRB7*) genes, and encodes a 12kDa membrane-anchored protein (*5*). By comparing 10 kinds of human mammary carcinoma cell lines and 38 kinds of normal tissue cells, Evans *et al*. reported that C35 was highly expressed in 7 kinds of carcinoma cell lines but barely expressed in normal cells except for Leydig cells (*5*). Overexpression of C35 was also detected in other cancer cells and tissues

*These authors contributed equally to this works.
***Address correspondence to:*
Dr. Ge Yan, Shandong Academy of Medical Sciences, Shandong Institute of Parasitical Disease, 11 Taibai Middle Road, Jining 272033, China.
E-mail: yange1965@163.com

such as colorectal cancer and prostate cancer (*6,7*). The conserved canonical immunoreceptor tyrosine-based activation (ITAM) motif located in its C-terminal end and the last four amino acids CVIL of C35 were proved to have an important role in cancer progression and metastasis (*7,8*). These studies suggested that C35 functions as an oncogene and highlight biomarker in breast cancer cell lines and has a potential application value in BC therapies. In this study, the extensive detection of C35 protein expression in 68 breast cancer tissues and 20 normal tissues was executed to investigate the clinicopathologic correlation, including differences of tumor types and age groups. The expression of C35 was also compared with the expression of the hormone receptor ER, PR and HER-2, in order to demonstrate the expression relationships among the genes; in addition, analysis of C35 expression pattern in different BC molecular subtypes was also evaluated.

2. Materials and Methods

2.1. *Source of sampless*

Cancer tissue samples and normal breast tissues were collected from the Second People's Hospital of Jining City in Shandong Province with the informed consent of patients, and were excised between July 2012 and January 2015. All of the 68 cancer samples were obtained from female inpatients and ranged in age from 34 to 81 years, with a mean and median age of 49 years. Normal tissue samples were derived from 20 cases of hyperplasia of mammary gland patients and mammary gland fibroma excision patients. Female patient age range was 17 to 38 years, with a median and mean age of 26.67 years. All of these samples were subjected to immunohistochemistry.

2.2. *Clinicopathologic characteristics of patients*

Inpatients involved in this study included 45 premenopausal patients and 23 postmenopausal patients. Samples ranged in degree of lymph node involvement, and included 43 axillary lymph node metastasis cases and 25 no metastasis cases. Of all the samples, 43 were invasive ductal carcinoma (IDC), 17 were invasive lobular carcinoma (ILC) and 8 were other carcinomas. Diameter of tumors ranged from 2.0 to 6.0 cm, 19 cases were less than 2 cm, 35 cases were 2~5cm and 14 cases were greater than 5 cm.

According to the clinical Tumor Node Metastasis (TNM) staging and confirmed by two qualified pathologists individually, samples were staged as 12 cases of stage I, 32 cases of stage II and 24 cases of stage III to IV. Samples were graded according to a modified Scarff-Bloom-Richardson (SBR) system by Elston Ellis, of which 14 were classified to Grade I (low malignant), 41 were classified to Grade II (moderate malignant), 13 were Grade III (highly malignant).

2.3. *Sample selection criteria*

Samples were selected according to four criteria: *1*) Have complete clinical and pathological records; *2*) All samples have been confirmed to be the primary breast cancer after surgery; *3*) None of the patients received preoperative treatment such as neoadjuvant chemotherapy, endocrinotherapy and radiotherapy; *4*) Surgical procedures included radical mastectomy, modified radical mastectomy and breast-conserving therpy plus axillary lymph node dissection. The study protocol was approved by the Hospital Ethics Review Committee.

Samples were excluded according to the following two criteria: *1*) Abandon bilateral primary breast cancer cases and complicated patients with other malignant tumor; *2*) According to National Comprehensive Cancer Network (NCCN) guidelines, abandon patients who have been undergoing postoperative treatment such as chemotherapy, radiotherapy and endocrine therapy in terms of their tumor stage and hormone receptor level.

2.4. *Immunohistochemistry*

Samples were fixed with 10% paraformaldehyde and made into 4 μm paraffin embedded serial sections. Immunohistochemical streptavidin-biotin complex (SABC) staining was performed according to the instruction of SABC immunohistochemical detection kit (Boster Biological Technology, Wuhan, China) rabbit anti-C35 polyclonal antibody (ZSGB-BIO, Beijing, China) at 1:100 dilution and rabbit anti-ER, PR and HER-2 monoclonal antibodies (Boster, Wuhan, China) at 1:20 dilution were used in this study.

ER and PR tumors were defined as positive only when the brownish yellow granules appeared in the cell nucleus. C35 positive staining was defined as when the brown or brownish yellow granules appeared in cell membrane. A final manual immunohistochemistry grade was devised by adding the staining score and positive proportion score together. The staining scores were evaluated according to the staining intensity as follows: 0 for unstained cells, 1 for cells stained pale yellow, 2 for cells stained brownish yellow, 3 for cells stained brown. Scores of 0 were considered negative, scores of 1 were considered weakly positive, scores of 2 were considered moderately positive, and scores of 3 were considered strongly positive. The positive proportion of stained cells was calculated according to semi-ration standard using cell counting estimation, and the method was as follows: first the highest intensity of tissue staining was found at low magnification, then a total of 100 cells were counted under five high power fields (HPF for 400×) to calculate the proportion of positive cells, and the positive proportion score was established on the basis of the following criteria: 1 for 0-10%, 2 for 10-25%, 3 for 26-50%, and 4 for > 50%

cell staining. The final positive grades were shown as 0~2 for (−), 3 for (+), 4~5 for (++) and 6 for (+++).

Cells stained brown or brownish yellow in plasma membrane or partly stained in cytoplasm were defined as HER-2 positive, while only cytoplasm staining should be defined as nonspecific staining. Positive immunohistological grades of HER-2 cells was assessed by the following standard: (−) for negative or nonspecific staining; (+) for > 10% discontinuous membrane coloration; (++) for > 10% with moderate intensity of membrane coloration consecutively; (+++) for > 10% with strong intensity of membrane coloration consecutively.

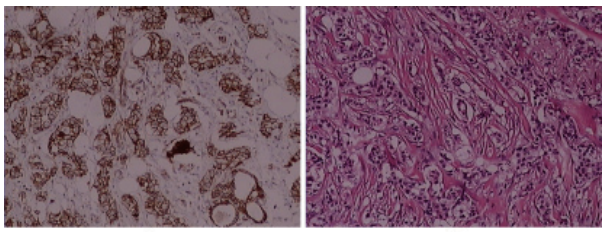

Figure 1. Immunohistochemistry of tissues derived from breast carcinomas and normal breast epithelia. C35 expression profile can be observed by SABC staining. (A) Breast carcinomas tissues stained intensely with a brownish yellow granules pattern for strong positivity of C35. **(B)** Negative expression of C35 in normal breast tissues. Magnification, ×100.

2.5. *Statistical analysis*

Statistical analysis was performed using the Statistical Package for the Social Sciences (SPSS) 18.0 (USA). A possible correlation between C35 expression and clinicopathological parameters was assessed using a chi-square (χ^2) test or Fisher's exact test. Differences with a p value less than 0.05 were considered to be statistically significant.

3. Results

3.1. *Expression of C35 protein in breast Carcinoma*

The overexpression of C35 protein in human breast carcinoma specimens was detected by immunohistochemical SABC staining of 68 breast cancers and 20 normal breast tissues. Results indicated that expression of C35 was mainly localized at the plasma membrane of breast cancer cells, with profiles of brown or brownish yellow granules, as shown in Figure 1A. At the same time, no positive staining existed in mesenchymal cells. For normal breast epithelium tissue, in contrast, only a minimal number of cells showed weakly positive staining, as shown in Figure 1B. The positive proportion of C35 expression in breast carcinomas and normal breast tissues was 82.35% (56/68) and 15.00% (3/20) respectively, with a statistically significant difference between the two

Table 1. Correlation between C35 positive expression and clinicopathological parameters

Clinicopathological parameters	C35, *n*	C35 (+)	C35 (−)	Positive rate (%)	χ^2	*p* value[a]
Age (year)						
≤ 50	36	31	5	86.1	0.744	0.389
> 50	32	25	7	78.1		
Menstrual status						
Regular status	45	39	6	86.7	0.939	0.333
Pausimenia	23	17	6	73.9		
Tumor diameter (cm)						
≤ 2 cm	19	15	4	78.9	0.562	0.755
2-5 cm	35	30	5	85.7		
> 5cm	14	11	3	78.6		
TNM stage[b]						
I	12	5	7	41.7	16.608	0.000**
II	32	29	3	90.6		
III + IV	24	22	2	91.7		
SBR grade[c]						
I	14	7	7	50.0	14.947	0.001**
II	41	39	2	95.1		
III	13	10	3	76.9		
Pathological type						
IDC	43	37	6	86.0	4.485	0.106
ILC	17	11	6	64.7		
Other	8	5	3	62.5		
Armpit Lymph node metastasis						
Yes	43	39	4	90.7	4.151	0.042*
No	25	17	8	68.0		

[a]), *$p < 0.05$; **$p < 0.01$. [b]), C35 (+) in the TNM stage columns: the differences between I and II, I and III + IV stages with *p* values less than 0.05, the difference between II and III + IV stages with a *p* value less than 0.01. [c]), C35 (+) in the SBR grade columns: the differences between I and II, I and III grades with *p* values less than 0.05, the difference between II and III + IV stages with a *p* value more than 0.05.

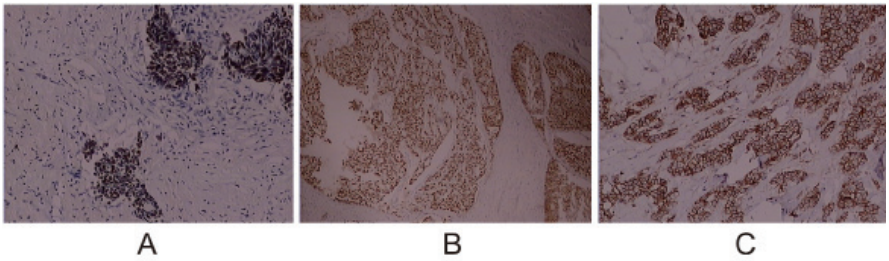

Figure 2. Expression of the other three biomarkers as determined by immunohistochemical SABC staining of the same BC samples used in C35 detection. (A) Positivity of ER and **(B)** PR tissues was stained with brownish yellow granules in cell nucleus. (C) Positivity of HER-2 tissues was stained with brownish yellow granules in plasma membrane or partly stained in cytoplasm. Magnification, ×100.

Table 2. Correlation between ER, PR and HER-2 positive expression and clinicopathological parameters

Clinicopathological parameters	*n*	ER(+)	χ^2	*p* value[a]	PR(+)	χ^2	*p* value[a]	HER-2(+)	χ^2	*p* value[a]
Age (year)										
≤ 50	36	17	0.082	0.774	16	0.337	0.561	26	2.658	0.103
> 50	32	14			12			17		
Menstrual status										
Regular status	45	23	1.636	0.201	15	3.379	0.066	35	0.002	0.964
Pausimenia	23	8			13			18		
Tumor diameter (cm)										
≤ 2 cm	19	11	1.816	0.403	9	0.493	0.782	8	6.784	0.034*
2-5 cm	35	15			14			23		
> 5cm	14	5			5			12		
TNM stage[b]										
I	12	9	10.847	0.004**	6	9.300	0.010*	6	6.526	0.038*
II	32	17			18			26		
III + IV	24	5			4			11		
SBR grade[c]										
I	14	11	9.077	0.011*	10	7.405	0.025*	6	9.275	0.010*
II	41	17			15			31		
III	13	3			3			6		
Pathological type										
IDC	43	24	6.070	0.048*	19	5.485	0.065	27	1.002	0.606
ILC	17	6			7			11		
Other	8	1			2			5		
Armpit Lymph node metastasis										
Yes	43	14	8.006	0.005**	13	5.783	0.016*	32	6.292	0.012**
No	25	17			15			11		

[a]), $*p < 0.05$; $**p < 0.01$. [b]), ER, PR and HER-2 (+) in the TNM stage columns: the differences between I and II, I and III + IV stages with *p* values less than 0.05, the difference between II and III + IV stages with a *p* value more than 0.05. [c]), ER, PR and HER-2 (+) in the SBR grade columns: the differences between I and II, I and III grades with *p* values less than 0.05, the difference between II and III + IV stages with a *p* value more than 0.05.

groups ($\chi^2 = 31.731$, $p < 0.01$).

3.2. *Correlations between C35 expression and clinicopathological parameters*

As the positive C35 staining results show in Table 1, C35 expression increases with tumor TNM stage and SBR grade progression. The expression of C35 among different clinical stages ($\chi^2 = 16.608$, $p < 0.01$) was significantly different, as well as in different histopathological grades ($\chi^2 = 14.947$, $p < 0.01$). In addition, increasing C35 was more prevalent among BC patients with regional armpit lymph node metastasis (90.7%) than in BC patients without lymph node metastasis (68.0%) ($\chi^2 = 4.151$, $p < 0.05$). However, a similar expression frequency of C35 was detected both in IDC and ILC, with no statistically significant difference ($\chi^2 = 4.485$, $p = 0.106$). Similarly, there was no significant association between C35 expression and other clinicopathological parameters such as age, menstrual status and tumor diameter ($p > 0.05$).

3.3. *Expression of ER, PR and HER-2 in Breast Carcinoma*

Expression of ER, PR and HER-2 detected by SABC staining are shown as Figure 2. The positive rate of ER, PR and HER-2 were 45.59 % (31/68), 41.18 % (28/68) and 63.24% (43/68) of total BC specimens respectively. Expression of ER, PR and HER-2 were analogously

Table 3. Relationships between C35 expression and expression of ER, PR and HER-2 in breast carcinoma

Groups	*n*	C35 (+)	C35 (-)	χ^2	*p* value	*r* value
ER						
positive	31	21	10	12.800	0.000	-0.035
negative	37	35	2			
PR						
positive	28	22	6	19.600	0.000	-0.083
negative	40	34	6			
HER-2						
positive	43	38	5	7.348	0.007	0.207
negative	25	18	7			

Table 4. Relationships between C35 expression and molecular subtypes of breast carcinoma

Molecular subtype	*n*	C35 (+)	C35 (-)	χ^2	*p* value
Luminal A subtype	26	21	5	2.922	0.404
Luminal B subtype	22	17	5		
Basal-like subtype	9	7	2		
HER-2 subtype	11	11	0		

associated with tumor SBR grade, TNM stage and lymph node metastasis, with a significant difference ($p < 0.05$) respectively. The increasing positive rate of HER-2 also can be seen in the advanced TNM stage and SBR grade, as well as in larger size of tumors ($p < 0.05$). When compared with different pathological types of BC, however, the expression of HER-2 was concordant in IDC and ILC ($p > 0.05$) whereas a significant difference was observed in ER paralleling tests ($p < 0.05$). Likewise, the expression of those three biomarkers show also no significant difference with patients age and menstrual status ($p > 0.05$), as shown in Table 2.

3.4. *Relationships between expression of C35 and other biomarkers*

Table 3 shows the relationships between expression of C35 and the other three biomarkers ER, PR and HER-2. Correlation analysis showed that the expression of C35 in BC samples has a positive correlation to the expression of HER-2 ($\gamma = 0.207$), whereas has negative correlations to the expressions of hormone receptors ER ($\gamma = -0.035$) and PR ($\gamma = -0.083$).

3.5. *Relationships between C35 expression and molecular subtypes of breast carcinoma*

To detect relationships between C35 and BC molecular subtypes, all of the 68 samples were divided into four main subtypes by immunohistochemistry (*9*). The molecular subtype criterion were as follows: *1*) Luminal A subtype: HER-2 negative but ER and/or PR positive (HER-2−/ER+ or HER-2−/PR+); *2*) Luminal B subtype: HER-2 positive, ER and/or PR positive (HER-2+/ER+/PR+ or HER-2+/ER−/PR+ or HER-2+/ER+/PR−); *3*) Basal-like subtype: ER, PR and HER-2 all negative (HER-2−/ER−/PR−); *4*) HER-2 subtype: only HER-2 positive (HER-2+/ER−/PR−). Table 4 shows that there was no significant difference between multiple molecular subtypes of BC and C35 positive expression according to chi square test result ($\chi^2 = 2.922$, $p > 0.05$).

4. Discussion

Recently, molecular biomarkers have been introduced to overcome the inherent subjectivity of BC involved in histopathology, such as ER, PR and HER-2 (*10*), and therapists tend to formulate a pointed therapeutic plan on the basis of biomarker expression results. Slamon *et al*. (*11*) reported that HER-2 protein overexpression can merely be detected in 13-20% of IDC patient tissues, and the expression levels rise with the increase of tumor clinical stage and histological grade. Moreover, overexpression of HER-2 was associated with improved clinical outcomes (*12*). Clinical trials have demonstrated that patients with HER-2 (+) BC could achieve a satisfactory therapeutic effect by using a humanized monoclonal antibody against HER-2 (trastuzumab) (*13*). However, the proportion of HER-2 protein overexpression patients is only 20-40 % (*11*), which limited the clinical use of trastuzumab in the majority of patients without HER-2+ BC. At the same time, the cytotoxicity of trastuzumab on the heart narrows the pool of candidates eligible for HER2-directed therapies (*13,14*).

TAM has been established as one of the most effective drugs in estrogen receptor-dependent BC treatment, and has been widely used as the first-line of anti-tumor drugs. Nevertheless, recent findings have shown that the frequent occurrence of drug resistance against TAM substantially reduced its anti-tumor efficacy, and the resistance mechanism of TAM remains unclear (*15*).

Consistent with previous study (5), our results demonstrated that a high level of C35 protein was frequently expressed in BC cells and tissues compared to normal breast cells, and the expression intensity difference was up to 10 times greater, thus it became a new attractive BC biomarker. In this study, the positive rate of C35 protein (82.35%) is higher than the other three biomarkers ER, PR and HER-2 at all stages. Increased expression level of C35 during tumor progression was also detected when correlating with SBR grade and TNM stage. Simultaneously, our results indicated that durative expression of C35 was associated with the clinical and pathological features of BC, since a higher positive rate was found in lymph node metastatic tumor tissues. Our results suggested that C35 expression might play an important role in tumor progression and lymphatic metastasis, in agreement with the conclusion presented previously

(*7,16,17*). Although these features were not independent prognostic factors, they were also associated with poor clinical outcome. At the same time, Dasgupta S *et al*. also indicated that down regulation of C35 results in reduced expression of MMP-9, uPA and VEGF in prostate cancer cells (*7*), which have been reported to be positively correlated with poor prognosis (*18*). Therefore C35 shows potential as a prognostic indicator for BC. In combination with previous results, C35 is involved in cancer cell migration and metastasis by prenylation of its C-terminal CAAX motif (*16*), has a functional role in prostate cancer infiltration (*7*) and drug resistance of ovarian (*17*) cancer, and hence might be a more appropriate and reliable biomarker for tumor diagnosis and prognosis, and is also likely to be a new therapeutic target for cancer treatment.

Our results found that C35 expression was independent of age and menstrual status of patients, but needs further evidence from similar research work using a larger panel of patients. In the present study, the positive rate of C35 expression was significantly higher than previous work (*5*), these differences might be related to clinicopathological factors. A majority of samples in this work occurred in advanced histological grade and clinical stage, or in BC with lymph node metastasis, which may attribute to a higher score for C35 expression.

Based on the previous study (*5*), C35 was strongly associated with the expression of HER-2 protein and inversely associated with clinical pathological features of BC such as pathological grade, clinical stage and lymphatic metastasis, and the frequency of C35 was higher than HER-2 at all stages (*14*), which was consistent with our results. At the same time, the correlation between C35 expression and four BC molecular subtypes was irrelevant ($p > 0.05$) in this study, and the expression of C35 highly overlapped the other three biomarkers, which indicated that C35 was prevalent in all those BC molecular subtypes.

In conclusion, our findings indicate that high frequency of C35 expression could occur in all stages of BC, has a significant correlation with the clinicopathological factors including disease progression and lymphatic metastasis, and is also positively related to traditional biomarker HER-2, suggesting C35 has a great potential to be a reliable diagnostic marker, or to develop a new C35-targeted therapy in the clinical treatment of BC.

Acknowledgements

This work was supported by grants from the National Natural Science Foundation of China (81041075, 31300617), the Science and Technology Development Program of Shandong Province (2006GG2302011), and the Natural Science Foundation of Shandong Province (ZR2015YL024, Q2007D04).

References

1. Fan L, Strasser-Weippl K, Li JJ, St Louis J, Finkelstein DM, Yu KD, Chen WQ, Shao ZM, Goss PE. Breast cancer in China. Lancet Oncol. 2014; 15:279-289.
2. Zheng G, Peng F, Ding R, Yu Y, Ouyang Y, Chen Z, Xiao Z, He Z. Identification of proteins responsible for the multiple drug resistance in 5-fluorouracil-induced breast cancer cell using proteomics analysis. J Cancer Res Clin Oncol. 2010; 136:1477-1488.
3. Rakha EA, Reis-Filho JS, Ellis IO. Combinatorial biomarker expression in breast cancer. Breast Cancer Res Treat. 2010; 120:293-308.
4. Early Breast Cancer Trialists' Collaborative Group. Effects of chemotherapy and hormonal therapy for early breast cancer on recurrence and 15-year survival: An overview of the randomised trials. Lancet. 2005; 365:1687-1717.
5. Evans EE, Henn AD, Jonason A, Paris MJ, Schiffhauer LM, Borrello MA, Smith ES, Sahasrabudhe DM, Zauderer M. C35 (C17orf37) is a novel tumor biomarker abundantly expressed in breast cancer. Mol Cancer Ther. 2006; 5:2919-2930.
6. Dong X, Huang Y, Kong L, Li J, Kou J, Yin L, Yang J. C35 is overexpressed in colorectal cancer and is associated with tumor invasion and metastasis. Biosci Trends. 2015; 9:117-121.
7. Dasgupta S, Wasson LM, Rauniyar N, Prokai L, Borejdo J, Vishwanatha JK. Novel gene C17orf37 in 17q12 amplicon promotes migration and invasion of prostate cancer cells. Oncogene. 2009; 28:2860-2872.
8. Katz E, Dubois-Marshall S, Sims AH, Faratian D, Li J, Smith ES, Quinn JA, Edward M, Meehan RR, Evans EE, Langdon SP, Harrison DJ. A gene on the HER2 amplicon, C35, is an oncogene in breast cancer whose actions are prevented by inhibition of Syk. Br J Cancer. 2010; 103:401-410.
9. Perou CM, Sorlie T, Eisen MB, *et al*. Molecular portraits of human breast tumors. Nature. 2000. 406:747-752.
10. Rakha EA, Reis-Filho JS, Ellis IO. Combinatorial biomarker expression in breast cancer. Breast Cancer Res Treat. 2010; 120:293-308.
11. Slamon DJ, Clark GM, Wong SG, Levin WJ, Ullrich A, McGuire WL. Human breast cancer: Correlation of relapse and survival with amplification of the HER-2/neu oncogene. Science. 1987; 235:177-182.
12. Press MF, Finn RS, Cameron D, *et al*. HER-2 gene amplification, HER-2 and epidermal growth factor receptor mRNA and protein expression, and lapatinib efficacy in women with metastatic breast cancer. Clin Cancer Res. 2008; 14:7861-7870.
13. Ward S, Pilgrim H, Hind D. Trastuzumab for the treatment of primary breast cancer in HER2-positive women: A single technology appraisal. Health Technol Assess. 2009; 13:1-6.
14. Piccart-Gebhart MJ, Procter M, Leyland-Jones B, *et al*. Trastuzumab after adjuvant chemotherapy in HER-2 positive breast cancer. N Engl J Med. 2005; 353:1659-1672.
15. Ghayad SE, Vendrell JA, Larbi SB, Dumontet C, Bieche I, Cohen PA. Endocrine resistance associated with activated ErbB system in breast cancer cells is reversed by inhibiting MARK or PI3K/Akt signaling pathways. Int J Cancer. 2010; 126:545-562.

16. Dasgupta S, Cushman I, Kpetemey M, Casey PJ, Vishwanatha JK. Prenylated c17orf37 induces filopodia formation to promote cell migration and metastasis. J Biol Chem. 2011; 286:25935-25946.
17. Leung TH, Wong SC, Chan KK, Chan DW, Cheung AN, Ngan HY. The interaction between C35 and ΔNp73 promotes chemo-resistance in ovarian cancer cells. Br J Cancer. 2013; 109:965-975.
18. Sheng S. The urokinase-type plasminogen activator system in prostate cancer metastasis. Cancer Metastasis Rev. 2001; 20:287-296.

(Received November 26, 2015; Revised December 23, 2015; Accepted December 27, 2015)

Original Article

DOI: 10.5582/bst.2015.01170

Serum expression levels of miR-17, miR-21, and miR-92 as potential biomarkers for recurrence after adjuvant chemotherapy in colon cancer patients

Nikolay V. Conev[1,2,*], Ivan S. Donev[1,2,*,], Assia A. Konsoulova-Kirova[1,2], Trifon G. Chervenkov[3,4], Javor K. Kashlov[5,2], Krasimir D. Ivanov[6,7]**

[1] *Clinic of Medical Oncology, UMHAT "St. Marina", Varna, Bulgaria;*
[2] *Department of Propedeutics of Internal Diseases, Medical University of Varna, Bulgaria;*
[3] *Laboratory of Immunology, UMHAT "St. Marina", Varna, Bulgaria;*
[4] *Department of Pediatrics and Medical genetics, Medical University of Varna, Bulgaria;*
[5] *Department of Internal Medicine, UMHAT "St. Marina", Varna, Bulgaria;*
[6] *Clinic of Surgery, UMHAT "St. Marina", Varna, Bulgaria;*
[7] *Department of General and Operative Surgery, Medical University of Varna, Bulgaria.*

Summary **The present study examined whether miR-17, miR-21, miR-29a, and miR-92 that are dysregulated in colon cancer (CC) can serve as potential predictive markers for relapse of disease after radical surgery and adjuvant chemotherapy. Real-time reverse transcription quantitative polymerase chain reaction was used to measure the expression levels of the miRNAs in serum samples from 37 patients with CC and 7 healthy individuals, tested as a control group. The area under the receiver operating characteristic curve (AUC) was then used to evaluate the predictive performance of the four miRNAs alone or in combination and compare it with carcinoembryonic antigen. The expression of miR-17, miR-21 and miR-92 were significantly higher in serum of patients with disease relapse. The AUCs for miR-17, miR-21, miR-92 for Nx patients were 0.844, 0.948, and 0.935, respectively ($p < 0.05$). Combining the four miRNAs for stage III patients increased the diagnostic performance, yielding an AUC of 0.881, with a sensitivity of 83.3% and a specificity of 85.7% ($p < 0.05$). Our study suggests that the expression levels of serum miR-21, miR-17, and miR-92 in patients with CC who underwent radical surgery and adjuvant chemotherapy may have diagnostic value for differentiating between recurred and non-recurred patients.**

Keywords: miRNA, marker, relapse, Nx

1. Introduction

Colorectal cancer (CRC) is the most commonly diagnosed gastrointestinal cancer worldwide with more than 1.2 million new cases and 600,000 deaths annually (*1*). Oncological management of colon cancer patients is based on the initial clinical staging of the disease. For patients without metastatic disease (M0), surgery is the first option, used with curative intention. Unfortunately, for 20-30% of the patients the prognosis is poor due to recurrence of the disease (*2*). 5 Fluorouracil (5-FU) based chemotherapy is the standard adjuvant treatment. In stage III patients, the benefit from additional adjuvant chemotherapy is confirmed in several large-scale trials and they have about 40% lower risk of recurrence, compared to patients who were stated on observation (*3,4*). In stage II patients, adjuvant treatment remains controversial (*5,6*). Survival rate is usually complicated by the side effects of chemotherapy. This is mainly ascribed to the lack of reliable markers that could predict development of disease relapse. Therefore, identification of such markers would be greatly beneficial for the individualized chemotherapy of patients with a high risk for recurrence of the disease.

Disease relapses after surgery alone or combined

*These authors contributed equally to this works.
***Address correspondence to:*
Dr. Ivan Shterev Donev, Clinic of Medical Oncology, UMHAT "St. Marina", 1 "Hristo Smirnenski" Blvd., Varna 9000, Bulgaria.
E-mail: ivan_donev75@abv.bg

with adjuvant treatment for colon cancer are a function of both degree of bowel wall penetration of the primary lesion and nodal status (*7*). Nx category includes patients with unknown nodal status. Last Surveillance, Epidemiology, and End Results (SEER) population-based colon cancer analysis includes 130,762 patients with colon cancer, among which 14% (n = 18,312) were defined as Nx (*7*). Despite the large number of Nx cases, the potential benefit of chemotherapy is not known (*8*) and there are only a few biomarkers that could predict recurrence of the disease in this group of patients (*9*).

miRNAs are a class of short (18-23 nucleotides in length), endogenous, non-protein-coding RNAs that play critical roles in diverse biological processes through negative post-transcriptional regulation (*10,11*). miRNAs can function as oncogenes or tumor suppressors by repressing cancer-related genes (*11,12*). Alterations of miRNA expression have been observed in a variety of human tumors, including colon cancer, and it was discovered that miRNAs are stably present in circulating blood at sufficient levels for use as blood-based biomarkers (*13,14*). Thus, identification of novel serum-based miRNAs as biomarkers for response to therapy or tumor recurrence could improve the outcome of the disease.

In this study, we investigated the serum levels of four miRNAs involved in tumor cell proliferation (miR-17, miR-92), survival (miR-21), and metastasis (miR-29a) in colon cancer patients (*15*). Blood samples were collected immediately after completion of adjuvant chemotherapy. We aimed to monitor the tumor biological behavior and the prediction capacity of the serum levels of miR 17, miR-92, miR-21 and miR-29a for recurrence of the disease in one year period.

2. Materials and Methods

2.1. *Ethics statement*

All procedures were approved by the Scientific Research Ethics Committee of Medical University "Prof. Dr. Paraskev Stoyanov", Varna. Blood samples were collected from 37 colon cancer patients and 7 healthy volunteers at the Medical Oncology Clinic, University Hospital "St. Marina", Varna after obtaining informed consent form (ICF) from all study participants. All patients with indications for adjuvant chemotherapy were discussed for participation in our trial and only subjects who agreed to participate and signed ICF were included.

2.2. *Patient selection*

All subjects in the study were of Caucasian race. Controls were matched to colon cancer patients by age. The characteristics of patients and controls are represented in Table 1. We included patients with colon cancer stage II (n = 6) and III (n = 13) as per American Joint Committee on Cancer (AJCC) Cancer Staging Manual, 7th ed., who have undergone radical surgery in our hospital; there was no residual disease or compromised edges post-surgery and patients have completed 5-FU based adjuvant chemotherapy. 18 patients had Nx lymph node status because the involvement of lymph nodes could not be determined (less than 12 lymph nodes examined). We obtained serum after last cycle of adjuvant chemotherapy and patients started follow-up regularly (every 3 months) with computed tomography (CT) or positron emission tomography PET-CT until progression for 1 year of follow-up.

2.3. *RNA isolation and real-time PCR*

Total RNA was extracted from 200 μL serum, using the miRNeasy mini kit (Qiagen) following the manufacturer's instructions. 5.6×10^8 copies cel-miR-39 synthetic RNA per sample were used as spike-in control (Qiagen). The RNA was eluted in 14 μL nuclease-free water supplied with the kit. Small RNAs were reverse transcribed with miScript II RT kit (Qiagen), using 5 μL of the eluted RNA and HiSpec buffer. Before use, cDNA was diluted as recommended. Quantitative real-time PCR was done on the StepOne

Table 1. Demographic and clinical features of patients and healthy subjects

Patients	
Sex %	
Male	43.2 (n = 16)
Female	56.8 (n = 21)
Age at diagnosis (yrs., mean, S.D.)	
Male	63.50 (7.694)
Female	64.86 (7.009)
Total	64.27 (7.241) Min. 44, Max. 77
Tumor localization (N, %)	
Colon ascendens	8 (21.6)
Colon descendens	6 (16.2)
Sigma	23 (62.2)
Stage (N, %)	
II	6 (16.2)
III	13 (35.1)
Nx (Stage N/A)	18 (48.6)
Grade (N, %)	
Gr 1 + Gr 2	32 (86.5)
Gr 3	5 (13.5)
Recurrence (N, %)	
Non recurrence	24 (64.9)
Recurrence	13 (35.1)
Recurrence on stage (N, %)	
II (n = 6)	0 (0)
III (n = 13)	6 (46.2)
Nx (n = 18)	7 (38.9)
Controls	
Sex %	
Male	42.9 (n = 3)
Female	57.1 (n = 4)
Age (yrs., mean, S.D.)	
	56.29 (10.704) Min. 38, Max. 69

Plus (Applied Biosystems) with miScript Sybr Green PCR kit and miScript Primer Assays (Qiagen). Relative quantities (RQ) of target miRNAs were calculated using method by the StepOne Software v2.0. The results were normalized using the spike-in control cel-miR-39 as a reference target and were expressed as relative quantity to a single reference sample (*16*). The relative levels of miRNA were normalized to cel-miR-39 and were calculated using the equation $2^{-\Delta\Delta Ct}$. RQ values for miRNA-17, miRNA-21, miRNA-29a or miRNA-92 were then normalized to the average expression of each of these miRNAs in healthy individual (*17*). Greater than the median RQ values of miRNAs we denoted as high expression levels, and values below or equal to the median RQ we denoted as low expression levels.

2.4. *Clinical and pathological features*

We collected demographical data (sex and age at initial staging), date and extent of surgery, as well as tumor characteristics: localization, TNM classification, histology of tumor, total number of histologically examined lymph nodes, and grade of differentiation. Associations of serum miR-17, miR-21, miR-29a, and miR-92 expression with clinicopathological parameters are represented in Table S1 (*http://www.biosciencetrends.com/docindex.php?year=2015&kanno=6*).

2.5. *Statistical analysis*

Statistical analysis was carried out with SPSS Statistics v.23 using descriptive statistics. Categorical features were summarized with frequencies and percentages. The Mann-Whitney *U* test, Pearson correlation, and χ^2 test or Fisher's exact test were used for comparison and estimation of correlations between miRNAs expression levels and clinicopathological characteristics such as tumor stage and grade, and age. Specificity and sensitivity of serum miRNAs expression levels for discriminating patients with recurrent disease (recurred patients, RP) from patients with non-recurrent disease (non-recurred patients, NP) at 1 year of follow-up were evaluated with receiver operating curve (ROC) analysis. Diagnostic accuracy of biomarkers was also determined by obtaining the largest possible area under the curve (AUC) in ROC analysis. The best linear combination of miRNA markers in the sense that the area under the ROC curve of this combination is maximized among all possible linear combinations was calculated according to the method of Su and Liu (*18*). Kaplan-Meier survival curves and the log-rank test were used to compare the survival differences between groups. Although our study was not powered enough to compare different subgroups, hazard ratios (HRs) and corresponding 95% confidence intervals (CIs) were calculated by Cox regression models. Two-tailed *p*-values (< 0.05) were considered as significant.

3. Results

3.1. *Expression of miRNAs in NP, RP and control groups*

Relative miRNA expression levels in serum samples of colon cancer patients (n = 37) who underwent curative surgery were obtained by using cel-miR-39 as reference genes for normalization. Relative quantification (RQ) values, calculated by the $2^{-\Delta\Delta Ct}$ method were used for evaluation of expression in patients. The Mann-Whitney test showed that there were no significant differences of RQ values of all 4 miRNAs between the control and NP group. Both miR-21 and miR-92 showed significant expression level differences between RP group with control and NP group (Figures 1B and 1D). In contrast, miR-17 showed significant difference only between RP group and NP group, but not between RP group and control group (Figure 1A). Expression level of miR-29a did not differ between groups (Figure 1C).

3.2. *Expression of miR-21 differs between and within stages*

There were no significant differences of RQ values of all miRNAs in patients with stage II, stage III and Nx except for miR-21, which differed between patients with stage II and III (Figure 2). Within stage III patients, none of the 4 miRNAs expression levels were different between RP and NP groups. However, within the Nx patients all miRNAs except miR-29a had significant differences in expression levels between RP *vs.* NP groups (Figures 3A, 3B and 3D).

3.3. *miR-21, miR-17 and miR-92 alone discriminate RP and NP groups*

After 1 year follow-up post adjuvant chemotherapy none of patients with stage II disease experienced recurrence. Six patients with stage III disease and 7 patients with Nx experienced recurrence after 1 year of follow-up. ROC analysis was performed to explore the potential value of analyzed miRNAs expression levels as noninvasive diagnostic biomarkers for recurrence after adjuvant chemotherapy (Figure 4). miR-21 allowed most accurate discrimination (AUC = 0.901, 95% CI: 0.788-1, $p < 0.001$) between RP and NP groups. At the optimal cutoff values of RQ, the sensitivity was 84.6% and specificity was 79.2% (Figure 4B). miR-92 and miR-17 could also discriminate RP and NP groups with the following AUC = 0.885 (95% CI: 0.778-0.991, $p < 0.001$) and with 84.6% sensitivity and 70.8% specificity (Figure 4D) and AUC = 0.814 (95% CI: 0.658-0.971, $p = 0.002$) and with 84.6% sensitivity

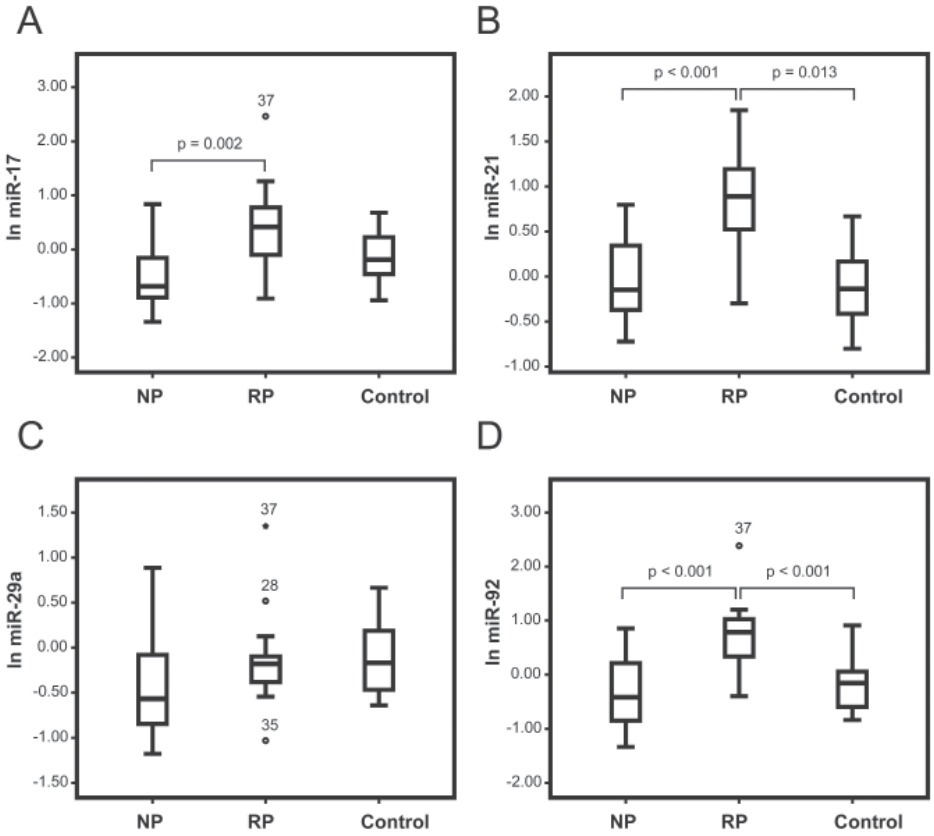

Figure 1. Box plots, representing serum miRNAs expression levels in NP (non-recurred patients), RP (recurred patients) and controls. Expression levels of miRNAs (scale of y axis: ln). The Mann-Whitney test was used to detect significant differences of RQ (relative quantities) values of all 4 miRNAs among control, NP and RP group. Two-tailed *p*-values (< 0.05) were considered as significant. **A**, miR-17; **B**, miR-21; **C**, miR-29a; **D**, miR-92.

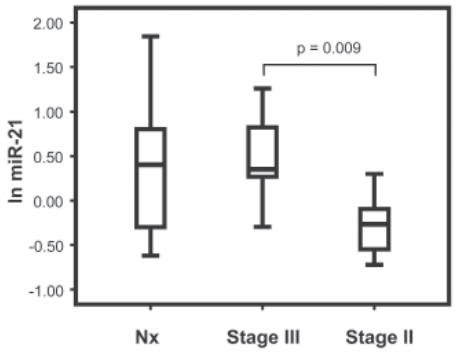

Figure 2. Box plots, representing serum miR-21 expression levels in patients with Nx, Stage III and II (scale of y axis: ln). The Mann-Whitney test was used to detect significant differences of RQ (relative quantities) values of miR-21 between Nx, Stage III and II. Two-tailed *p*-values (< 0.05) were considered as significant.

and 66.7% specificity (Figure 4A) at the optimal cutoff values of RQ, respectively. miR-29a discriminates RP and NP groups with the following AUC = 0.670 (95% CI: 0.493-0.846, $p = 0.092$) and with 53.8% sensitivity and 70.8% specificity at the optimal cutoff values of RQ, but the result did not reach statistical significance (Figure 4C). For comparison, carcinoembryonic antigen (CEA) after adjuvant chemotherapy has lower power to discriminate RP and NP groups AUC= 0.655 (95% CI: 0.472-0.839, $p = 0.123$) with 61.5% sensitivity and 62.5% specificity, but the result did not reach statistical significance (Figure 4E).

3.4. *miR-21, miR-17 and miR-92 alone or in combination discriminate RP and NP groups within stage III and Nx patients*

The potential value of analyzed miRNAs as biomarkers for recurrence after adjuvant chemotherapy within stage III and Nx patients is shown in Table 2. Because none of the studied biomarkers could discriminate accurately in stage III between RP and NP groups, we constructed multimarker ROC analysis. The combination of all 4 biomarkers discriminates RP and NP groups with the following AUC = 0.881 (95% CI: 0.655-1, $p = 0.022$) and with 83.3% sensitivity and 85.7% specificity at the optimal cutoff values of RQ (Figure 4F). In patients with Nx disease only expression levels of miR-29a were not good enough to discriminate between patients with recurrence and no recurrence of the disease (Table 2). CEA after adjuvant chemotherapy has similar power to discriminate recurrence in stage III and Nx patients (Table 2).

3.5. *No correlation of miRNA expression levels with disease free survival, age and CEA*

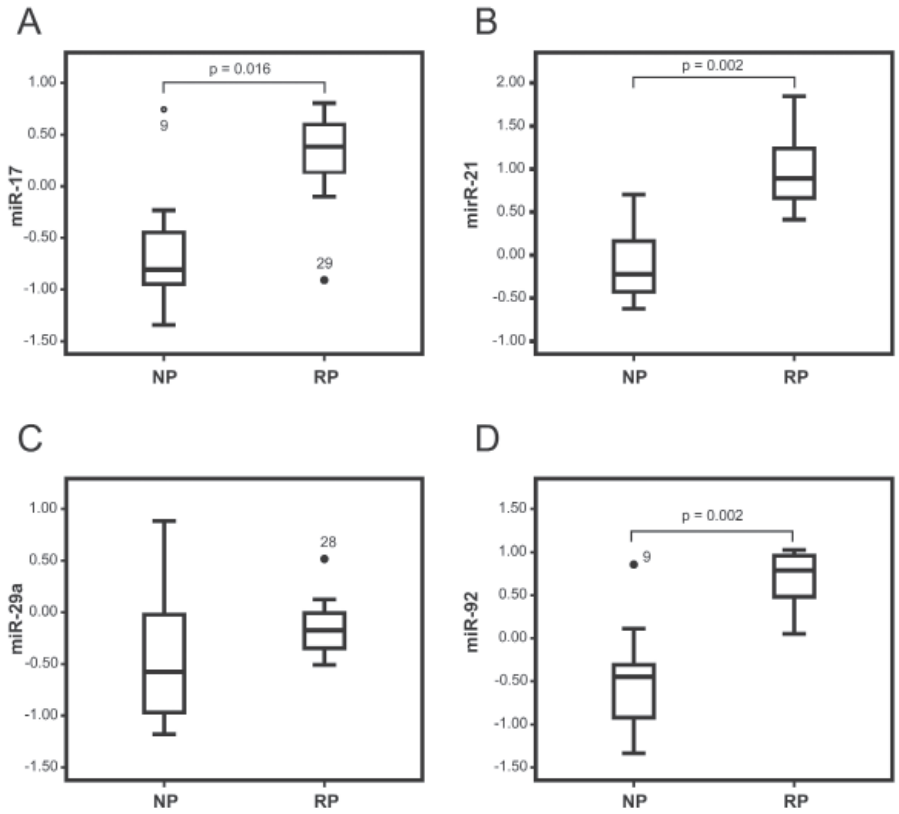

Figure 3. Box plots, representing serum miRNAs expression levels in Nx group in RP (recurred patients) and NP (non-recurred patients). Expression levels of miRNAs (scale of y axis: ln). The Mann-Whitney test was used to detect significant differences of RQ (relative quantities) values of all 4 miRNAs between NP and RP group. Two-tailed *p*-values (< 0.05) were considered as significant. **A**, miR-17; **B**, miR-21; **C**, miR-29a; **D**, miR-92.

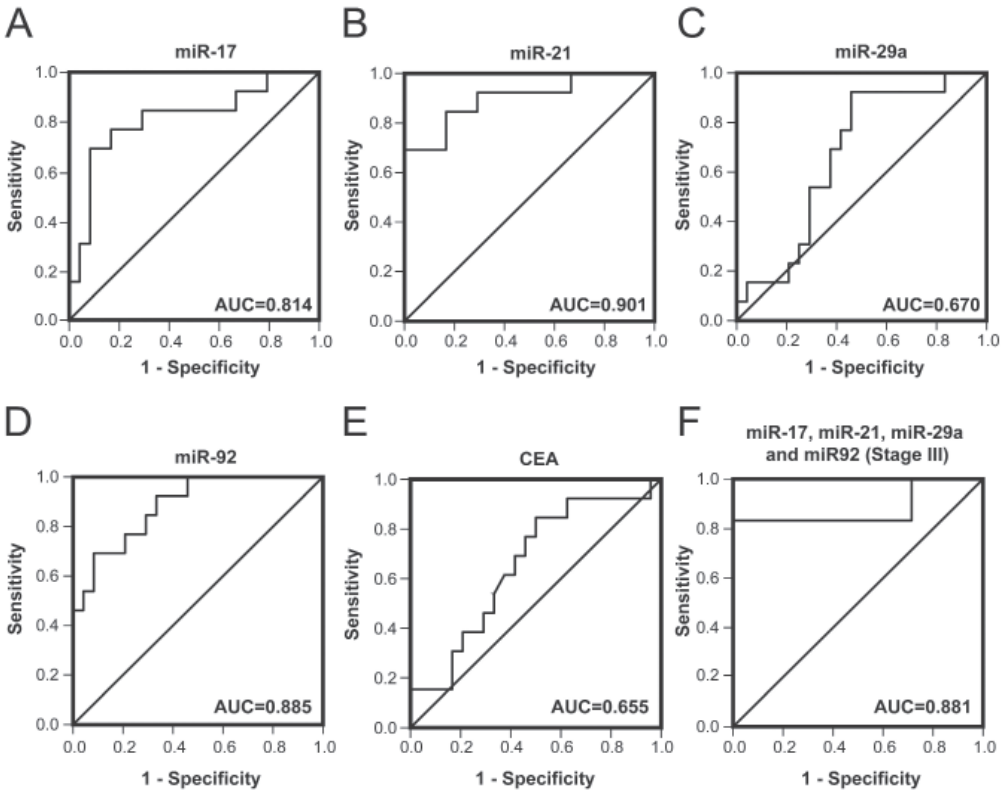

Figure 4. Receiver operating curve (ROC) curve analysis, using four miRNAs and CEA (carcinoembryonic antigen) to differentiate RP (recurred patients) from NP (non-recurred patients). Diagnostic accuracy of biomarkers was determined by obtaining the largest possible area under the curve (AUC) in ROC analysis. **A**, miR-17; **B**, miR-21; **C**, miR-29a; **D**, miR-92; **E**, CEA; **F**, Multimarker ROC analysis, using four miRNAs in stage III patients.

Table 2. Result from Receiver operating curve (ROC) analysis according to data by using four miRNAs and CEA (carcinoembryonic antigen) to differentiate RP (recurred patients) from NP (non-recurred patients)

Patients	Biomarkers	AUC (95% CI)	*p*-value	Sensitivity (%)	Specificity (%)
Stage III	miR-17	0.738	0.153	66.7	85.7
	miR-21	0.738	0.153	66.7	85.7
	miR-29a	0.452	0.775	50.0	42.9
	miR-92	0.786	0.086	66.7	85.8
	CEA	0.643	0.391	66.7	57.1
Nx	miR-17	0.844	0.016	85.7	81.8
	miR-21	0.948	0.002	85.7	81.8
	miR-29a	0.701	0.16	85.7	63.6
	miR-92	0.935	0.002	85.7	90.9
	CEA	0.662	0.258	71.4	59.5

Disease free survival (DFS) was calculated as the time from the date of surgery to the date of documented recurrence of the disease. Colon cancer patients with high expression levels of any miRNAs had no significant differences in DFS compared with those with low expression levels of miRNAs (Figure S1, *http://www.biosciencetrends.com/docindex.php?year=2015&kanno=6*). In univariate analysis, older age, stage of disease, sex, histologic grade and expression levels of miRNAs were not associated with poor 1 year DFS (Table S2, *http://www.biosciencetrends.com/docindex.php?year=2015&kanno=6*).

Pearson correlation tests did not detect significant correlation between the DFS and the serum levels of the miRNAs studied. We also did not observe correlation between age and expression levels of the studied miRNAs. Furthermore, none of the 4 miRNAs correlated with serum level of CEA after adjuvant chemotherapy. However, strong correlation was observed between miR-17 and miR-92 ($r = 0.971$, $p < 0.001$, Figure S2), moderate correlation between miR-21 and miR-92 ($r = 0.492$, $p = 0.002$, Figure S2, *http://www.biosciencetrends.com/docindex.php?year=2015&kanno=6*) and weak correlation between miR-17 and miR-21 ($r = 0.360$, $p = 0.029$, Figure S2).

4. Discussion

Previous studies have identified multiple circulating miRNAs that are differently expressed and dysregulated in colon cancer patients compared with control healthy people (*11,19,20*). Several lines of evidence have suggested that miRNAs might serve as potential biomarkers for the diagnosis and prognosis of patients with colon cancer (*19,21-23*).

The goal of our study was to identify potential biomarkers that could predict early recurrence after adjuvant treatment. Additionally we included in our analysis patients with unknown lymph node status (Nx patients). Usually dysregulated miRNAs are associated with wide variety of cancers (*24*). To increase the sensitivity and specificity of our assay we used miR-21, miR-17, miR-29a and miR-92 which have been shown to be upregulated in colon cancer patients (*25*). ROC analysis in our study showed that upregulation of any of miR-21, miR-92 and miR-17 in serum is an accurate biomarker and can distinguish colon cancer patients with recurrence from patients without recurrence with high sensitivity and specificity (Figure 4). In stage III patients, only the combination of all miRNAs reached statistically significant result in distinguishing RP from NP, which might be as a result of the small sample size. All miRNAs except miR-29a outperformed CEA serum levels in predicting recurrence. The sensitivity and specificity of ROC curve for prediction of recurrence on the basis of CEA only was low, which is consistent with other research (*26*).

Only a few studies have evaluated the expression levels of miRNAs after curative surgical resection of the primary tumor (*21,27,28*) and have looked for a diagnostic correlation between serum levels of miRNAs and post-adjuvant levels of CEA. In the present study the expression levels and the diagnostic significance of 4 circulating miRNAs (miR-17, miR-21, miR-29a and miR-92) from blood samples of colon cancer patients, who underwent radical surgery of the primary tumor and adjuvant chemotherapy were correlated with the serum levels of CEA (measured after end of adjuvant chemotherapy) and the stage of the disease.

Previous studies have found higher levels of circulating miR-17, miR-21, miR-29a and miR-92 as compared to healthy individuals and some of those miRNAs were associated with poor survival, independent of other clinicopathological factors (*28-31*). Among the most important target genes of miR-17 and miR-92 are the E2F family of transcription factors (Figure 5) that drive the progression from the G1 into the S phase of the cell cycle (*15*). Thus, increased levels of miR-17 and miR-92 promote tumor cell proliferation. Crucial target of miR-21 is PTEN (phosphatidylinositol-3,4,5-trisphosphate 3-phosphatase) which negatively regulates the PI3K (phosphatidylinositol-4,5-bisphosphate 3-kinase) pathway (*15*). As a result, increased level of miR-21 promotes tumor cell survival (Figure 5). In one study it was shown that the serum levels of miR-21 statistically

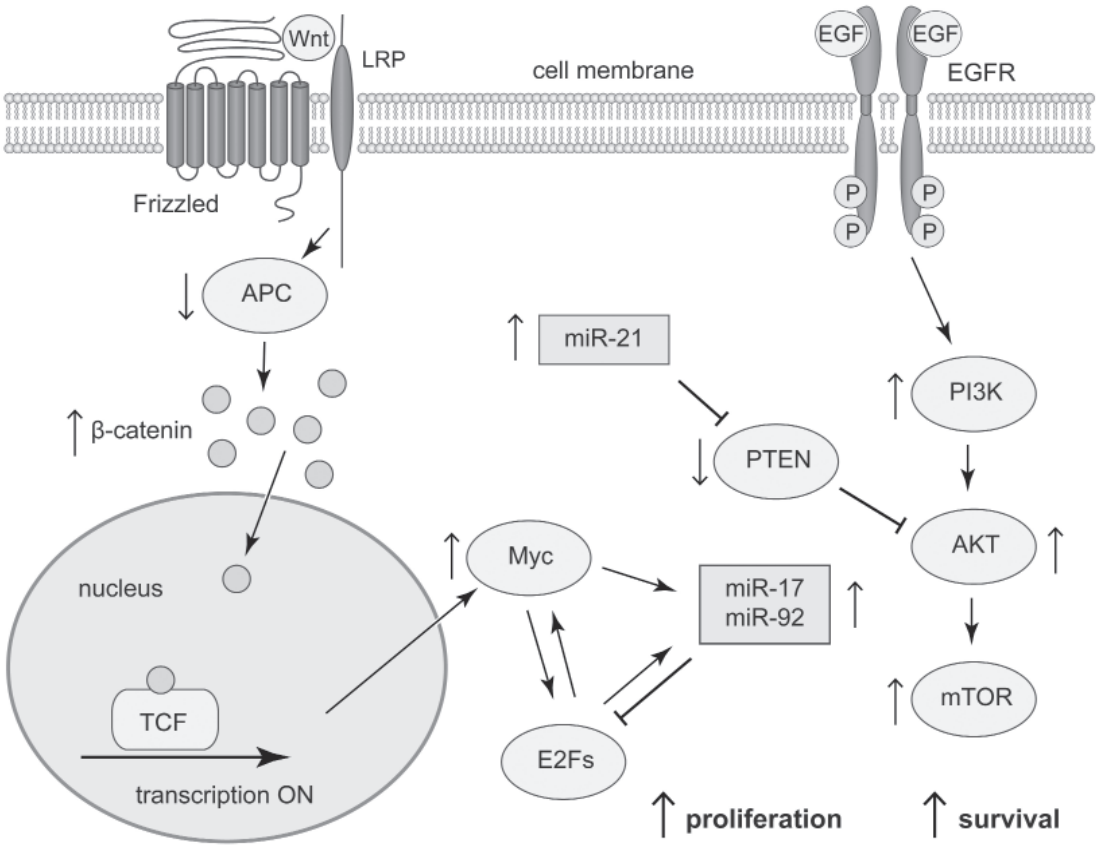

Figure 5. Targets of the studied microRNAs: miR-17 and miR-92 promote cell proliferation through regulation of E2Fs, whereas miR-21 promotes cell survival through regulation of PTEN. AKT, protein kinase B; APC, adenomatous polyposis coli; E2Fs, E2F family of transcription factors; EGF, epidermal growth factor; EGFR, EGF receptor; LRP, low-density lipoprotein receptor-related protein; mTOR, mammalian target of rapamycin; P, phosphorylated site; PI3K, phosphatidylinositol-4,5-bisphosphate 3-kinase; PTEN, phosphatidylinositol-3,4,5-trisphosphate 3-phosphatase; TCF, T cell factor; Wnt, wingless/integrase-1.

significantly plummeted after surgery in the subset of patients with potentially curative surgeries (*21*). Others demonstrated that stromal miR-21 expression was related to the expression of E-cadherin and metastasis-associated protein 1 in colorectal cancer and high miR-21 expression in stage III patients was not associated with poor DFS (*32*). Stage II colorectal cancer patients with high levels of miR-21 are at higher risk for tumor recurrence and should be considered for more intensive treatment (*32*). We found from our panel of miRNAs that only miR-21 had significantly altered expression levels in patients with III *vs.* II stage disease, which may reflect the tumor burden or may indicate noncurative surgeries. Patients with recurrence of the disease had significantly higher expression levels in Nx group for all miRNAs except miR-29a which again may reflect the tumor burden or may indicate noncurative surgeries.

There is considerable sample-to-sample variability in both protein and lipid content of serum samples, which could affect efficiency of RNA extraction (*33*). To ensure the accuracy of our assay, including variability in polymerase chain reaction amplification efficiencies, we used the novel method for normalization of experimental miRNA data using spiked-in synthetic, nonhuman mature miRNA from *Caenorhabditis elegans* (*33*). Although our approach of quantifying relative expression of serum miRNAs is widely used, absolute quantitation of serum miRNAs expression levels may further improve the translation of these data into a clinically viable diagnostic test for early detection of disease relapse.

Inadequate examination of lymph nodes may lead to tumor understaging and subsequent treatment failure (*34*). Many factors affect the number of lymph nodes examined, including extent of surgical resection, patient age, tumor location, and pathology techniques. Population-based data suggest that only 37% of colon cancer patients have adequate lymph node evaluation (*35*).

Colon cancer patients may benefit from discovering prognostic markers that can identify those individuals that are more likely to recur by selecting patients that are suitable for adjuvant therapy. Several miRNAs (miR-192, miR-215, miR-140, miR-129, let-7, miR-21, miR-181b, miR-200 s) were found to be associated with chemoresistance by regulating key cell death pathways (*24*). High levels of miR-21 may partly be responsible for poor response to 5-FU; therefore, patients with high miR-21 expression are at high-risk for disease recurrence (*36*). In colon cancer cell lines it was demonstrated that increased miR-21 expression reduced apoptosis and G2/

M arrest due to damage by 5-FU (*37*).

In summary, the most important finding in our study is that miR-17, miR-21 and miR-92 alone in Nx or in combination in stage III patients may help detecting early recurrence of colon cancer after radical surgery and adjuvant chemotherapy with high accuracy in clinical practice. Our results suggest that patients with elevated serum levels of miR-17, miR-21 and miR-92 should undergo more intensive follow-up in order to increase the possibility for early relapse detection and potential subsequent curative interventions. To our knowledge our study, despite its small sample size, is one of the few, testing potential biomarkers that could predict disease recurrence in patients with Nx colon cancer. Future studies may further evaluate the potential use of miR-17, miR-21 and miR-92 in post-operative surveillance, which may provide an opportunity for early detection of recurrent disease.

References

1. Jemal A, Bray F, Center MM, Ferlay J, Ward E, Forman D. Global cancer statistics. CA Cancer J Clin. 2011; 61:69-90.
2. O'Connell MJ, Campbell ME, Goldberg RM, Grothey A, Seitz JF, Benedetti JK, Andre T, Haller DG, Sargent DJ. Survival following recurrence in stage II and III colon cancer: Findings from the ACCENT data set. J Clin Oncol. 2008; 26:2336-2341.
3. Andre T, Boni C, Navarro M, Tabernero J, Hickish T, Topham C, Bonetti A, Clingan P, Bridgewater J, Rivera F, de Gramont A. Improved overall survival with oxaliplatin, fluorouracil, and leucovorin as adjuvant treatment in stage II or III colon cancer in the MOSAIC trial. J Clin Oncol. 2009; 27:3109-3116.
4. Sargent D, Shi Q, Yothers G, Van Cutsem E, Cassidy J, Saltz L, Wolmark N, Bot B, Grothey A, Buyse M, de Gramont A, Adjuvant Colon Cancer End-points G. Two or three year disease-free survival (DFS) as a primary end-point in stage III adjuvant colon cancer trials with fluoropyrimidines with or without oxaliplatin or irinotecan: Data from 12,676 patients from MOSAIC, X-ACT, PETACC-3, C-06, C-07 and C89803. Eur J Cancer. 2011; 47:990-996.
5. Chau I, Cunningham D. Adjuvant therapy in colon cancer – what, when and how? Ann Oncol. 2006; 17:1347-1359.
6. Quasar Collaborative G, Gray R, Barnwell J, McConkey C, Hills RK, Williams NS, Kerr DJ. Adjuvant chemotherapy versus observation in patients with colorectal cancer: A randomised study. Lancet. 2007; 370:2020-2029.
7. Gunderson LL, Jessup JM, Sargent DJ, Greene FL, Stewart AK. Revised TN categorization for colon cancer based on national survival outcomes data. J Clin Oncol. 2010; 28:264-271.
8. Wolpin BM, Meyerhardt JA, Mamon HJ, Mayer RJ. Adjuvant treatment of colorectal cancer. CA Cancer J Clin. 2007; 57:168-185.
9. Drebber U, Lay M, Wedemeyer I, Vallbohmer D, Bollschweiler E, Brabender J, Monig SP, Holscher AH, Dienes HP, Odenthal M. Altered levels of the onco-microRNA 21 and the tumor-supressor microRNAs 143 and 145 in advanced rectal cancer indicate successful neoadjuvant chemoradiotherapy. Int J Oncol. 2011; 39:409-415.
10. Bartel DP. MicroRNAs: Genomics, biogenesis, mechanism, and function. Cell. 2004; 116:281-297.
11. Slack FJ, Weidhaas JB. MicroRNA in cancer prognosis. N Engl J Med. 2008; 359:2720-2722.
12. Jansson MD, Lund AH. MicroRNA and cancer. Mol Oncol. 2012; 6:590-610.
13. Chen X, Ba Y, Ma L, *et al*. Characterization of microRNAs in serum: A novel class of biomarkers for diagnosis of cancer and other diseases. Cell Res. 2008; 18:997-1006.
14. Mitchell PS, Parkin RK, Kroh EM, *et al*. Circulating microRNAs as stable blood-based markers for cancer detection. Proc Natl Acad Sci U S A. 2008; 105:10513-10518.
15. Slaby O, Svoboda M, Michalek J, Vyzula R. MicroRNAs in colorectal cancer. In: MicroRNAs in Cancer Translational Research (Cho WCS, ed. Springer, Dordrecht, Netherlands, 2011; pp. 107-133.
16. Livak KJ, Schmittgen TD. Analysis of relative gene expression data using real-time quantitative PCR and the $2^{-\Delta\Delta CT}$ method. Methods. 2001; 25:402-408.
17. Subramani A, Alsidawi S, Jagannathan S, Sumita K, Sasaki AT, Aronow B, Warnick RE, Lawler S, Driscoll JJ. The brain microenvironment negatively regulates miRNA-768-3p to promote K-ras expression and lung cancer metastasis. Sci Rep. 2013; 3:2392.
18. Su JQ, Liu JS. Linear combinations of multiple diagnostic markers. J Am Stat Assoc. 1993; 88:1350-1355.
19. Ogata-Kawata H, Izumiya M, Kurioka D, Honma Y, Yamada Y, Furuta K, Gunji T, Ohta H, Okamoto H, Sonoda H, Watanabe M, Nakagama H, Yokota J, Kohno T, Tsuchiya N. Circulating exosomal microRNAs as biomarkers of colon cancer. PLoS One. 2014; 9:e92921.
20. Wang CJ, Zhou ZG, Wang L, Yang L, Zhou B, Gu J, Chen HY, Sun XF. Clinicopathological significance of microRNA-31, -143 and -145 expression in colorectal cancer. Dis Markers. 2009; 26:27-34.
21. Toiyama Y, Takahashi M, Hur K, Nagasaka T, Tanaka K, Inoue Y, Kusunoki M, Boland CR, Goel A. Serum miR-21 as a diagnostic and prognostic biomarker in colorectal cancer. J Natl Cancer Inst. 2013; 105:849-859.
22. Corte H, Manceau G, Blons H, Laurent-Puig P. MicroRNA and colorectal cancer. Dig Liver Dis. 2012; 44:195-200.
23. Schetter AJ, Okayama H, Harris CC. The role of microRNAs in colorectal cancer. Cancer J. 2012; 18:244-252.
24. Mishra PJ. MicroRNAs as promising biomarkers in cancer diagnostics. Biomark Res. 2014; 2:19.
25. Dong Y, Wu WKK, Wu CW, Sung JJY, Yu J, Ng SSM. MicroRNA dysregulation in colorectal cancer: A clinical perspective. Br J Cancer. 2011; 104:893-898.
26. Peng Y, Zhai Z, Li Z, Wang L, Gu J. Role of blood tumor markers in predicting metastasis and local recurrence after curative resection of colon cancer. Int J Clin Exp Med. 2015; 8:982-990.
27. Luo X, Burwinkel B, Tao S, Brenner H. MicroRNA signatures: Novel biomarker for colorectal cancer? Cancer Epidemiol Biomarkers Prev. 2011; 20:1272-1286.
28. Li J, Liu Y, Wang C, Deng T, Liang H, Wang Y, Huang D,

Fan Q, Wang X, Ning T, Liu R, Zhang CY, Zen K, Chen X, Ba Y. Serum miRNA expression profile as a prognostic biomarker of stage II/III colorectal adenocarcinoma. Sci Rep. 2015; 5:12921.
29. Brunet Vega A, Pericay C, Moya I, Ferrer A, Dotor E, Pisa A, Casalots A, Serra-Aracil X, Oliva JC, Ruiz A, Saigi E. microRNA expression profile in stage III colorectal cancer: Circulating miR-18a and miR-29a as promising biomarkers. Oncol Rep. 2013; 30:320-326.
30. Rothschild SI. microRNA therapies in cancer. Mol Cell Ther. 2014; 2:7.
31. Huang Z, Huang D, Ni S, Peng Z, Sheng W, Du X. Plasma microRNAs are promising novel biomarkers for early detection of colorectal cancer. Int J Cancer. 2010; 127:118-126.
32. Kang WK, Lee JK, Oh ST, Lee SH, Jung CK. Stromal expression of miR-21 in T3-4a colorectal cancer is an independent predictor of early tumor relapse. BMC Gastroenterol. 2015; 15:2.
33. Kroh EM, Parkin RK, Mitchell PS, Tewari M. Analysis of circulating microRNA biomarkers in plasma and serum using quantitative reverse transcription-PCR (qRT-PCR). Methods. 2010; 50:298-301.
34. Wolpin BM, Mayer RJ. Systemic treatment of colorectal cancer. Gastroenterology. 2008; 134:1296-1310.
35. Baxter NN, Virnig DJ, Rothenberger DA, Morris AM, Jessurun J, Virnig BA. Lymph node evaluation in colorectal cancer patients: A population-based study. J Natl Cancer Inst. 2005; 97:219-225.
36. Schetter AJ, Leung SY, Sohn JJ, Zanetti KA, Bowman ED, Yanaihara N, Yuen ST, Chan TL, Kwong DL, Au GK, Liu CG, Calin GA, Croce CM, Harris CC. MicroRNA expression profiles associated with prognosis and therapeutic outcome in colon adenocarcinoma. JAMA. 2008; 299:425-436.
37. Valeri N, Gasparini P, Braconi C, Paone A, Lovat F, Fabbri M, Sumani KM, Alder H, Amadori D, Patel T, Nuovo GJ, Fishel R, Croce CM. MicroRNA-21 induces resistance to 5-fluorouracil by down-regulating human DNA MutS homolog 2 (hMSH2). Proc Natl Acad Sci U S A. 2010; 107:21098-21103.

(Received December 11, 2015; Revised December 19, 2015; Accepted December 25, 2015)

Original Article

DOI: 10.5582/bst.2015.01163

Pancreatic adenocarcinoma: the impact of preneoplastic lesion pattern on survival

Yves Flattet[1], Takamune Yamaguchi[2], Snezana Andrejevic-Blant[1], Nermin Halkic[2,*]

[1] *Department of Pathology, University Hospital CHUV, Lausanne, Switzerland;*
[2] *Department of Visceral Surgery, University Hospital CHUV, Lausanne, Switzerland.*

Summary **Pancreatic adenocarcinoma is associated with a very poor prognosis, characterized with a 5-year survival rate of only 5%. Surgery is the only curative treatment for selected patients. Nevertheless, recurrence is very frequent. Identifying prognostic factors is thus warranted. Like numerous other tumors, adenocarcinomas are preceded by preneoplastic lesions. The role and the impact of these lesions remain unclear. This study aimed to assess the impact of the preneoplastic lesion pattern and histo-morphological features, on survival after pancreatic resection. Thirty-five patients who underwent pancreatic resection for pancreatic adenocarcinoma were identified from a prospective database of a single center, between 2003 and 2008. We considered demographics, tumor characteristics and type of treatment. The major outcome was survival. Analyzes were separated into two groups, according to the preneoplastic lesions: Pancreatic intraepithelial neoplasia (PanIN)-related carcinomas and intracanalar papillary mucinous neoplasia (IPMN)-related carcinomas. The former were more frequent, accounting for 63% (22/35). Moreover, they displayed more aggressive features, with a higher tumor stage ($p = 0.01$) and higher rate of positive lymph nodes ($p = 0.019$). Lymphatic ($p = 0.009$) and perinervous ($p = 0.019$) invasions were also more frequent. Survival was negatively influenced by PanIN preneoplastic lesions ($p = 0.015$), T3-4 tumor stage ($p = 0.038$), positive lymph nodes ($p = 0.044$), lymphatic ($p = 0.019$) and vascular ($p = 0.029$) invasions. Pancreatic adenocarcinoma displays different behavior according to its preneoplastic lesion. Indeed, PanIN-related adenocarcinoma showed more aggressive features and lower survival rate. Preneoplastic lesions may represent predictive factors for survival. Their role and predictive value should be investigated more thoroughly.**

Keywords: PanIN, IPMN, pancreatic resection

1. Introduction

Pancreatic adenocarcinoma represents the fourth leading cause of death by cancer, worldwide (*1*). Its aggressive pattern is partially due to the silent course of the disease, with symptoms like jaundice or weight loss occurring late (*1*). Although surgery may be curative for early stages (*2*), overall recurrence rate are high while 5-year survival rate only reaches 5% (*3*). Significant advances have been made in the understanding of the biology and mechanisms of pancreatic cancer, during the last decade. Adenocarcinoma of the pancreas seems to result from successive mutations. A continuum of lesions may be observed between normal parenchyma and adenocarcinoma (*4-7*). The most frequent preneoplastic lesions that usually precede pancreatic adenocarcinoma are subdivided into two types: pancreatic intraepithelial neoplasia (PanINs) and intracanalar papillary mucinous neoplasia (IPMN) (*8-11*). The former is a peripheral lesion affecting small pancreatic ducts (< 5mm in diameter), which is often described, in ductal adenocarcinoma. IPMN are less frequent lesions, usually occurring in the main pancreatic duct or its principle branches (*11*). Characterized by a size greater than 5 mm, they are more likely to be visible on imaging, compared to PanIN. As with PanIN, IPMN appear to follow an adenoma-carcinoma sequence with three continuous steps: low grade adenoma, borderline

**Address correspondence to:*
Dr. Nermin Halkic, Department of Visceral Surgery, University Hospital CHUV, Rue du Bugnon 46, 1011 Lausanne, Switzerland.
E-mail: nermin.halkic@chuv.ch

neoplasia, and carcinoma in situ (*12*).

Both preneoplastic lesions, PanIN and IPMN, follow a sequence of events leading to adenocarcinoma. Notwithstanding, tumor progression may be different depending on the preneoplastic lesion (*9*). Studies have described the trend for PanINs leading into ductal adenocarcinoma, and for IPMN evolving toward mucinous adenocarcinoma. Although ductal- and mucinous adenocarcinomas obviously display different outcomes, the impact of various tumor characteristics, like the pattern of preneoplastic lesions remains unclear. In this study, we aimed to analyze the impact of histo-morphological tumors' characteristics on survival, in the setting of pancreatic resection for adenocarcinoma.

2. Materials and Methods

Thirty-five patients who underwent pancreatic resection for adenocarcinoma of the pancreas were identified from prospective databases for pancreas surgery, in the Division of Visceral Surgery at University Hospital of Lausanne (CHUV), between 2003 and 2008. A complete preoperative workup was performed to determine whether the disease was completely resectable and each case had been previously discussed in a tumor board. Surgical procedures were performed by conventional pancreatic resection including pancreaticoduodenectomy and distal splenopancreatectomy. Distal splenopancreatectomy was performed through exclusive abdominal incision or laparoscopic procedure. The artery-first approach was not performed in pancreaticoduodenectomy and reconstruction was done by pancreaticogastrostomy or pancreaticojejunostomy according to pancreas texture (*13*). Patients' demographics, tumor characteristics, type of treatment and survival were analyzed. We considered: age, gender, type of surgery, histological type of tumor, preneoplastic lesion, TNM stage, tumor grade, lymphatic invasion, vascular invasion, neural invasion, margins status, adjuvant therapy and survival (DFS-disease free survival). Due to a limited number of patients, and in order to perform pertinent statistical analyzes, several classes of items were regrouped. Indeed, high grade tumors (G2 and G3) were grouped and compared to low grade tumors (G1). Tumor stages T1/2 were compared to T3/4 stages. The IPMN lesions were classified as low-grade (adenoma) and high grade (borderline neoplasia and carcinoma in situ). The margins status were separated into margins > 0.1cm and margins ≤ 0.1cm. Clinical follow-up was analyzed according to tumor-free survival, survival with disease, death without disease and death with disease.

The overall survival curves were determined using the Kaplan-Meier method and were compared using the log-rank test. A multivariate analysis was performed using a Cox proportional hazards model. A significant value of 0.05 was used in all tests. The statistical analysis was done using SPSS v20 statistical software, Chicago, IL.

3. Results

3.1. *Patients and tumors*

Patients' characteristics are summarized in Table 1. Median age was 69 years while men accounted for 57% (20/35). Tumors were separated in two groups, based on the preneoplastic lesion (Table 1). A majority of tumors were related to PanIN 63% (22/35) while 13 adenocarcinomas (37%) were related to IPMN. Although, the 2 groups were comparable in regard to several characteristics, they were significantly different for the following variables: tumor stage ($p = 0.01$), lymph node ($p = 0.019$), lymphatic invasion ($p = 0.009$) and perineural invasion ($p = 0.019$). Moreover, PanIN-related tumors more frequently required pancreaticoduodenectomy.

3.2. *PanIN-related adenocarcinomas*

They displayed aggressive features with 86% stage T3-4. Moreover, 73% had lymphatic metastasis. Distant metastasis accounted for 14% while a majority presented a high tumor grade G2-3 (86%). Vascular and perinervous invasion were highlighted in 46% and 91%, respectively. Treatment was mostly pancreaticoduodenectomy (91%) while pathological R0 resection was carried out in 46%. Furthermore, 64% of patients received adjuvant therapy.

3.3. *IPMN-related adenocarcinomas*

This subtype of tumors displayed less aggressive features than PanIN-related adenocarcinoma. However, we identified 39% as T3-4 stage, 31% with positive lymph nodes while distant metastasis concerned 15% (2/13). In term of invasion, tumors invaded vessels, lymphatics and nerves in 39%, 31% and 54%, respectively. Surgery was relatively well balanced between pancreaticoduodenectomy (61.5%) and distal splenopancreatectomy (38.5%). Pathological R0 resection was carried out in 54%, and half of the patients received an adjuvant treatment.

3.4. *Survival*

The impact on survival was analyzed for each variable and is described in Table 2. Demographics did not show a significant difference for survival rate. As mentioned above, PanIN-related adenocarcinomas displayed more aggressive features than IPMN-related ones. Indeed, these findings influenced survival with a significantly lower survival rate in the former group ($p = 0.015$, Figure 1). Lymph node metastasis was also identified

Table 1. Characteristics of patients, tumors and treatments

Characteristics	*n* (%) PanIN-related adenocarcinoma (*n* = 22)	*n* (%) IPMN-related adenocarcinoma (*n* = 13)	*p* value
Patients			
Age			0.552
< 70 years	11 (50)	7 (53.8)	
> 70 years	11 (50)	6 (46.2)	
Gender			0.482
Men	12 (54.5)	8 (61.5)	
Women	10 (45.5)	5 (38.5)	
Tumors			
Subtypes			0.004*
Ductal	0	8 (61.5)	
Mucinous	22 (100)	5 (38.5)	
Preneoplastic lesion			
PanIN 1a-b	16 (72.7)	0	
PanIN 2-3	6 (27.3)	0	
IPMN Adenoma	0	4 (30.8)	
IPMN borderline-CiS	0	9 (69.2)	
Stage			0.01*
T1-2	3 (13.6)	8 (61.5)	
T3-4	19 (86.4)	5 (38.5)	
Lymph node metastasis			0.019*
N+	16 (72.7)	4 (30.8)	
N−	6 (27.3)	9 (69.2)	
Metastases			0.626
M+	3 (13.6)	2 (15.4)	
M−	19 (86.4)	11 (84.6)	
Tumor grade			0.103
G1	3 (13.6)	5 (38.5)	
G2-3	19 (86.4)	8 (61.5)	
Lymphatic invasion			0.009*
Yes	17 (77.3)	4 (30.8)	
No	5 (22.7)	9 (69.2)	
Vascular invasion			0.482
Yes	10 (45.5)	5 (38.5)	
No	12 (54.5)	8 (61.5)	
Perineural invasion			0.019*
Yes	20 (90.9)	7 (53.8)	
No	2 (9.1)	6 (46.2)	
Treatment			
Type of surgery			0.05*
Pancreaticoduodenectommy	20 (90.9)	8 (61.5)	
Distal splenopancreatectomy	2 (9.1)	5 (38.5)	
Margins			0.621
≤ 1 mm	12 (54.5)	7 (53.8)	
> 1 mm	10 (45.5)	6 (46.2)	
Adjuvant therapy			0.340
Yes	14 (63.6)	6 (50)	
No	8 (36.4)	6 (50)	

as a prognostic factor and was associated with lower survival ($p = 0.038$, Figure 2).

The invasion of adjacent tissues by the tumor appeared to influence survival, via three mechanisms: direct invasion ($p = 0.038$), vascular invasion ($p = 0.029$) and lymphatic invasion ($p = 0.019$), while perinervous invasion was not associated with poorer outcomes ($p = 0.119$). None of the therapeutic variables influenced survival in our study. Multivariate analysis did not detect any significant impact on survival for the studied variables.

4. Discussion

This study assessed the impact of preneoplastic lesion pattern and histo-morphological features of pancreatic adenocarcinoma, on survival after pancreatic resection. Although, pancreatic adenocarcinoma may be classified according to their subtype: ductal *vs*. mucinous, the preneoplastic lesion pattern appeared to play an important role (*9*). Indeed, PanIN-related tumors displayed more aggressive characteristics than IPMN-related ones. These findings were translated into survival with poorer prognosis in the PanIN-related group. The survival rate at 1-, 3- and 5-years were 69%, 58% and 58% for IPMN-related tumors while it only reached 45%, 19% and 9% for PanIN-related adenocarcinomas.

Tremendous effort has permitted a significant improvement in understanding tumorigenesis of pancreatic adenocarcinoma and precancerous lesions, during the last decade (*14-16*). The pathological

Table 2. Predictive factors of survival

Items	Survival (month) 95% CI	*p* value
Demographics		
Age		0.074
< 70 years	21.7-43	
> 70 years	8.2-11.1	
Gender		0.805
Men	16.8-32.5	
Women	17.1-53	
Tumors		
Subtypes		0.293
Ductal	18.4-43.4	
Mucinous	18-40.1	
Preneoplastic lesion		0.015*
PanIn-related adenocarcinoma	10-32.1	
IPMN-related adenocarcinoma	27-51.6	
PanIN		0.233
PanIN 1a-b	22.7-65.9	
PanIN 2-3	13.7-28	
IPMN		0.029*
IPMN Adenoma	12-35.3	
IPMN borderline-CiS	27.9-55.9	
Stage		0.038*
T1-2	26.2-52.6	
T3-4	13.1-38.1	
Lymph node metastasis		0.044*
N+	11.7-25.3	
N−	33.5-72.3	
Metastases		0.555
M+	11-32.6	
M−	22.3-50	
Tumor grade		0.471
G1	13.9-40.2	
G2-3	16.9-42.4	
Lymphatic invasion		0.019*
Yes	11.4-24.5	
No	36.8-76	
Vascular invasion		0.029*
Yes	9.4-21.4	
No	27-61.3	
Perineural invasion		0.119
Yes	16.5-40.2	
No	20.1-43.7	
Treatment		
Type of surgery		0.291
Pancreaticoduodenectommy	16.5-43.5	
Distal splenopancreatectomy	19.1-41.1	
Margins		0.934
≤ 1 mm	16.1-31.5	
> 1 mm	18.2-55.7	
Adjuvant therapy		0.854
Yes	17.8-32.2	
No	17.5-58.2	

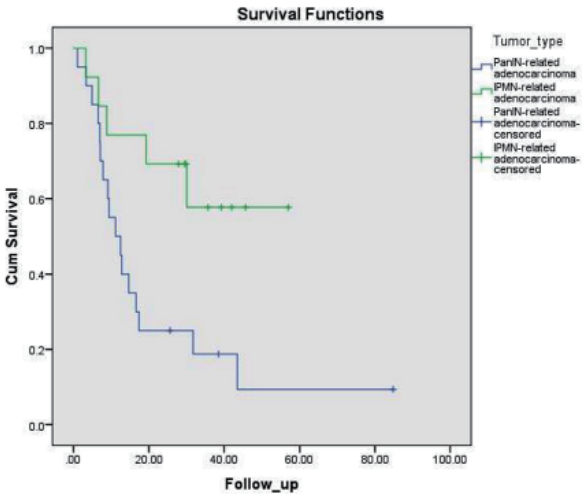

Figure 1. Survival and preneoplastic lesion pattern.

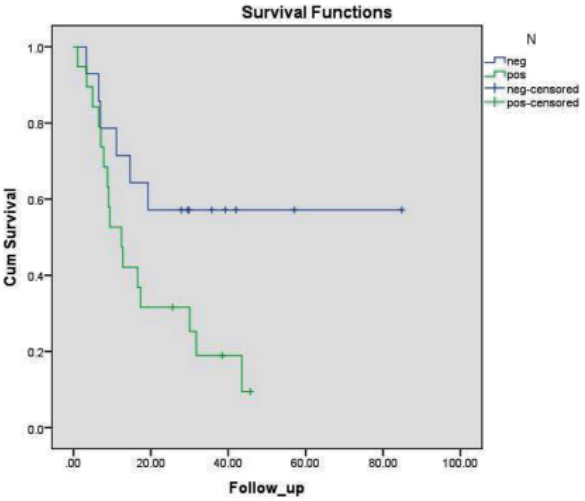

Figure 2. Survival and lymph nodes stage.

characteristics and molecular mechanisms have rapidly evolved, leading to new classification of preneoplastic lesions (*8*). Notwithstanding, the relationship between these findings and the clinical setting is not obvious yet.

This study displays some limitations. The retrospective design leads to missing data and missing variables. Moreover, the number of included patients is relatively low. Based on these potential biases, results should be interpreted with caution.

In a landmark article, Andea *et al*. showed the association between PanIN and ductal adenocarcinomas (*9*). Therefore, the need to address and treat these progressive lesions at an early stage is crucial. Of note, the influence of preneoplastic lesion pattern on survival after resection has rarely or not been addressed, to our knowledge. Based on our results, preneoplastic lesions may play an important role. At least, they may reflect different oncogenic pathways, according to their respective type. Pancreatic adenocarcinomas are heterogeneous tumors with poor prognosis while prognostic tools as biomarkers are somewhat lacking. Identifying subclasses is thus a critical step for the future.

The relatively small number of cases (n = 35) was a limitation of our study. This may be the reason why well-known risk factors, such as perinervous invasion, were not associated with poorer outcomes. This result should be confirmed in a future study carried out in a larger cohort of patients.

In summary, this study supports the influence of preneoplastic lesions on survival, after pancreatic resection for adenocarcinoma. PanIN-related lesions displayed more aggressive features than IPMN-related ones, leading to a lower survival rate. Further studies are needed in order to explore the role of precancerous lesions of the pancreas, in more depth.

Acknowledgements

The authors wish to thank Dr. S. Ferrone for the gift of the anti-HMW-MAA mAb.

References

1. Hidalgo M. Pancreatic cancer. N Engl J Med. 2010; 362:1605-1617.
2. Shaib Y, Davila J, Naumann C, El-Serag H. The impact of curative intent surgery on the survival of pancreatic cancer patients: a U.S. Population-based study. Am J Gastroenterol. 2007; 102:1377-1382.
3. Dusch N, Weiss C, Strobel P, Kienle P, Post S, Niedergethmann M. Factors predicting long-term survival following pancreatic resection for ductal adenocarcinoma of the pancreas: 40 years of experience. J Gastrointest Surg. 2014; 18:674-681.
4. Singh M, Maitra A. Precursor lesions of pancreatic cancer: molecular pathology and clinical implications. Pancreatology. 2007; 7:9-19.
5. Sipos B, Frank S, Gress T, Hahn S, Klöppel G. Pancreatic intraepithelial neoplasia revisited and updated. Pancreatology. 2009; 9:45-54.
6. Zamboni G, Hirabayashi K, Castelli P, Lennon AM. Precancerous lesions of the pancreas. Best Pract Res Clin Gastroenterol. 2013; 27:299-322.
7. Cooper CL, O'Toole SA, Kench JG. Classification, morphology and molecular pathology of premalignant lesions of the pancreas. Pathology. 2013; 45:286-304.
8. Hruban RH, Maitra A, Goggins M. Update on pancreatic intraepithelial neoplasia. Int J Clin Exp Pathol. 2008; 1:306-316.
9. Andea A, Sarkar F, Adsay VN. Clinicopathological correlates of pancreatic intraepithelial neoplasia: a comparative analysis of 82 cases with and 152 cases without pancreatic ductal adenocarcinoma. Mod Pathol. 2003; 16:996-1006.
10. Takaori K. Current understanding of precursors to pancreatic cancer. J Hepatobiliary Pancreat Surg. 2007; 14:217-223.
11. Adsay NV, Conlon KC, Zee SY, Brennan MF, Klimstra DS. Intraductal papillary-mucinous neoplasms of the pancreas: an analysis of in situ and invasive carcinomas in 28 patients. Cancer. 2002; 94:62-77.
12. Andrejevic-Blant S, Kosmahl M, Sipos B, Klöppel G. Pancreatic intraductal papillary-mucinous neoplasms: a new and evolving entity. Virchows Arch. 2007; 451:863-869.
13. Kokudo T, Uldry E, Demartines N, Halkic N. Pulmonary embolism: specific risk factor after pancreas resection? Pancreas. 2014; 43:891-894.
14. Yonezawa S, Higashi M, Yamada N, Yokoyama S, Goto M. Significance of mucin expression in pancreatobiliary neoplasms. J Hepatobiliary Pancreat Sci. 2010; 17:108-124.
15. Nagata K, Horinouchi M, Saitou M, Higashi M, Nomoto M, Goto M, Yonezawa S. Mucin expression profile in pancreatic cancer and the precursor lesions. J Hepatobiliary Pancreat Surg. 2007; 14:243-254.
16. Basturk O, Khayyata S, Klimstra DS, Hruban RH, Zamboni G, Coban I, Adsay NV. Preferential expression of MUC6 in oncocytic and pancreatobiliary types of intraductal papillary neoplasms highlights a pyloropancreatic pathway, distinct from the intestinal pathway, in pancreatic carcinogenesis. Am J Surg Pathol. 2010; 34:364-370.

(Received November 27, 2015; Revised December 27, 2015; Accepted December 28, 2015)

Original Article

DOI: 10.5582/bst.2015.01143

Exclusion criteria for assuring safety of single-incision laparoscopic cholecystectomy

Yoshikuni Kawaguchi, Takeaki Ishizawa, Rihito Nagata, Junichi Kaneko, Yoshihiro Sakamoto, Taku Aoki, Yasuhiko Sugawara, Kiyoshi Hasegawa, Norihiro Kokudo*

Hepato-Biliary-Pancreatic Surgery Division, Department of Surgery, Graduate School of Medicine, The University of Tokyo, Tokyo, Japan.

Summary **Despite increasing popularity of single-incision laparoscopic cholecystectomy (SILC), indication criteria assuring safety of SILC has yet to be established. In the present study, the subjects consisted of 146 consecutive patients undergoing conventional laparoscopic cholecystectomy (CLC) or SILC. SILC was indicated after excluding patients who met following criteria: age > 75 years, obesity, operative scar, cardiopulmonary diseases, acute cholecystitis, choledocholithiasis and abnormal bile duct anatomy. Thirty-four patients were excluded from the SILC candidates (moderate/high-risk CLC group). Among the 112 potential candidates, SILC was indicated for 23 patients (21%, SILC group) and the remaining 89 patients (79%) underwent CLC (low-risk CLC group). In the SILC group, operation time was longer than in the low-risk CLC group (171 [113-286] *vs.* 126 [72-240] min, $p < 0.01$), but the periods requiring painkiller was shorter. That led to reduced length of hospital stay compared to low-risk CLC group (2 [2-4] *vs.* 4 [2-12] days, $p < 0.01$). Between the low-risk CLC and moderate/high-risk CLC group, operation time was significantly longer and amount of blood loss was larger in the latter group. No complications were encountered in the SILC group. SILC can be indicated safely as far as appropriate criteria is adopted for excluding patients in whom complicated laparoscopic procedures are needed.**

Keywords: Conventional multiport laparoscopic cholecystectomy, fluorescence cholangiography, single-incision laparoscopic cholecystectomy

1. Introduction

Single-incision laparoscopic cholecystectomy (SILC), which was first introduced by Navarra *et al*. (*1*), is increasingly gaining popularity presumably because SILC has definite advantage in improving cosmesis after laparoscopic cholecystectomy (LC) (*2,3*). In some institutions favoring SILC over conventional multiport laparoscopic cholecystectomy (CLC), incidence of SILC reached 50% among all the LC procedures (*4,5*). In contrast, SILC has potential disadvantages compared to CLC in terms of longer operative time (*6*), increased cost for specialized laparoscopic instruments (*7*), a higher bile duct injury rate (*8*), and occurrence of umbilical hernia (*3,9*). In order to safely adopt SILC in clinical practice, we need strict criteria for indication of SILC, which have not been indicated clearly even in the guideline of LC by the Society of American Gastrointestinal and Endoscopic Surgeons (*10*).

In the authors' institution, SILC has been performed after setting definite exclusion criteria comprising patients' background factors and gallstones/cholecystitis conditions. The present study evaluated intra- and post-operative outcomes of SILC compared to those of CLC with the aim to consider appropriate criteria for indicating SILC safely to patients who opt for single-incision surgery.

2. Materials and Methods

2.1. *Patients*

The subjects consisted of 146 consecutive patients who underwent LC for cholecystolithiasis, gallbladder

**Address correspondence to:*
Dr. Norihiro Kokudo, Hepato-Biliary-Pancreatic Surgery Division, Department of Surgery, Graduate School of Medicine, The University of Tokyo, 7-3-1 Hongo, Bunkyo-ku, Tokyo 113-8655, Japan.
E-mail: KOKUDO-2SU@h.u-tokyo.ac.jp

polyps, or acute cholecystitis at The University of Tokyo between December 2009 and April 2012. Exclusion criteria for SILC were determined as follows: age > 75 years, obesity (BMI > 30 kg/m^2), operative scar in the upper abdomen, concomitant cardiopulmonary diseases, acute cholecystitis, choledocholithiasis, abnormal bile duct anatomy detected by routine preoperative cholangiography on computed tomography, magnetic resonance images, or fluoroscopy. These criteria were set to secure the safety based on the studies which indicated higher postoperative morbidity rate following CLC for patients with higher age (*11*), the higher grade in American Society of Anesthesiologists score (*11*), and complicated and/or acute gallstone disease (*11-13*). SILC was indicated for patients who met the criteria and opted for SILC after being presented explanation on the potential benefits and disadvantages of this procedure. CLC and SILC were performed or guided by surgeons who have experienced general surgery and LC for more than 10 years. All operations were performed after obtaining informed consent from each patient, and patient anonymity was preserved.

2.2. *Surgical techniques*

For CLC, patients were placed in the supine position under general anesthesia as well as epidural anesthesia. The trocar for laparoscopy was placed via the umbilical region, and 2 to 3 trocars were generally placed on the epigastric region and on the right side of the umbilicus. For SILC, on the other hand, patients were placed in the supine position with legs spread apart under general anesthesia with local anesthesia around the umbilicus. SILS port (Covidien, Mansfield, MA, USA) and a 5.4 mm-flexible laparoscope were used. A 2 mm visceral tractor (Mini Loop Retractor II; Covidien) was also used to lift the fundus of the gallbladder (*14*). The procedure was performed through Semi-cross method, holding an articulating instrument (Roticulator Endo Grasp; Covidien) with the left hand and a straight instrument with the right hand (*15*). The triangle of Calot was dissected to reach "critical view of safety" (*16*), while using fluorescence cholangiography (*17-20*) with preoperative and intravenous injection of ICG at any time during the procedures (Figure 1 and supplementary video 1, *http://biosciencetrends.com/docindex.php?year=2015&kanno=6*). When the isolation of the cystic duct was not completed within one hour after the incision, the second trocar was then placed to facilitate laparoscopic procedures. During this study period, intraoperative drip infusion cholangiography using meglumine iotroxate (*21*) (Figure 2) as well as fluorescence cholangiography was also routinely performed for both LC and SILC at the authors' institution. The cystic duct was ligated and divided after confirming the anatomy of the common bile duct using drip infusion cholangiography and fluorescence cholangiography, and consequently, the gallbladder was removed from the liver and retrieved. In principle, a drainage tube was not placed.

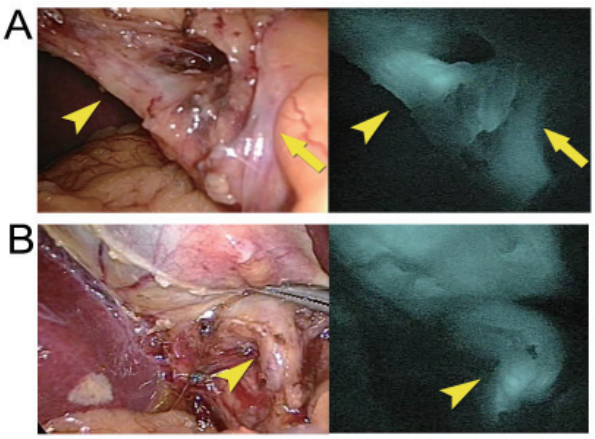

Figure 1. Fluorescence cholangiography during SILC. (A) Fluorescence cholangiography (right) after dissection of the triangle of Calot identifies the cystic duct (arrow head) and the common bile duct (arrow). **(B)** The cystic duct (arrow) is isolated and clearly visualized on fluorescence images. Please see supplementary video 1.

Figure 2. Drip infusion cholangiography. Drip infusion cholangiography was performed to confirm the relationship between the common bile duct (arrowheads) and clips made at the cystic duct (arrow).

2.3. *Postoperative management*

The catheter for the epidural anesthesia in CLC was removed on postoperative day 2. Non steroid anti-inflammatory drug was administered intravenously or orally to relieve postoperative pain depending on patients' complaint. Patients were discharged from the hospital when levels of C-reacitive protein and hepato-

biliary enzyme in blood were confirmed to be within normal limit on PODs 1 and/or 3 and when they had recovered from impaired activities of daily living. Follow-up was conducted for at least 6 months after surgery.

2.4. *Statistical analysis*

The subjects were divided into the following three groups: patients who met the exclusion criteria for SILC and underwent CLC (moderate/high-risk CLC group), those who were potential candidates of SILC but underwent CLC (Low-risk CLC group), and those who were potential candidates of SILC and actually underwent SILC (SILC group). Background characteristics and postoperative outcomes were compared between the Low-risk CLC group and the SILC group. Intraoperative factors were compared among the low-risk CLC group, the moderately/high-risk CLC group, and the SILC group.

Categorical variables are expressed in numerical figures (%), and were compared between groups using Fisher's exact test or the chi-square test. Continuous variables were expressed as median values (with range), and were compared using the Wilcoxon's rank-sum test. In the analysis of intraoperative factors among the three groups, the Steel-Dwass test was used following Kruskal-Wallis test. p values < 0.05 were considered as denoting statistical significance. Statistical analysis was conducted using JMP software (version 9.0.2; SAS Institute Inc., Cary, NC).

3. Results

3.1. *Background characteristics*

The treatment flow in the study population is shown in Figure 3. Among the 146 patients, 34 (23%) patients were excluded from the candidates of SILC (the moderate/high risk-CLC group) due to high age (n = 13), obesity (n = 11), acute cholecystitis (n = 3), surgical scar in the upper abdomen (n = 2), and abnormal bile duct anatomy on preoperative cholangiography (n = 5). Of the remaining 112 candidates of SILC, 23 (21 %) patients opted for SILC and 89 patients (79%) underwent CLC. Between the 23 patients in the SILC group and the 89 patients in the low risk-CLC group, the former group included younger patients and larger ratio of female patients (Table 1).

3.2. *Intraoperative outcomes*

Intraoperative factors are summarized in Table 2. Operation time in the low-risk CLC group was significantly shorter than that in the SILC group (126 [72-240] min *vs*. 171 [113-286] min, $p < 0.01$) and also than that in the moderate/high-risk CLC group

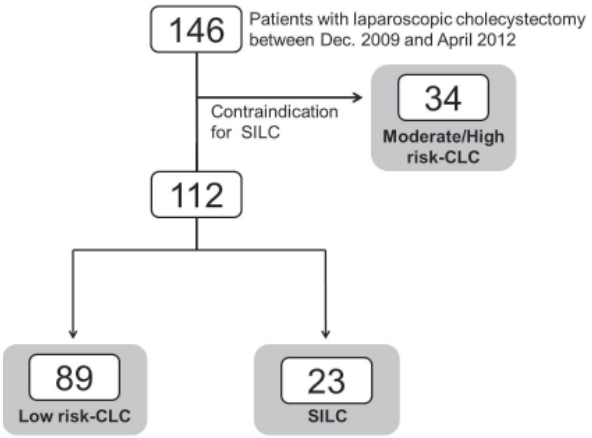

Figure 3. The treatment flow of study population. SILC, single-incision laparoscopic cholecystectomy; CLC, conventional multiport laparoscopic cholecystectomy; Low risk-CLC, CLC for patients who were the potential candidate of SILC but underwent CLC; Moderate/high risk-CLC, CLC for patients who met the exclusion criteria for SILC and underwent CLC.

Table 1. Background characteristics of SILC vs. low risk-CLC

Variables	SILC (n = 23)	Low risk-CLC (n = 89)	p value
Age (y)*	45 [19-65]	59 [22-75]	< 0.01
Gender			
Female	17 (74%)	39 (44%)	< 0.01
Male	6 (26%)	50 (56%)	
BMI (kg/m^2)*	21 [16-30]	23 [16-30]	0.116
Indication			0.308
Stones	23 (100%)	84 (95%)	
Polypoid lesions	0	3 (3%)	
Both	0	2 (2%)	

BMI, body mass index. *Median [range].

Table 2. Intraoperative outcomes among SILC, low risk-CLC, and moderate/high risk-CLC

Variables	SILC (n = 23)	Low risk-CLC (n = 89)	Moderate/High risk-CLC (n = 34)
Operation time (m)*	171 [113-286][a]	126 [72-240][a,b]	150 [100-343][b]
Estimated blood loss (mL)*	3 [0-50]	3 [0-100]b	5 [0-250][b]
Additional trocar placement	2 (9%)	0	0
Conversions to laparotomy†	0	1 (1%)†	1 (4%)†
Intraoperative complications‡	0	0	1‡

* Median [range]. † Intraoperatively diagnosed as gallbladder carcinoma. ‡ Anaphylaxis after intravenous injection of iodinated contrast material. [a] p < 0.05 between the SILC group and the low-risk CLC group. [b] p < 0.05 between the low-risk CLC group and the moderate/high -risk CLC group.

Table 3. Postoperative outcome of SILC vs. low risk-CLC

Variables	SILC (n = 23)	Low risk-CLC (n = 89)	p value
Postoperative complications	0	2†	
Use of postoperative painkiller			
None	6 (26%)	11 (12%)	0.122
≤ 3 days	22 (96%)	46 (52%)	< 0.01
Hospital stay (d)*	2 [2-4]	4 [2-12]	< 0.01

* Median [range]. † Pleural effusion (n = 1) and intra-abdominal abscess (n = 1).

(126 [72-240] min *vs*. 150 [100-343] min, $p < 0.023$). Estimated blood loss in the low-risk CLC was similar to that in the SILC group but smaller than that in the moderate/high-risk CLC group (low risk-CLC 3 [0-100] mL *vs*. moderate/high-risk CLC 5 [0-250] mL, $p = 0.017$). In the SILC group, additional trocars were needed in 2 patients (9%, one patient with BMI 29.9 kg/m^2 and severe adhesion around the liver and the gallbladder and the other patient with severe inflammation around the hepatoduodenal ligament). No intraoperative complication was observed in the SILC group. Conversion to laparotomy was needed for one patient (1%) in the low-risk CLC group and one patient (4%) in the moderate/high-risk CLC group due to the diagnosis of gallbladder carcinoma in the intraoperative pathological findings.

3.3. *Postoperative outcomes*

Postoperative complications (Clavien-Dindo classification [22] grade II or more) developed only in the Low risk-CLC group (pleural effusion and intra-abdominal abscess, Table 3). No bile leak was encountered in the SILC group or in the Low risk-CLC group. Postoperative hospital stay was significantly shorter in the SILC group than in the Low risk-CLC group (2 [2-4] days *vs*. 4 [2-12] days, $p < 0.01$). Patients in the SILC group needed postoperative for shorter periods compared to those in the Low risk-CLC group (Table 3).

4. Discussion

In the present study, LC has been performed in 146 consecutive patients using the definite exclusion criteria for SILC. According to our criteria, 77% of the patients undergoing LC were defined as potential candidates for SILC, and of those, 23 patients decided to undergo SILC. In the SILC group, additional trocars were needed in two patients (9%) and no conversion to open surgery was required. Although operation time was significantly longer in the SILC group than in the low risk-CLC group, SILC led to better postoperative outcomes in terms of length of hospital stay and painkiller use most likely due to its less-invasiveness without increasing risk of operative complications compared to CLC. These results suggest that SILC can be applied safely to patients who prefer better cosmetic outcomes if appropriate indication criteria for SILC is established.

In the previous series, some authors have proposed exclusion criteria for SILC consisting of clinical factors such as BMI > 35 or 40 kg/m^2 (*4,22,23*), cholecystitis (*4,22*), abdominal scar (*4,22,23*), choledocholithiasis (*4,23*), pacemaker (*22*), and pregnancy (*22*) (Table 4). Since operation time of SILC tend to be longer than that in the CLC, it is reasonable to consider patients with a high risk of general anesthesia and clinical factors that can further prolong operation time as contraindications for SILC. Since operation time of SILC tend to be longer than that in the CLC, it is reasonable to consider patients with a high risk of general anesthesia and clinical factors that can further prolong operation time as contraindications for SILC. The long operation time in our series was most likely due to unskilled surgical skills for single incision technique in addition to the application of intraoperative ICG-fluorescence imaging. In the present series, on the other hand, we regarded patients as having moderate/high risk of LC and contraindication for SILC if they met any of the followings: higher age, obesity, operative scar in the upper abdomen, concomitant cardiopulmonary diseases, acute cholecystitis, choledocholithiasis, and abnormal bile duct anatomy. Indeed, operation time and estimated blood loss in the moderate/high-risk CLC group were unfavorable compared to those in the low-risk CLC group, suggesting that our criteria may serve to assure safety of SILC. In contrast, our indication criteria for SILC are stricter than those used in the previous series in terms of restrictions in age and BMI. In particular, routine use of preoperative cholangiographic images to evaluate bile duct anatomy may be a debatable issue, but we believe that preoperative cholangiography and/or intraoperative fluorescence cholangiography (*18,19*) is essential for reducing risk of bile duct injury especially in patients undergoing SILC. As single-incision surgery techniques advance, indications of SILC can be expanded gradually in future.

Interestingly, only 20% of potential candidates of SILC decided to undergo SILC after informed consent, most likely because the majority of patients in the present series prioritized safety of surgery over the advantages SILC demonstrated thorough randomized controlled trials (*2,3*), including better cosmetic outcomes, less postoperative pain, and shorter length of hospital stay compared to CLC. If further advancements in surgical techniques, such as robotic surgery (*24*) and intraoperative fluorescence cholangiography (*17-20,25*), enhance safety of SILC, the role of SILC in the treatment of cholecystolithiasis/cholecystitis may gain more presence in future.

In conclusion, SILC can be safely applied to patients

Table 4. Indication criteria and operative outcomes of SILC

Source	Exclusion criteria for SILC	*N* (indication rate of SILC, %)	Female sex, *N* (%)	Age (y)	BMI (kg/m^2)	Operation time (m)*	Additional port (%)	Conversion (%)	Complication† (%)	Pain (*vs.* CLC)	HS (d)*
Karim, *et al.* (*4*), 2012	warfarin, BMI > 40, cholecystitis, abdominal scar, choledocholithiasis	45 (25)	36 (80)	46 [20-73]	24 [21-27]	75 [42-120]	N.S.	0	0	Same	0.9 [0.5-2]
Culp, *et al.* (*5*), 2012	N.S.	62 (50)	N.S.	45 [22-84]	N.S.	65 [35-141]	N.S.	N.S.	0	N.S.	0.4 [0-6]
Khambaty, *et al.* (*26*), 2011	Malignant disease	N.A.	N.S.	44.9	29.5	82	24	0	2†	Same	1.2
Curcillo, *et al.* (*27*), 2010	Malignant disease	100 (100)	240 (81)	46 [16-87]	N.S.	71	N.S.	1.4	9‡	N.S.	1.5
Rivas, *et al.* (*23*), 2010	Choledocholithiasis, previous abdominal surgery, BMI > 35	N.A.	85 (85)	34 [17-66]	30 [17-43]	51 [23-120]	13	0	N.S.	N.S.	N.S.
Elsey, *et al.* (*28*), 2010	Malignant disease	N.A.	160 (67)	39		40	3	0.4	2§	N.S.	1
Dominguez, *et al.* (*22*), 2009	Upper abdominal scar, BMI > 40, cholecystitis, pacemaker, pregnancy	N.A.	31 (78)	48 [27-68]	28 [21-37]	93 [55-130]	0	0	3¶	N.S.	N.S.
Current study	age > 75 years, BMI > 30, operative scar, cardiopulmonary diseases, cholecystitis, choledocholithiasis, abnormal bile duct anatomy	23 (16)	17 (74)	45 [19-65]	22 [16-30]	171 [113-286]	8	0	0	Less	2 [2-4]

N.A., not applicable; N.S., not stated.

* Median [range].

† Oozing from the gallbladder fossa (*n* = 1) and postoperative endoscopic retrograde cholangiopancreatography for retained stone (*n* = 1).

‡ wound seroma (*n* = 9), intraoperative bile or bag spillage (*n* = 5), umbilical abscess (*n* = 3), umbilical hematoma (*n* = 2), ileus (*n* = 2), postoperative endoscopic retrograde cholangiopancreatography for retained stone (*n* = 1), biliary stricture at 1 year (*n* = 1), laceration to the falciform ligament (*n* = 1), wound infection (*n* = 1), acute renal failure (n = 1), and iatrogenic skin laceration to the wound (*n* = 1).

§ port site hematoma (*n* = 3) and skin dehiscence at umbilical site (*n* = 2).

¶ wound infection at umbilicus (*n* = 1).

who desire better cosmetic outcomes if appropriate exclusion criteria are established through consideration of potential risks that SILC poses in prolonged operation time and bile duct injury.

Acknowledgements

This work was supported by grants from the Takeda Science Foundation, the Kanae Foundation for the Promotion of Medical Science, and the Ministry of Education, Culture, Sports, Science and Technology of Japan (No. 23689060 and No. 23249067).

References

1. Navarra G, Pozza E, Occhionorelli S, Carcoforo P, Donini I. One-wound laparoscopic cholecystectomy. Br J Surg. 1997; 84:695.
2. Bucher P, Pugin F, Buchs NC, Ostermann S, Morel P. Randomized clinical trial of laparoendoscopic single-site versus conventional laparoscopic cholecystectomy. Br J Surg. 2011; 98:1695-1702.
3. Marks JM, Phillips MS, Tacchino R, Roberts K, Onders R, DeNoto G, Gecelter G, Rubach E, Rivas H, Islam A, Soper N, Paraskeva P, Rosemurgy A, Ross S, Shah S. Single-incision laparoscopic cholecystectomy is associated with improved cosmesis scoring at the cost of significantly higher hernia rates: 1-year results of a prospective randomized, multicenter, single-blinded trial of traditional multiport laparoscopic cholecystectomy *vs* single-incision laparoscopic cholecystectomy. J Am Coll Surg. 2013; 216:1037-1047; discussion 1047-1038.
4. Karim MA, Ahmed J, Mansour M, Ali A. Single incision *vs*. conventional multiport laparoscopic cholecystectomy: A comparison of two approaches. Int J Surg. 2012; 10:368-372.
5. Culp BL CV, Arnold DT. Single-incision laparoscopic cholecystectomy versus traditional four-port cholecystectomy. Proc (Bayl Univ Med Cent). 2012; 25:319-323.
6. Aprea G, Coppola Bottazzi E, Guida F, Masone S, Persico G. Laparoendoscopic single site (LESS) versus classic video-laparoscopic cholecystectomy: A randomized prospective study. J Surg Res. 2011; 166:e109-112.
7. Henriksen NA, Al-Tayar H, Rosenberg J, Jorgensen LN. Cost assessment of instruments for single-incision laparoscopic cholecystectomy. JSLS. 2012; 16:353-359.
8. Joseph M, Phillips MR, Farrell TM, Rupp CC. Single incision laparoscopic cholecystectomy is associated with a higher bile duct injury rate: A review and a word of caution. Ann Surg. 2012; 256:1-6.
9. Erdas E, Dazzi C, Secchi F, Aresu S, Pitzalis A, Barbarossa M, Garau A, Murgia A, Contu P, Licheri S, Pomata M, Farina G. Incidence and risk factors for trocar site hernia following laparoscopic cholecystectomy: A long-term follow-up study. Hernia. 2012; 16:431-437.
10. Guidelines for the Clinical Application of Laparoscopic Biliary Tract Surgery: Society of American Gastrointestinal and Endoscopic Surgeons. *http://wwwsagesorg*.
11. Veen EJ, Bik M, Janssen-Heijnen ML, De Jongh M, Roukema AJ. Outcome measurement in laparoscopic cholecystectomy by using a prospective complication registry: Results of an audit. Int J Qual Health Care. 2008; 20:144-151.
12. Georgiades CP, Mavromatis TN, Kourlaba GC, Kapiris SA, Bairamides EG, Spyrou AM, Kokkinos CN, Spyratou CS, Ieronymou MI, Diamantopoulos GI. Is inflammation a significant predictor of bile duct injury during laparoscopic cholecystectomy? Surg Endosc. 2008; 22:1959-1964.
13. Kholdebarin R, Boetto J, Harnish JL, Urbach DR. Risk factors for bile duct injury during laparoscopic cholecystectomy: A case-control study. Surg Innov. 2008; 15:114-119.
14. Abe N, Takeuchi H, Ueki H, Yanagida O, Masaki T, Mori T, Sugiyama M, Atomi Y. Single-port endoscopic cholecystectomy: A bridge between laparoscopic and translumenal endoscopic surgery. J Hepatobiliary Pancreat Surg. 2009; 16:633-638.
15. Chiu CG, Nguyen NH, Bloom SW. Single-incision laparoscopic appendectomy using conventional instruments: An initial experience using a novel technique. Surg Endosc. 2011; 25:1153-1159.
16. Strasberg SM, Hertl M, Soper NJ. An analysis of the problem of biliary injury during laparoscopic cholecystectomy. J Am Coll Surg. 1995; 180:101-125.
17. Aoki T, Murakami M, Yasuda D, Shimizu Y, Kusano T, Matsuda K, Niiya T, Kato H, Murai N, Otsuka K, Kusano M, Kato T. Intraoperative fluorescent imaging using indocyanine green for liver mapping and cholangiography. J Hepatobiliary Pancreat Sci. 2010; 17:590-594.
18. Ishizawa T, Bandai Y, Ijichi M, Kaneko J, Hasegawa K, Kokudo N. Fluorescent cholangiography illuminating the biliary tree during laparoscopic cholecystectomy. Br J Surg. 2010; 97:1369-1377.
19. Ishizawa T, Kaneko J, Inoue Y, Takemura N, Seyama Y, Aoki T, Beck Y, Sugawara Y, Hasegawa K, Harada N, Ijichi M, Kusaka K, Shibasaki M, Bandai Y, Kokudo N. Application of fluorescent cholangiography to single-incision laparoscopic cholecystectomy. Surg Endosc. 2011; 25:2631-2636.
20. Kawaguchi Y, Ishizawa T, Masuda K, Sato S, Kaneko J, Aoki T, Beck Y, Sugawara Y, Hasegawa K, Kokudo N. Hepatobiliary surgery guided by a novel fluorescent imaging technique for visualizing hepatic arteries, bile ducts, and liver cancers on color images. J Am Coll Surg. 2011; 212:e33-39.
21. Ochiai T, Yamazaki S, Ohta K, Takahashi M, Iwai T, Irie T, Noguchi N, Takamatsu S, Kawamura T, Teramoto K, Arii S. Is drip infusion cholecystocholangiography (DIC) an acceptable modality at cholecystectomy for cholecystolithiasis, considering the frequency of bile duct maljunction and intraoperative bile duct injury? J Hepatobiliary Pancreat Surg. 2004; 11:135-139.
22. Dominguez G, Durand L, De Rosa J, Danguise E, Arozamena C, Ferraina PA. Retraction and triangulation with neodymium magnetic forceps for single-port laparoscopic cholecystectomy. Surg Endosc. 2009; 23:1660-1666.
23. Rivas H, Varela E, Scott D. Single-incision laparoscopic cholecystectomy: Initial evaluation of a large series of patients. Surg Endosc. 2010; 24:1403-1412.
24. Buchs NC, Pugin F, Azagury DE, Jung M, Volonte F, Hagen ME, Morel P. Real-time near-infrared fluorescent cholangiography could shorten operative time during

robotic single-site cholecystectomy. Surg Endosc. 2013; 27:3897-3901.
25. Ishizawa T, Tamura S, Masuda K, Aoki T, Hasegawa K, Imamura H, Beck Y, Kokudo N. Intraoperative fluorescent cholangiography using indocyanine green: A biliary road map for safe surgery. J Am Coll Surg. 2009; 208:e1-4.
26. Khambaty F, Brody F, Vaziri K, Edwards C. Laparoscopic versus single-incision cholecystectomy. World J Surg. 2011; 35:967-972.
27. Curcillo PG, 2nd, Wu AS, Podolsky ER, *et al*. Single-port-access (SPA) cholecystectomy: A multi-institutional report of the first 297 cases. Surg Endosc. 2010; 24:1854-1860.
28. Elsey JK, Feliciano DV. Initial experience with single-incision laparoscopic cholecystectomy. J Am Coll Surg. 2010; 210:620-624, 624-626.

(Received October 27, 2015; Revised December 21, 2015; Accepted December 27, 2015)

Original Article

DOI: 10.5582/bst.2015.01114

The relationship between the tip position of an indwelling venous catheter and the subcutaneous edema

Ryoko Murayama[1,*], Toshiaki Takahashi[2], Hidenori Tanabe[1,3], Koichi Yabunaka[2], Makoto Oe[1], Maiko Oya[2], Miho Uchida[4], Chieko Komiyama[4], Hiromi Sanada[2]

[1] *Department of Advanced Nursing Technology, Graduate School of Medicine, The University of Tokyo, Tokyo, Japan;*
[2] *Department of Gerontological Nursing/Wound Care Management, Division of Health Science and Nursing, Graduate School of Medicine, The University of Tokyo, Tokyo, Japan;*
[3] *Terumo Corporation, Tokyo, Japan;*
[4] *Department of Nursing, The University of Tokyo Hospital, Tokyo, Japan.*

Summary **The present observational study aimed to clarify the relationship between the tip position of an indwelling venous catheter and the subcutaneous edema using ultrasonography images. Data were obtained before catheter removal in a medical ward of a university hospital in Tokyo, Japan. Two hundred peripheral intravenous catheters (PIVCs) from 154 patients were observed just before removal. We analyzed data for 194 PIVCs from 150 patients. Subcutaneous edema was observed in 43.8% of ultrasonography images. According to the univariate analysis, insertion site, PIVC tip contact with the vessel wall, and irritant drug's presence were selected as independent variables for logistic regression analysis. Both irritant drug and PIVC tip contact were associated with the presence of subcutaneous edema [adjusted odds ratio (OR) = 2.68, 95% confidence interval (CI) = 1.14-6.33; and OR = 2.01, 95% CI = 1.04-3.88, respectively]. To the best of our knowledge, this is the first study to use ultrasonography to simultaneously observe PIVC tip position and subcutaneous edema. Using ultrasonography to observe PIVC may be a useful method to understand these mechanisms. Medical staff should select an appropriate vein and indwelling catheter to avoid contact of PIVC tip with the vessel wall. Further studies exploring the causality of the relationship between subcutaneous edema, catheter placement, and thrombus formation is required. In addition, further development of nursing skills and medical devices to reduce mechanical stress is required.**

Keywords: Intravenous therapy, peripheral intravenous catheters, subcutaneous tissue, ultrasonography

1. Introduction

Intravenous therapy using a peripheral intravenous catheter (PIVC) is a common and useful method for peripheral venous administration of medicine or fluid (*1-3*). However, treatment interruptions frequently occur in intravenous therapy because of accidental removal or signs and symptoms indicating complications (*4-6*). These problems not only lead to uncomfortable experiences for patients but are also costly in terms of repeated PIVC insertion (*7,8*).

Infiltration is one of the problems of intravenous therapy, because it can result in serious complications, including skin loss and necrosis (*9*). A report from the Veterans Administration of Puget Sound Health Care System showed that 33.7% of all complications during IV therapy with PIVC occurred because of infiltration (*10*). Therefore, clarifying the causes of infiltration can help prevent catheter failures.

The Infusion Nurses Society Standards of Practice Infiltration Scale defines infiltration as inadvertent leakage of a non-vesicant solution into surrounding

**Address correspondence to:*
Dr. Ryoko Murayama, Department of Advanced Nursing Technology, Graduate School of Medicine, The University of Tokyo, 7-3-1 Hongo, Bunkyo-ku, Tokyo, 113-8655, Japan.
E-mail: rymurayama-tky@umin.ac.jp

tissue; grade 1 clinical criteria is edema of < 1 inch (2.5 cm) in any direction (*11*). Edema is observed as swelling surrounding the insertion site of an indwelling catheter. In contrast, subcutaneous edema surrounding the insertion site of an indwelling catheter can also be observed using ultrasonography (US) (*12*), a portable, non-invasive method that does not result in radiation exposure.

Doellman *et al*. reported that risk factors for infiltration and extravasation have been commonly regarded as mechanical factors (vein size and condition, catheter size and stability, insertion site, patient activity, insertion frequency, and power injector use), physiological factors (clot formation, thrombus, fibrin sheath, and lymphedema), and pharmacological factors (pH, osmolarity, vasoconstrictive potential, and cytotoxicity) (*13*). In the present study, we focused on mechanical factors because the subcutaneous tissue and vessel wall are damaged by inserting the needle, and an indwelling catheter might also continuously stimulate the vessel wall during placement. PIVC directly injures the subcutaneous tissue and vessel walls, followed by repairing of the vessel wall by blood clotting (*14*) and occurrence of edema as an inflammatory reaction in the subcutaneous tissue. Stimulation due to catheterization, particularly the catheter tip position, may be directly related to subcutaneous edema.

We used US to observe the situation of the indwelling catheter in the vein just before catheter removal. Clarifying the relationship between the position of an indwelling catheter in the vein and complications such as subcutaneous edema can facilitate the development of catheter placement skills and devices to prevent stimulation of the vessel wall. Therefore, the present study aimed to clarify the relationship between the tip position of an indwelling venous catheter and the image of subcutaneous edema using US.

2. Materials and Methods

2.1. *Study design and participants*

The present study used a prospective observational approach. Data were obtained just before catheter removal in a medical ward of a university hospital in Tokyo, Japan, from January to June 2014. The study sample included hospitalized adult patients who received IV therapy. Catheter removal was from 6:00 AM to 9:00 PM every weekday. Exclusion criteria were as follows: patients who received chemotherapy, those who were under 20 years of age, those who had low cognitive levels, and those who had a condition that made it difficult to cooperate with the research.

2.2. *Data collection procedure*

Researchers were notified by the nurse or physician when a catheter was to be removed due to catheter failure, routine replacement, or completion of IV therapy. US examination was performed at bedside just before catheter removal. Characteristics of PIVC placement, such as insertion site, catheter size, and catheterization duration, were also recorded.

In addition, the researchers observed signs, such as swelling, redness, induration, bleeding, and symptoms, such as pain. Patient characteristics, such as age, sex, and history of present illness and intravenous fluid therapy, were collected from patients' medical records.

2.3. *US scanning technique*

We used US diagnostic equipment (Hitachi Aloka Medical Ltd., Tokyo, Japan) with linear-array transducers (5-18.0 MHz). The focal range and image depth were set at 1.5-2 cm to determine the correct display range. Echo gain was set at 25 and the dynamic range at 65. Ultrasound gel (Aquasonic 100; Parker Laboratories Inc., Fairfield, NJ, USA) and gel pads (Sonar Pad; Nippon Bxi Inc., Tokyo, Japan) were used because transducer pressure resulted in vein disfiguration (Figure 1).

US examinations were performed by two researchers who received US training. The PIVC tip positions were the anatomic landmarks for identifying the US scanning point, with scanning starting at the insertion site and performed for more than 5 cm on both the short and long axes.

2.4. *Data analysis*

2.4.1. *US images analysis*

The PIVC tip position, intravenous thrombus, and edema of the subcutaneous fat layer were assessed by a certified sonographer with over 10 years of experience. The definitions of thrombus and subcutaneous edema were based on our previous study (*12*). Intravenous thrombus was defined as a marked echogenic mass with an uneven surface. Subcutaneous edema was defined by a homogeneous cobblestone appearance in the subcutaneous fat layer due to excessive fluid in the interstitium and a slightly edematous dermis. Presence or absence of subcutaneous edema and intravenous thrombus was determined using both transverse and longitudinal US images.

The PIVC tip position was defined as clear contact with the vessel wall; presence or absence of contact was determined using transverse US images.

2.4.2. *Statistical analysis*

Chi-square or Mann-Whitney *U* tests were used to compare PIVC placement between two patient groups (with and without subcutaneous edema).

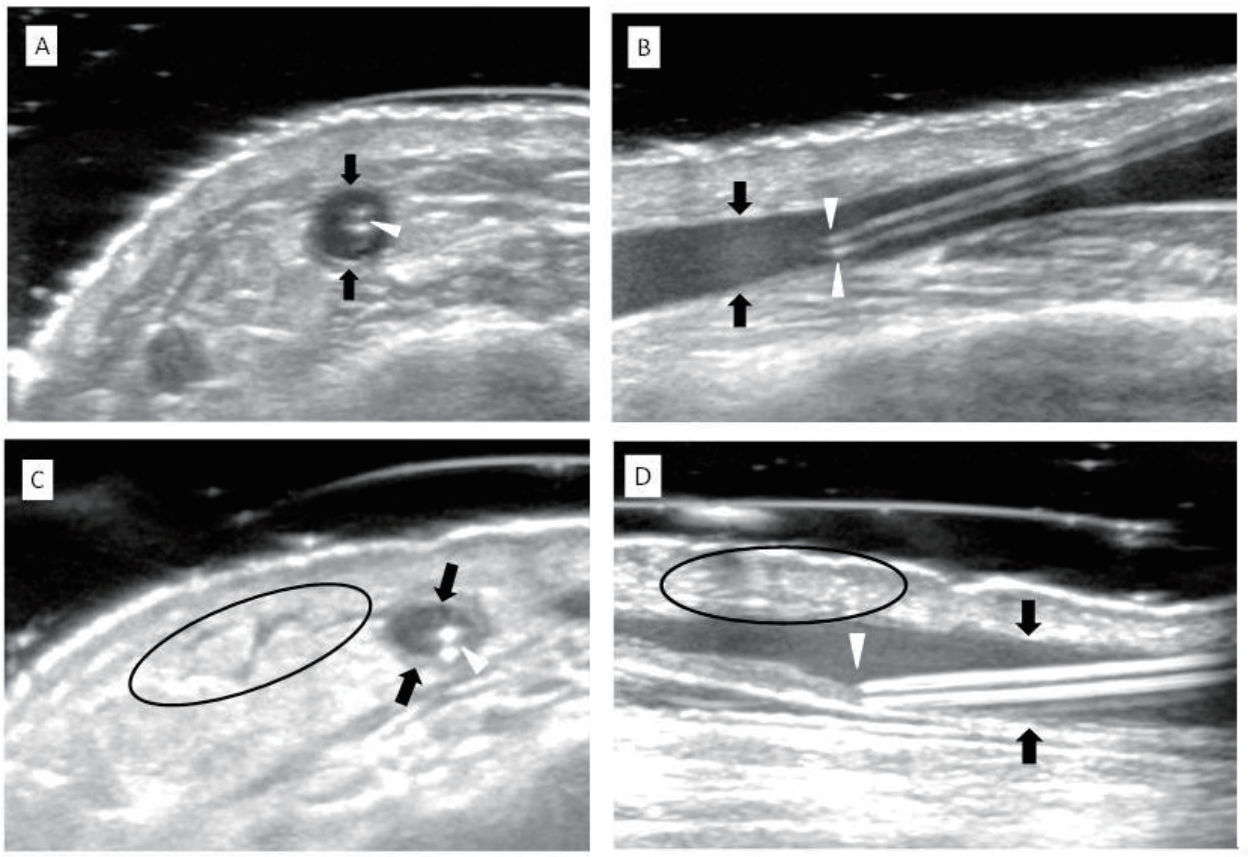

Figure 1. Ultrasonography findings of subcutaneous tissue, blood vessel, and peripheral intravenous catheter placement. **A:** Normal findings (transverse image), **B**: Normal findings (longitudinal image), **C**: PIVC tip in contact with the vessel wall (transverse image), **D**: PIVC tip in contact with the vessel wall (longitudinal image). Ultrasonography images showing the vessel wall (arrows), PIVC tip (arrowheads), and subcutaneous edema (circle).

The insertion site was classified as forearm or others (upper arm, dorsum of hand, wrist, cubital fossa and dorsum of foot) and the duration of catheterization was classified as < 96 h or ≥ 96 h based on the study facility's policy as specified by the Guidelines for the Prevention of Intravascular Catheter-Related Infections (*15*).

The subjective observation of the presence or absence of infiltration [edema (swelling), pain, cool-to-touch] was based on the Infusion Nurses Society Standards of Practice Infiltration Scale, with presence being more than grade 1 criteria (*11*).

Information about intravenous fluids, including antibiotic and irritant drug administration, was collected from patients' medical charts. We defined an irritant drug as having a pH < 5 or a ratio of osmotic pressure ≥ 3, based on the Infusion Nursing Standards of Practice (*16*). Multivariate logistic regression analysis was used to define the relationships between each factor in the univariate analysis that showed $p < 0.2$ with subcutaneous edema.

All two-tailed p-values of < 0.05 were considered significant. Data were analyzed using the Statistical Package for Social Sciences Version 21.0 (IBM SPSS Statistics for Windows, Version 21.0. Armonk, NY: IBM Corp.).

2.5. *Ethical considerations*

Before participation, all patients and their families were informed about the purpose of the study, methods of measurement, management of individual information, consideration of safety, and right to withdraw from participation at any time. Written consent was obtained from all participating patients.

This study was approved by the Research Ethics Committee of the Graduate School of Medicine at the University of Tokyo (#10348).

3. Results

3.1. *Participants and PIVC characteristics*

In total, 293 patients consented to participate in the present study. Two hundred PIVCs from 154 patients were observed just before removal. Six PIVCs were excluded from analysis because US images were not obtained. Data for 194 PIVCs from 150 patients were analyzed. Of the participants, 88 (58.7%) were male; the mean age was 69.7 years, with a standard deviation

(SD) of 12.7 years (range, 25-92 years). In addition, 81 patients (54%) had neoplasms (Table 1).

The most common catheter size was 22 gauge (81.4%) and almost all were inserted into the forearm (91.8%). The duration of catheterization was almost within 96 h (82.0%).

3.2. *US findings*

Subcutaneous edema was observed in 85 (43.8%) US images and was associated with the presence of infiltration ($p < 0.001$). Intravenous thrombus before PIVC removal was observed in 112 (60.9%) images, and PIVC tip was in clear contact with the vessel wall in 60 (33.3%) images.

Table 1. Participants characteristics

Items	(n = 150)
Age (years), mean (SD)	69.7 (12.7)
Sex, *n* (%)	
Male	88 (58.7)
Female	62 (41.3)
History of present illness, *n* (%)	
Neoplasms	81 (54.0)
Digestive system	50 (33.4)
Circulatory system	8 (5.3)
Certain infectious	5 (3.3)
Musculoskeletal system and connective tissue	3 (2.0)
Nervous system	2 (1.3)
Respiratory system	1 (0.7)

Note. History of present illness was classified based on ICD-10.

3.3. *Risk factors associated with subcutaneous edema*

Patient characteristics, such as age and sex, and PIVC characteristics, such as catheter size, insertion site, and catheterization duration, were not associated with subcutaneous edema. The number of PIVCs used to administer irritant drug during catheterization was 36 (18.6%), which was significantly associated with subcutaneous edema ($p = 0.009$) and thrombus ($p = 0.001$). In this research, all irritant drugs were BFLUID®. The presence of PIVC tip contact was also associated with subcutaneous edema ($p = 0.038$). Intravenous thrombus was associated with subcutaneous edema ($p = 0.047$) (Table 2).

Following univariate analysis, insertion site, irritant drug, and presence of PIVC tip contact's presence were included as independent variables for logistic regression analysis. The sex and age of patients were included as control variables. Multicollinearity was considered to be present between PIVC tip contact with the vessel wall and intravenous thrombus; therefore, intravenous thrombus was excluded. Administration of an irritant drug and presence of PIVC tip contact were associated with the presence of subcutaneous edema [adjusted odds ratio (OR) = 2.68, 95% confidence ratio

Table 2. Characteristics of peripheral intravenous catheter placement

Items	Total catheter (n = 194)	Without edema[a] (n = 109)	With edema[a] (n = 85)	p-value
Age (years), median [interquartile range]	72.5 [15.3]	73.0 [15.0]	72.0 [17.0]	0.321[d]
Sex, *n* (%)				0.377[e]
Male	115 (59.3)	68 (62.4)	47 (55.3)	
Female	79 (40.7)	41 (37.6)	38 (44.7)	
Catheter size, *n* (%)				0.418[d]
20 gauge	4 (2.1)	2 (1.8)	2 (2.4)	
22 gauge	158 (81.4)	87 (79.8)	71 (83.5)	
24 gauge	32 (16.5)	20 (18.3)	12 (14.1)	
Insertion site, *n* (%)				0.125[e]
Forearm	178 (91.8)	103 (94.5)	75 (88.2)	
Others[b]	16 (8.2)	6 (5.5)	10 (11.8)	
Duration of catheterization, *n* (%)				0.852[e])
< 96 hours	159 (82.0)	90 (82.6)	69 (81.2)	
≥ 96 hours	35 (18.0)	19 (17.4)	16 (18.8)	
Antibiotics, n (%)				0.312[e]
Presence	94 (48.5)	49 (45.0)	45 (52.9)	
Absence	100 (51.5)	60 (55.0)	40 (47.1)	
Irritant drug[c], *n* (%)				0.009[e]*
Presence	36 (18.6)	13 (11.9)	23 (27.1)	
Absence	158 (81.4)	96 (88.1)	62 (72.9)	
PIVC tip in contact with the vessel wall, *n* (%) (n = 180)				0.038[e]*
Presence	60 (33.3)	27 (26.5)	33 (42.3)	
Absence	120 (66.7)	75 (73.5)	45 (57.7)	
Intravenous thrombus, *n* (%) (n = 184)				0.047[e]*
Presence	112 (60.9)	57 (54.3)	55 (69.6)	
Absence	72 (39.1)	48 (45.7)	24 (30.4)	

[a] Presence of edema of the subcutaneous fat layer before catheter removal by ultrasound. [b] Others: upper arm, dorsum of hand, wrist, cubital fossa, dorsum of foot, [c] Irritant drug: pH < 5 or ratio of osmotic pressure ≥ 3, [d] Mann-Whitney U test, [e] χ^2–test. *$p < 0.05$.

Table 3. Logistic regression analysis of risk factors associated with subcutaneous edema

Items	Odds ratio (95% CI)			
	Crude	*p*-value	Adjusted	*p*-value
Patient characteristics				
Sex (1: male, 0: female)	0.75 (0.42,1.33)	0.377	0.84 (0.44,1.60)	0.587
Age (years)	1.01 (0.99,1.03)	0.429	1.01 (0.99,1.04)	0.443
Insertion site (1: others, 0: forearm)	2.29 (0.80,6.57)	0.125	2.41 (0.80,7.29)	0.119
Irritant drug (1: presence, 0: absence)	2.74 (1.29,5.81)*	0.009	2.68 (1.14,6.33)*	0.025
PIVC tip in contact with the vessel wall (1: presence, 0: absence)	2.04 (1.09,3.82)*	0.038	2.01 (1.04, 3.88)*	0.038

$n = 180$, $^*p < 0.05$, Hosmer & Lemeshow test: $p = 0.694$.

(CI) = 1.14-6.33; and OR = 2.01, 95% CI = 1.04-3.88, respectively] (Table 3).

4. Discussion

To the best of our knowledge, this is the first study using US to simultaneously examine PIVC tip position and subcutaneous edema. We found that the PIVC tip position was associated with subcutaneous edema.

We focused on mechanical factors, one of the risk factors for infiltration and extravasation, because the subcutaneous tissue and vessel wall get damaged by inserting the needle. An indwelling catheter may also continuously stimulate the vessel wall during placement. Everitt prospectively observed intravenous catheters (fine-bore polyurethane) and vein caliber using B-mode ultrasound (7.5 MHz transducer), and suggested that the complication of infusion might be related to intravenous thrombus and that the initiating event was venous endothelial trauma by venipuncture and abrasion at the catheter tip or delivery of the feed (*17*). However, Everitt made no reference to the presence or absence of subcutaneous edema. In contrast, LaRue and Peterson suggested that the toxicant is no more diluted when a catheter's tip is positioned perpendicularly to the vessel wall; therefore, it may promote the incidence of chemically-induced phlebitis and subcutaneous edema (*18*). However, they did not observe the position of the catheter within the vein.

Our results showed that one third of PIVC tip was clearly in contact with the vessel wall. It is noteworthy that the presence of subcutaneous edema was not only associated with irritant infusate but also associated with PIVC tip contact. This suggests that venous endothelial cells are directly damaged by mechanical stimulation from PIVC tip. Consequently, subcutaneous edema may have been formed as an inflammatory reaction to mechanical stimulation. In addition, venous endothelial cells might be damaged by chemical stimulation from PIVC tip positioned near the vessel wall. Extreme pH and high osmolarity relative to blood also affect venous endothelial cell damage and cause the infusate to escape venous circulation (*13,19*).

Although a relationship between the mechanism of the vessel wall damage and an increase in complications has not yet been revealed in detail (*20*), healthcare providers should carefully consider PIVC placement and the tip position in the vein. PIVC observation using US may be a useful method to develop understanding of these mechanisms. Medical staff should select an appropriate vein and indwelling catheter to avoid contact between PIVC tip and the vessel wall. Furthermore, even if PIVC tip is in contact with the vessel wall, developments in catheter design or material might reduce stimulation and inflammatory reactions.

As we performed US observation just before catheter removal, we could not determine how long PIVC tip had stimulated a vascular wall. Moreover, it is not known exactly how PIVC position leads to complications. Further study exploring the causality of the relationship between subcutaneous edema, catheter placement, and thrombus formation is needed. In addition, further development is needed in nursing skills and medical devices to reduce mechanical stress.

Acknowledgements

We deeply appreciate all participants and medical staff who collaborated and helped us in our research. This research project was funded by a grant from the Japanese Ministry of Education, Culture, Sports, Science and Technology (Grant-in-Aid for Exploratory Research, 2014-2015, #26670915).

References

1. Hadaway L. Short peripheral intravenous catheters and infections. J Infus Nurs. 2012; 35:230-240.
2. Zingg W, Pittet D. Peripheral venous catheters: an under-evaluated problem. Int J Antimicrob Agents. 2009; 34S:S38-S42.
3. Chaiyakunapruk N, Veenstra DL, Lipsky BA, Sullivan SD, Saint S. Vascular catheter site care: The clinical and economic benefits of chlorhexidine gluconate compared with povidone iodine. Clin Infect Dis. 2003; 37:764-771.
4. Maki DG, Ringer M. Risk factors for infusion-related phlebitis with small peripheral venous catheters. A randomized controlled trial. Ann Intern Med. 1991; 114:845-854.

5. Rickard CM, Webster J, Wallis MC, Marsh N, McGrail MR, French V, Foster L, Gallagher P, Gowardman JR, Zhang L, McClymont A, Whitby M. Routine versus clinically indicated replacement of peripheral intravenous catheters: a randomised controlled equivalence trial. 2012; 380:1066-1074.
6. Wallis MC, McGrail M, Webster J, Marsh N, Gowardman J, Playford EG, Rickard CM. Risk factors for peripheral intravenous catheter failure: a multivariate analysis of data from a randomized controlled trial. Infect Control Hosp Epidemiol. 2014; 35:63-68.
7. González López JL, Arribi Vilela A, Fernández del Palacio E, Olivares Corral J, Benedicto Martí C, Herrera Portal P. Indwell times, complications and costs of open vs. closed safety peripheral intravenous catheters: a randomized study. J Hosp Infect. 2014; 86:117-126.
8. Tuffaha HW, Rickard CM, Webster J, Marsh N, Gordon L, Wallis M, Scuffham PA. Cost-effectiveness analysis of clinically indicated versus routine replacement of peripheral intravenous catheters. Appl Health Econ Health Policy. 2014; 12:51-58.
9. Hadaway L. Infiltration and extravasation: preventing a complication of IV catheterization. Am J Nurs. 2007; 107:64-72.
10. Royer T. Improving short peripheral IV outcomes: A clinical trial of two securement methods. JAVA. 2003; 8:45-49.
11. Infusion Nursing Society. Infusion nursing standards of practice. J Infus Nurs. 2006; 29(1S):S59-60.
12. Yabunaka K, Murayama R, Takahashi T, Tanabe H, Kawamoto A, Oe M, Arai R, Sanada H. Ultrasonographic appearance of infusion via the peripheral intravenous catheters. J Nurs Sci Eng. 2015; 2:40-46.
13. Doellman D, Hadaway L, Bowe-Geddes LA, Franklin M, LeDonne J, Papke-O'Donnell L, Pettit J, Schulmeister L, Stranz M. Infiltration and extravasation: update on prevention and management. J Infus Nurs. 2009; 32:203-211.
14. Lanbeck P, Odenholt I, Paulsen O. Antibiotics differ in their tendency to cause infusion phlebitis: a prospective observational study. Scand J Infect Dis. 2002; 34:512-519.
15. O'Grady NP, Alexander M, Dellinger EP, Gerberding JL, Heard SO, Maki DG, Masur H, McCormick RD, Mermel LA, Pearson ML, Raad II, Randolph A, Weinstein RA. Guidelines for the prevention of intravascular catheter-related infections. Centers for Disease Control and Prevention. MMWR Recomm Rep. 2002; 51(RR-10):1-29.
16. Infusion Nursing Society. Infusion nursing standards of practice. J Infus Nurs. 2011; 34(1S):S5.
17. Everitt NJ. Effect of prolonged infusion on vein calibre: a prospective study. Ann R Coll Surg Engl. 1999; 81:109-112.
18. LaRue GD, Peterson M. The impact of dilution on intravenous therapy. J Infus Nurs. 2011; 34:117-123.
19. Thomas MV, Stranz M, Masoorli S, Hadaway LC. The diverse and conflicting standards and practices in infusion therapy. JAVA. 2002; 7:9-25.
20. Tagalakis V, Kahn S, Libman M, Blosteinet M. The epidemiology of peripheral vein infusion thrombophlebitis: a critical review. Am J Med. 2002; 113:146-151.

(Received August 28, 2015; Revised December 23, 2015; Accepted December 26, 2015)

Brief Report

DOI: 10.5582/bst.2015.01171

Alantolactone exhibited anti-herpes simplex virus 1 (HSV-1) action *in vitro*

Caidan Rezeng[1], Dongping Yuan[2], Jun Long[2], Dengdeng Suonan[1], Fang Yang[1], Wenyuan Li[1], Li Tong[1,*], Pengcuo Jiumei[3,*]

[1] *Traditional Chinese and Tibetan Medicine of Medical College, Qinghai University, Xining, Qinghai, China;*
[2] *Pharmacy College, Nanjing University of Chinese Medicine, Nanjing, Jiangsu, China;*
[3] *Qinghai Jiumei Traditional Tibetan Hospital, Xining, Qinghai, China.*

Summary **The aim of this study was to determine the inhibitory action of alantolactone, a gradient of traditional Chinese medicine Inulae Radix (Tu-Mu-Xiang), on herpes simplex virus 1 (HSV-1). African green monkey kidney cells (Vero cells) were infected with HSV-1 and the protective effects of alantolactone on Vero cells were examined. At concentrations of 10^{-6}, 10^{-7}, and 10^{-8} g/mL, alantolactone did not have a marked harmful effect on the viability of Vero cells according to an MTT assay. Based on the cytopathic effect (CPE) and MTT assays, alantolactone at these concentrations exhibited antiviral action and protected cells from being damaged by HSV-1. Results indicated that alantolactone had potent anti-HSV-1 action and provided evidence for use of Inulae Radix in the treatment of HSV-1 infection.**

Keywords: Herpes simplex virus (HSV), Inulae Radix, alantolactone, cytopathic effect (CPE)

1. Introduction

Viral infections are serous conditions and are usually difficult to treat at the current point in time (*1*). Herpes simplex virus (HSV) can primarily be divided into two serotypes, *i.e*. HSV-1 and HSV-2, and infection with HSV can lead to herpes simplex encephalitis, genital herpes, or cervical cancer, and is a risk factor for fetal congenital malformation (*2,3*). HSV-1 infection is a common and widespread disease that is characterized by lifelong persistence and periodic reactivation (*4*). Ribavirin is the one of the main drugs that is currently used to treat HSV-1 infection (*5*). However, mounting evidence has shown that the virus is becoming resistant to this drug due to long-term use (*6,7*). Consequently, the pressing challenge is to develop novel drugs to treat HSV-1 infection.

Traditional Chinese medicine (TCM) has attracted considerable attention in the search for antivirals because TCM has obvious advantages in the treatment of viral infections and TCM has a broad range of applications (*8*). Inulae Radix (Tu-Mu-Xiang) is a typical TCM that is usually used to treat bacterial or viral infection in China. Thus, the current study examined the anti-HSV-1 action of alantolactone, a main component found in Inulae Radix, *in vitro*.

2. Materials and Methods

2.1. *Agents*

Alantolactone was obtained from Shanghai Yuanye Biological Technology Co. Ltd. (Shanghai, China). For an *in vitro* assay, alantolactone was first dissolved in dimethyl sulfoxide (DMSO; Sigma-Aldrich) and further diluted in RPMI-1640 media (Hyclone) before use. Injectable ribavirin was purchased from Sanjing Pharmaceutical Co., Ltd. (Harbin, Heilongjiang, China). HSV-1 was obtained from the School of Basic Medicine, Nanjing University of Traditional Chinese Medicine (Nanjing, Jiangsu, China).

2.2. *Cell line and cell culture*

African green monkey kidney cells (Vero cells) were

**Address correspondence to:*
Dr. Li Tong, Traditional Chinese and Tibetan Medicine of Medical College, Qinghai University, Xining, Qinghai, China.
E-mail: qhdx2011@126.com

Dr. Pengcuo Jiumei, Qinghai Jiumei Traditional Tibetan Hospital, Xining, Qinghai, China.
E-mail: qhzhzyyjzhx@126.com

Table 1. Anti-HSV-1 action of alantolactone evaluated with a CPE-based assay

Experiments No.	Virus-free cells	Infected cells	Ribavirin	Alantolactone concentration (g/mL)				
				10^{-6}	10^{-7}	10^{-8}	10^{-9}	10^{-10}
1	-	++++	-	+	-	-	++	+++
2	-	++++	-	+	+	-	++	+++
3	-	++++	-	-	-	++	+++	++++

−, none of the cells exhibited a cytopathic effect; +, 0-25% of cells exhibited a cytopathic effect; ++, 25-50% of cells exhibited a cytopathic effect; +++, 50-75% of cells exhibited a cytopathic effect; ++++, 75-100% of cells exhibited a cytopathic effect.

obtained from the School of Basic Medicine, Nanjing University of Traditional Chinese Medicine. Briefly, cells were cultured in RPMI 1640 supplemented with 10% fetal bovine serum (FBS) at 37°C in a humid atmosphere (5% CO_2-95% air). Cells were harvested by brief incubation in 0.02% (w/v) ethylenediaminetetraacetic acid (EDTA) in PBS.

2.3. *Assay of the cytopathic effect (CPE) of the virus*

A CPE-based assay was used to determine the structural changes in the host cells that are caused by viral invasion. Common examples of CPE include rounding of infected cells, fusion with adjacent cells to form syncytia, and the appearance of nuclear or cytoplasmic inclusion bodies (*9*). '−' was recorded when none of the cells exhibited cytopathic effect; '+' was recorded when 0-25% of cells exhibited a cytopathic effect; '++' was recorded when 25-50% of cells exhibited a cytopathic effect; '+++' was recorded when 50-75% of cells exhibited a cytopathic effect; and '++++' was recorded when 75-100% of cells exhibited a cytopathic effect.

2.4. *MTT assay*

Cells (1×10^4 per well) seeded in 96-well plates were exposed to increasing concentrations of alantolactone for specified times. After incubation for 72 h, a 3-(4,5-dimethylthiazol-2-yl)-2,5-diphenyltetrazolium bromide (MTT) assay was performed by adding 20 μL of MTT (5 mg/mL, Sigma-Aldrich) for 4 h (*10*). Light absorbance of the solution was measured at 490 nm on a microplate reader (Perkin-Elmer, USA).

3. Results and Discussion

3.1. *Toxicity of the virus*

Vero cells seeded in 96-well plates were exposed to decreasing concentrations of HSV-1 (10^{-1}, 10^{-2}, 10^{-3}, 10^{-4}, 10^{-5}, 10^{-6}, 10^{-7}, 10^{-8}, or 10^{-9} of stock virus solution) for 1 h. The virus solution was then removed. The cells were subsequently cultured in RPMI-1640 media for 72 h. A CPE-based assay was used to determine the damage caused by HSV-1 in Vero cells. Results indicated that Vero cells were all infected when the dilution of the virus was above 10^{-3}, and the tissue culture 50% infective dose (TCID50) was calculated to be $10^{-6.33}$ according to the Reed-Muench method.

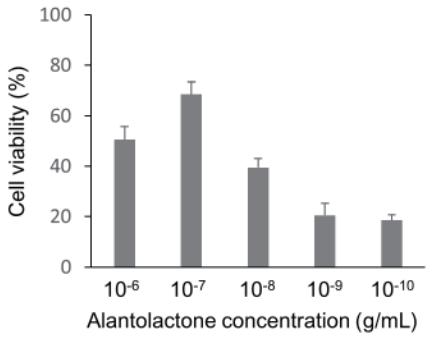

Figure 1. Alantolactone increased the viability of Vero cells infected with HSV-1.

3.2. *Effects of alantolactone on the viability of Vero cells*

Vero cells seeded in 96-well plates were exposed to increasing concentrations of alantolactone for 72 h. The cells were then subjected to an MTT assay. Results revealed no obvious cytotoxic effects when the concentration of alantolactone was lower than 10^{-6} g/mL. In order to avoid the harmful effects of alantolactone on Vero cells, the concentration of alantolactone was set below 10^{-6} g/mL in the following antiviral assay.

3.3. *Antiviral action of alantolactone on HSV-1*

The effects of alantolactone on HSV-1 were determined using a CPE-based assay and an MTT assay. Results of the CPE-based assay indicated that alantolactone at a concentration of 10^{-6}, 10^{-7}, or 10^{-8} g/mL markedly inhibited viral infection (Table 1). However, alantolactone at a concentration of 10^{-7} g/mL exhibited more potent antiviral action. The reason why alantolactone had less potent antiviral activity at 10^{-6} g/mL than at 10-7 g/mL might be because a higher concentration of alantolactone has more of a cytotoxic effect on Vero cells, thus reducing the resistance of Vero cells to viral infection. Similar results were obtained using the MTT assay (Figure 1). Cell viability increased markedly when the alantolactone concentration was 10^{-6}, 10^{-7}, or 10^{-8} g/

mL. Alantolactone at a concentration of 10^{-7} g/mL provided the most protection from HSV-1 infection. The IC_{50} of alantolactone was determined to be $10^{-7.4}$ g/mL.

The present study examined the antiviral action of alantolactone on HSV-1. Given the possible cytotoxic effects of alantolactone on Vero cells, the effects of alantolactone on the cell viability of Vero cells were first determined using an MTT assay. Results indicated that alantolactone at concentrations below 10^{-6} g/mL did not have a marked effect on the cell viability on Vero cells. Alantolactone at a concentration of 10^{-6}, 10^{-7}, or 10^{-8} g/mL inhibited viral infection and the viability of Vero cells increased markedly at these concentrations. These results suggest that alantolactone had antiviral action against HSV-1 *in vitro* and they provide evidence for use of Inulae Radix to treat HSV-1 infection. Studies to examine the antiviral action of alantolactone *in vivo* and the mechanisms underlying the action of alantolactone are warranted in the future.

Acknowledgements

This Project was supported by the National Natural Science Foundation of China (Project No. 81160469).

References

1. Erdemli HK, Akyol S, Armutcu F, Akyol O. Antiviral properties of caffeic acid phenethyl ester and its potential application. J Intercult Ethnopharmacol. 2015; 4:344-347.
2. Sauerbrei A, Bohn-Wippert K, Kaspar M, Krumbholz A, Karrasch M, Zell R. Database on natural polymorphisms and resistance-related non-synonymous mutations in thymidine kinase and DNA polymerase genes of herpes simplex virus types 1 and 2. J Antimicrob Chemother. 2016; 71:6-16.
3. Piret J, Boivin G. Innate immune response during herpes simplex virus encephalitis and development of immunomodulatory strategies. Rev Med Virol. 2015; 25:300-319.
4. Kennedy PG, Rovnak J, Badani H, Cohrs RJ. A comparison of herpes simplex virus type 1 and varicella-zoster virus latency and reactivation. J Gen Virol. 2015; 96:1581-1602.
5. Ding X, Sanchez DJ, Shahangian A, Al-Shyoukh I, Cheng G, Ho CM. Cascade search for HSV-1 combinatorial drugs with high antiviral efficacy and low toxicity. Int J Nanomedicine. 2012; 7:2281-2292.
6. Marcelletti JF. Synergistic inhibition of herpesvirus replication by docosanol and antiviral nucleoside analogs. Antiviral Res. 2002; 56:153-166.
7. Andronova VL, Grokhovskii SL, Surovaia AN, Deriabin PG, Gurskii GV, Galegov GA. Research of suppression of the herpes simplex virus reproduction with drug resistance using a combination 15-Lys-bis-Nt with some antiherpetic drugs. Vopr Virusol. 2014; 59:38-41.
8. Huang J, Su D, Feng Y, Liu K, Song Y. Antiviral herbs--Present and future. Infect Disord Drug Targets. 2014; 14:61-73.
9. Ichinose T, Musyoka TM, Watanabe K, Kobayashi N. Evaluation of antiviral activity of Oligonol, an extract of Litchi chinensis, against betanodavirus. Drug Discov Ther. 2013; 7:254-260.
10. Chen J, Wang W, Wang H, Liu X, Guo X. Combination treatment of ligustrazine piperazine derivate DLJ14 and adriamycin inhibits progression of resistant breast cancer through inhibition of the EGFR/PI3K/Akt survival pathway and induction of apoptosis. Drug Discov Ther. 2014; 8:33-41.

(Received September 27, 2015; Revised December 14, 2015; Accepted December 27, 2015)

Subject Index (2015)

Policy Forum

Reviews

Original Articles

2015; 9(3):169-181. (DOI: 10.5582/bst.2015.01011)

Evaluation of medical staff and patient satisfaction of Chinese hospitals and measures for improvement.
Li M, Huang CY, Lu XC, Chen SY, Zhao P, Lu HZ
2015; 9(3):182-189. (DOI: 10.5582/bst.2015.01043)

Prevalence of 7 virulence genes of *Legionella* strains isolated from environmental water sources of public facilities and sequence types diversity of *L. pneumopila* strains in Macau.
Xiong LN, Zhao HB, Mo ZY, Shi L
2015; 9(4):214-220. (DOI: 10.5582/bst.2015.01075)

High copy numbers and N terminal insertion position of influenza A M2E fused with hepatitis B core antigen enhanced immunogenicity.
Sun XC, Wang YL, Dong CW, Hu JQ, Yang LP
2015; 9(4):221-227. (DOI: 10.5582/bst.2015.01060)

Products of dentin matrix protein-1 degradation by interleukin-1β-induced matrix metalloproteinase-3 promote proliferation of odontoblastic cells.
Hase N, Ozeki N, Hiyama T, Yamaguchi H, Kawai R, Kondo A, Nakata K, Mogi M
2015; 9(4):228-236. (DOI: 10.5582/bst.2015.01092)

Protective effects on vascular endothelial cell in *N'*-nitro-*L*-arginine (*L*-NNA)-induced hypertensive rats from the combination of effective components of *Uncaria rhynchophylla* and *Semen Raphani*.
Li YL, Yang WQ, Zhu QJ, Yang JG, Wang Z
2015; 9(4):237-244. (DOI: 10.5582/bst.2015.01087)

Dual regulating effect of Ningdong granule on extracellular dopamine content of two kinds of Tourette's syndrome rat models.
Zhao L, Qi FH, Zhang F, Wang ZX, Mu LM, Wang Y, En Q, Li JJ, Du YF, Li AY
2015; 9(4):245-251. (DOI: 10.5582/bst.2015.01088)

The diagnostic value of contrast-enhanced ultrasound in differentiating small renal carcinoma and angiomyolipoma.
Chen L, Wang L, Diao XH, Qian WQ, Fang L, Pang Y, Zhan J, Chen Y
2015; 9(4):252-258. (DOI: 10.5582/bst.2015.01080)

The Chinese version of monitoring and evaluation system strengthening tool for human immunodeficiency virus (HIV) capacity building: Development and evaluation.
Zhao R, Chen R, Zhang B, Ma Y, Qin X, Hu Z
2015; 9(4):259-265. (DOI: 10.5582/bst.2015.01111)

A systematic review and meta-analysis of feasibility, safety and efficacy of associating liver partition and portal vein ligation for staged hepatectomy (ALPPS) versus two-stage hepatectomy (TSH).
Sun ZP, Tang W, Sakamoto Y, Hasegawa K, Kokudo N
2015; 9(5):284-288. (DOI: 10.5582/bst.2015.01139)

Transarterial Y90 radioembolization versus chemoembolization for patients with hepatocellular carcinoma: A meta-analysis.
Zhang YF, Li YM, Ji H, Zhao X, Lu HW
2015; 9(5):289-298. (DOI: 10.5582/bst.2015.01089)

Adenovirus-mediated P311 inhibits TGF-β1-induced epithelialmesenchymal transition in NRK-52E cells *via* TGF-β1-Smad-ILK pathway.
Qi FH, Cai PP, Liu X, Peng M, Si GM
2015; 9(5):299-306. (DOI: 10.5582/bst.2015.01129)

Brief Reports

Case Report

Commentary

News

Letter

BST
BioScience Trends

Guide for Authors

1. Scope of Articles

BioScience Trends is an international peer-reviewed journal. BioScience Trends devotes to publishing the latest and most exciting advances in scientific research. Articles cover fields of life science such as biochemistry, molecular biology, clinical research, public health, medical care system, and social science in order to encourage cooperation and exchange among scientists and clinical researchers.

2. Submission Types

Original Articles should be well-documented, novel, and significant to the field as a whole. An Original Article should be arranged into the following sections: Title page, Abstract, Introduction, Materials and Methods, Results, Discussion, Acknowledgments, and References. Original articles should not exceed 5,000 words in length (excluding references) and should be limited to a maximum of 50 references. Articles may contain a maximum of 10 figures and/or tables.

Brief Reports definitively documenting either experimental results or informative clinical observations will be considered for publication in this category. Brief Reports are not intended for publication of incomplete or preliminary findings. Brief Reports should not exceed 3,000 words in length (excluding references) and should be limited to a maximum of 4 figures and/or tables and 30 references. A Brief Report contains the same sections as an Original Article, but the Results and Discussion sections should be combined.

Reviews should present a full and up-to-date account of recent developments within an area of research. Normally, reviews should not exceed 8,000 words in length (excluding references) and should be limited to a maximum of 100 references. Mini reviews are also accepted.

Policy Forum articles discuss research and policy issues in areas related to life science such as public health, the medical care system, and social science and may address governmental issues at district, national, and international levels of discourse. Policy Forum articles should not exceed 2,000 words in length (excluding references).

Case Reports should be detailed reports of the symptoms, signs, diagnosis, treatment, and follow-up of an individual patient. Case reports may contain a demographic profile of the patient but usually describe an unusual or novel occurrence. Unreported or unusual side effects or adverse interactions involving medications will also be considered. Case Reports should not exceed 3,000 words in length (excluding references).

News articles should report the latest events in health sciences and medical research from around the world. News should not exceed 500 words in length.

Letters should present considered opinions in response to articles published in BioScience Trends in the last 6 months or issues of general interest. Letters should not exceed 800 words in length and may contain a maximum of 10 references.

3. Editorial Policies

Ethics: BioScience Trends requires that authors of reports of investigations in humans or animals indicate that those studies were formally approved by a relevant ethics committee or review board.

Conflict of Interest: All authors are required to disclose any actual or potential conflict of interest including financial interests or relationships with other people or organizations that might raise questions of bias in the work reported. If no conflict of interest exists for each author, please state "There is no conflict of interest to disclose".

Submission Declaration: When a manuscript is considered for submission to BioScience Trends, the authors should confirm that 1) no part of this manuscript is currently under consideration for publication elsewhere; 2) this manuscript does not contain the same information in whole or in part as manuscripts that have been published, accepted, or are under review elsewhere, except in the form of an abstract, a letter to the editor, or part of a published lecture or academic thesis; 3) authorization for publication has been obtained from the authors' employer or institution; and 4) all contributing authors have agreed to submit this manuscript.

Cover Letter: The manuscript must be accompanied by a cover letter signed by the corresponding author on behalf of all authors. The letter should indicate the basic findings of the work and their significance. The letter should also include a statement affirming that all authors concur with the submission and that the material submitted for publication has not been published previously or is not under consideration for publication elsewhere. The cover letter should be submitted in PDF format. For example of Cover Letter, please visit http://www.biosciencetrends.com/downcentre.php (Download Centre).

Copyright: A signed JOURNAL PUBLISHING AGREEMENT (JPA) form must be provided by post, fax, or as a scanned file before acceptance of the article. Only forms with a hand-written signature are accepted. This copyright will ensure the widest possible dissemination of information. A form facilitating transfer of copyright can be downloaded by clicking the appropriate link and can be returned to the e-mail address or fax number noted on the form (Please visit Download Centre). Please note that your manuscript will not proceed to the next step in publication until the JPA Form is received. In addition, if excerpts from other copyrighted works are included, the author(s) must obtain written permission from the copyright owners and credit the source(s) in the article.

Suggested Reviewers: A list of up to 3 reviewers who are qualified to assess the scientific merit of the study is welcomed. Reviewer information including names, affiliations, addresses, and e-mail should be provided at the same time the manuscript is submitted online. Please do not suggest reviewers with known conflicts of interest, including participants or anyone with a stake in the proposed research; anyone from the same institution; former students, advisors, or research collaborators (within the last three years); or close personal contacts. Please note that the Editor-in-Chief may accept one or more of the proposed reviewers or may request a review by other qualified persons.

Language Editing: Manuscripts prepared by authors whose native language is not English should have their work proofread by a native English speaker before submission. If not, this might delay the publication of your manuscript in BioScience Trends.

The Editing Support Organization can provide English proofreading, Japanese-English translation, and Chinese-English translation services to authors who want to publish in BioScience Trends and need assistance before submitting a manuscript. Authors can visit this organization directly at http://www.iacmhr.com/iac-eso/support.php?lang=en. IAC-ESO was established to facilitate manuscript preparation by researchers whose native language is not English and to help edit works intended for international academic journals.

4. Manuscript Preparation

Manuscripts should be written in clear, grammatically correct English and submitted as a Microsoft Word file in a single-column format. Manuscripts must be paginated and typed in 12-point Times New Roman font with 24-point line spacing. Please do not embed figures in the text. Abbreviations should be used as little as possible and should be explained at first mention unless the term is a well-known abbreviation (*e.g.* DNA). Single words should not be abbreviated.

Title Page: The title page must include 1) the title of the paper (Please note the title should be short, informative, and contain the major key words); 2) full name(s) and affiliation(s) of the author(s), 3) abbreviated names of the author(s), 4) full name, mailing address, telephone/fax numbers, and e-mail address of the corresponding author; and 5) conflicts of interest (if you have an actual or potential conflict of interest to disclose, it must be included as a footnote on the title page of the manuscript; if no conflict of

interest exists for each author, please state "There is no conflict of interest to disclose"). Please visit Download Centre and refer to the title page of the manuscript sample.

Abstract: The abstract should briefly state the purpose of the study, methods, main findings, and conclusions. For article types including Original Article, Brief Report, Review, Policy Forum, and Case Report, a one-paragraph abstract consisting of no more than 250 words must be included in the manuscript. For News and Letters, a brief summary of main content in 150 words or fewer should be included in the manuscript. Abbreviations must be kept to a minimum and non-standard abbreviations explained in brackets at first mention. References should be avoided in the abstract. Key words or phrases that do not occur in the title should be included in the Abstract page.

Introduction: The introduction should be a concise statement of the basis for the study and its scientific context.

Materials and Methods: The description should be brief but with sufficient detail to enable others to reproduce the experiments. Procedures that have been published previously should not be described in detail but appropriate references should simply be cited. Only new and significant modifications of previously published procedures require complete description. Names of products and manufacturers with their locations (city and state/country) should be given and sources of animals and cell lines should always be indicated. All clinical investigations must have been conducted in accordance with Declaration of Helsinki principles. All human and animal studies must have been approved by the appropriate institutional review board(s) and a specific declaration of approval must be made within this section.

Results: The description of the experimental results should be succinct but in sufficient detail to allow the experiments to be analyzed and interpreted by an independent reader. If necessary, subheadings may be used for an orderly presentation. All figures and tables must be referred to in the text.

Discussion: The data should be interpreted concisely without repeating material already presented in the Results section. Speculation is permissible, but it must be well-founded, and discussion of the wider implications of the findings is encouraged. Conclusions derived from the study should be included in this section.

Acknowledgments: All funding sources should be credited in the Acknowledgments section. In addition, people who contributed to the work but who do not meet the criteria for authors should be listed along with their contributions.

References: References should be numbered in the order in which they appear in the text. Citing of unpublished results, personal communications, conference abstracts, and theses in the reference list is not recommended but these sources may be mentioned in the text. In the reference list, cite the names of all authors when there are fifteen or fewer authors; if there are sixteen or more authors, list the first three followed by *et al.* Names of journals should be abbreviated in the style used in PubMed. Authors are responsible for the accuracy of the references. Examples are given below:

Example 1 (Sample journal reference):
Inagaki Y, Tang W, Zhang L, Du GH, Xu WF, Kokudo N. Novel aminopeptidase N (APN/CD13) inhibitor 24F can suppress invasion of hepatocellular carcinoma cells as well as angiogenesis. Biosci Trends. 2010; 4:56-60.

Example 2 (Sample journal reference with more than 15 authors):
Darby S, Hill D, Auvinen A, *et al.* Radon in homes and risk of lung cancer: Collaborative analysis of individual data from 13 European case-control studies. BMJ. 2005; 330:223.

Example 3 (Sample book reference):
Shalev AY. Post-traumatic stress disorder: diagnosis, history and life course. In: Post-traumatic Stress Disorder, Diagnosis, Management and Treatment (Nutt DJ, Davidson JR, Zohar J, eds.). Martin Dunitz, London, UK, 2000; pp. 1-15.

Example 4 (Sample web page reference):
Ministry of Health, Labour and Welfare of Japan. Dietary reference intakes for Japanese. *http://www.mhlw.go.jp/houdou/2004/11/h1122-2a.html* (accessed June 14, 2010).

Tables: All tables should be prepared in Microsoft Word or Excel and should be arranged at the end of the manuscript after the References section. Please note that tables should not in image format. All tables should have a concise title and should be numbered consecutively with Arabic numerals. If necessary, additional information should be given below the table.

Figure Legend: The figure legend should be typed on a separate page of the main manuscript and should include a short title and explanation. The legend should be concise but comprehensive and should be understood without referring to the text. Symbols used in figures must be explained.

Figure Preparation: All figures should be clear and cited in numerical order in the text. Figures must fit a one- or two-column format on the journal page: 8.3 cm (3.3 in.) wide for a single column, 17.3 cm (6.8 in.) wide for a double column; maximum height: 24.0 cm (9.5 in.). Please make sure that the symbols and numbers appeared in the figures should be clear. Please make sure that artwork files are in an acceptable format (TIFF or JPEG) at minimum resolution (600 dpi for illustrations, graphs, and annotated artwork, and 300 dpi for micrographs and photographs). Please provide all figures as separate files. Please note that low-resolution images are one of the leading causes of article resubmission and schedule delays. All color figures will be reproduced in full color in the online edition of the journal at no cost to authors.

Units and Symbols: Units and symbols conforming to the International System of Units (SI) should be used for physicochemical quantities. Solidus notation (*e.g.* mg/kg, mg/mL, mol/mm^2/min) should be used. Please refer to the SI Guide www.bipm.org/en/si/ for standard units.

Supplemental data: Supplemental data might be useful for supporting and enhancing your scientific research and BioScience Trends accepts the submission of these materials which will be only published online alongside the electronic version of your article. Supplemental files (figures, tables, and other text materials) should be prepared according to the above guidelines, numbered in Arabic numerals (*e.g.*, Figure S1, Figure S2, and Table S1, Table S2) and referred to in the text. All figures and tables should have titles and legends. All figure legends, tables and supplemental text materials should be placed at the end of the paper. Please note all of these supplemental data should be provided at the time of initial submission and note that the editors reserve the right to limit the size and length of Supplemental Data.

5. Submission Checklist

The Submission Checklist will be useful during the final checking of a manuscript prior to sending it to BioScience Trends for review. Please visit Download Centre and download the Submission Checklist file.

6. Online Submission

Manuscripts should be submitted to BioScience Trends online at http://www.biosciencetrends.com. The manuscript file should be smaller than 5 MB in size. If for any reason you are unable to submit a file online, please contact the Editorial Office by e-mail at office@biosciencetrends.com.

7. Accepted Manuscripts

Proofs: Galley proofs in PDF format will be sent to the corresponding author via e-mail. Corrections must be returned to the editor (proof-editing@biosciencetrends.com) within 3 working days.

Offprints: Authors will be provided with electronic offprints of their article. Paper offprints can be ordered at prices quoted on the order form that accompanies the proofs.

Page Charge: Page charges will be levied on all manuscripts accepted for publication in BioScience Trends ($140 per page for black white pages; $340 per page for color pages). Under exceptional circumstances, the author(s) may apply to the editorial office for a waiver of the publication charges at the time of submission.

(*Revised February 2013*)

Editorial and Head Office:
Pearl City Koishikawa 603
2-4-5 Kasuga, Bunkyo-ku
Tokyo 112-0003 Japan
Tel: +81-3-5840-8764
Fax: +81-3-5840-8765
E-mail: office@biosciencetrends.com

BST
BioScience Trends

JOURNAL PUBLISHING AGREEMENT (JPA)

Manuscript No.:

Title:

Corresponding Author:

The International Advancement Center for Medicine & Health Research Co., Ltd. (IACMHR Co., Ltd.) is pleased to accept the above article for publication in BioScience Trends. The International Research and Cooperation Association for Bio & Socio-Sciences Advancement (IRCA-BSSA) reserves all rights to the published article. Your written acceptance of this JOURNAL PUBLISHING AGREEMENT is required before the article can be published. Please read this form carefully and sign it if you agree to its terms. The signed JOURNAL PUBLISHING AGREEMENT should be sent to the BioScience Trends office (Pearl City Koishikawa 603, 2-4-5 Kasuga, Bunkyo-ku, Tokyo 112-0003, Japan; E-mail: **office@biosciencetrends.com**; Tel: **+81-3-5840-8764**; Fax: **+81-3-5840-8765**).

1. Authorship Criteria

As the corresponding author, I certify on behalf of all of the authors that:
1) The article is an original work and does not involve fraud, fabrication, or plagiarism.
2) The article has not been published previously and is not currently under consideration for publication elsewhere. If accepted by BioScience Trends, the article will not be submitted for publication to any other journal.
3) The article contains no libelous or other unlawful statements and does not contain any materials that infringes upon individual privacy or proprietary rights or any statutory copyright.
4) I have obtained written permission from copyright owners for any excerpts from copyrighted works that are included and have credited the sources in my article.
5) All authors have made significant contributions to the study including the conception and design of this work, the analysis of the data, and the writing of the manuscript.
6) All authors have reviewed this manuscript and take responsibility for its content and approve its publication.
7) I have informed all of the authors of the terms of this publishing agreement and I am signing on their behalf as their agent.

2. Copyright Transfer Agreement

I hereby assign and transfer to IACMHR Co., Ltd. all exclusive rights of copyright ownership to the above work in the journal BioScience Trends, including but not limited to the right 1) to publish, republish, derivate, distribute, transmit, sell, and otherwise use the work and other related material worldwide, in whole or in part, in all languages, in electronic, printed, or any other forms of media now known or hereafter developed and the right 2) to authorize or license third parties to do any of the above.

I understand that these exclusive rights will become the property of IACMHR Co., Ltd., from the date the article is accepted for publication in the journal BioScience Trends. I also understand that IACMHR Co., Ltd. as a copyright owner has sole authority to license and permit reproductions of the article.

I understand that except for copyright, other proprietary rights related to the Work (*e.g.* patent or other rights to any process or procedure) shall be retained by the authors. To reproduce any text, figures, tables, or illustrations from this Work in future works of their own, the authors must obtain written permission from IACMHR Co., Ltd.; such permission cannot be unreasonably withheld by IACMHR Co., Ltd.

3. Conflict of Interest Disclosure

I confirm that all funding sources supporting the work and all institutions or people who contributed to the work but who do not meet the criteria for authors are acknowledged. I also confirm that all commercial affiliations, stock ownership, equity interests, or patent-licensing arrangements that could be considered to pose a financial conflict of interest in connection with the article have been disclosed.

Corresponding Author's Name (Signature):

Date: